COLLISION OF CHARGED PARTICLES FROM ATOMS AND MOLECULES

THESIS

Submitted to the University of Roorkee
for the award of the degree
of
DOCTOR OF PHILOSOPHY
in
PHYSICS

By

MUKESH KUMAR

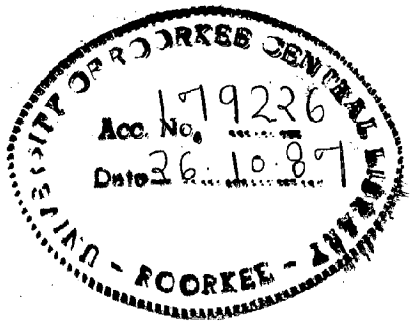

DEPARTMENT OF PHYSICS
UNIVERSITY OF ROORKEE
ROORKEE-247 667 (INDIA)

MARCH, 1986

DEDICATED
TO
MY MOTHER

CANDIDATE'S DECLARATION

I hereby certify that the work which is being presented in the thesis entitled 'COLLISION OF CHARGED PARTICLES FROM ATOMS AND MOLECULES' in fulfilment of the requirement for the award of the Degree of Doctor of Philosophy, submitted in the Department of Physics, University of Roorkee, is an authentic record of my own work carried out during a period from August, 1982 to March, 1986 under the supervision of Dr.A.N. Tripathi.

The matter embodied in this thesis has not been submitted by me for the award of any other degree.

Mukesh Kumar
(Mukesh Kumar)
Candidate's Signature

CERTIFICATE

This is to certify that the above statement made by the candidate is correct to the best of my knowledge.

A N Tripathi
(A.N. Tripathi)
Signature of Supervisor

Dated March 18, 1986

ACKNOWLEDGEMENT

I feel privileged to express my sincere gratitude to Dr. A.N. Tripathi, Reader in Physics, University of Roorkee, Roorkee for his invaluable guidance. His affable inspiration helped me sift the bran of complexities from the problem. His unfeigned efforts to give me carte blanche speak volumes of his unrelenting zest of making me self-reliant in trackling the problems. With his refreshing approach, he was instrumental in creating an ambienceconducive to productive research work.

It gives me immense pleasure to express my deep sense of gratitude towards Dr. Rajesh Srivastava, for his collaboration and useful discussions.

I am indebted to Prof. S.K. Joshi, Head, Department of Physics, for providing various research facilities in the department. I am also grateful to Prof. M.K. Srivastava, Dr. S.N.Singh, Dr. K.C.Mathur and Dr. Deepak Kumar for their constant encouragement during the course of this work.

I am also grateful to Prof. V.H. Smith,Jr. for his collaboration.

The alacrity of my ambidextrous colleagues (Dr.Mohan Lal, Mr. K.S.Baliyan, Miss Indira Khurana, Miss Sushma Saxena, Miss Sadhna Sharma, Mr. Arun Katiyar, Mr. Arvind Kumar Jain, Mr. Kamal and Mr. Pangantiwar, Miss K.Jain) to bring the thesis to the present form left a lasting impression on me. They put the paraphernalia of their limited resources at my disposal. This, besides giving an immense physical help, served as a morale booster.

To see me with a doctorate was a long-cherished ambition of my father. He is no more to relish the fulfilment of his ambition. I can feel his glistening eyes on his blithesome face, showering blessings from the heavenly abode.

Acknowledgement is made to the Director of Computer Centre (RURCC) for providing the computer facilities.

This research was supported in part by the Council of Scientific and Industrial Research, India.

Sri R.C.Sharma deserves my special thanks for the neat typing work which he carried out so painstakingly.

RESUME

The work reported in the thesis contains the results of the author's attempt to study the scattering of intermediate and high energy electrons or positrons by simple atomic and molecular target system, using the various quantum mechanical approaches. The whole work has been divided into three main categories. Under the first category we have studied the inelastic scattering of electron by simple atoms like helium and lithium using various perturbative methods. Under the second category, we have studied the positron impact excitation of helium using same perturbative approaches and in the last category we have calculated the elastic, inelastic, total high energy electron and x-ray scattering from the ten electron systems Ne, HF, H_2O, NH_3 and CH_4 using SCF-MO wavefunction obtained in double zeta quality basis of Gaussian contracted wavefunctions within the framework of the first Born approximation.

The thesis has been written in seven Chapters. The first Chapter gives a brief review of previous work and various quantum mechanical approaches which have been used in different manner. Among the various quantum mechanical approaches, the perturbative models such as distorted wave and its variants, eikonal Born series, modified Glauber approximation, first Born approximation are worth mentioning. In all these approaches the central idea has been to pay

attention to the second order term and attempt to calculate it as accurately as possible. This chapter forms the groundwork to the work reported in subsequent chapters.

In recent years it has been noticed that the theoretical calculations suffer from two sources of uncertainties (i) adoption of an approximate model within the frame work of which the calculation is carried out (ii) choice of the bound state wavefunction to represent the initial and final states of the atomic targets as input to evaluate the scattering amplitude in that particular model. In the subsequent chapters, i.e., 2,3, and 4 we have tried to minimise these uncertainties. For example, the Chapter 2 present our study of electron impact excitation of helium (1^1S-2^1S,2^1P) in the energy range (50-500 eV) using the Coulomb-Born model. Closed form expressions for scattering amplitudes have been obtained with Fourier-decomposition of interaction potential and then the use of accurate correlated wavefunctions. The results of the present calculations have been compared with other available theoretical calculations and the experimental measurements.

Chapter 3 contains the results of our calculation for the differential and total inelastic scattering cross-section, using electron impact excitation (1^1S - 2^1S, 2^1P) of helium in distorted wave approximation (beyond Coulomb Born model as reported in Chapter 2) at intermediate and high energies. The effect of the distortion of incident electron, contribution due to polarization of the target

and the exchange effect are appropriately taken in both the initial and final channels. Fourier decomposition of interaction potential between the projectile and target is taken and an accurate form factor has been used to calculate the transition matrix. The resulting radial Schrödinger equation was solved by a standard noniterative procedure given by Marriott and Percival (Proc.Phys.Soc. 72 121(1958)). The present results show very good agreement with experiment.

In Chapter 4, we extend our study (as outlined in Chapter 2 and 3) for 2^1S and 2^1P transition of helium atom by positron impact. As is well known that the positron impact studies differ from its similar counterpart study by electron in two ways (i) No exchange effects are present (iii) the static distortion potential now bears a negative sign. In this way we have carried out this study on the same footing as has been done for electron impact. Present results are compared with the earlier theoretical estimates.

The Chapter 5, presents our results of electron impact excitation of 3s state of lithium in the energy range 20-200 eV. Differential cross-sections for this transition are obtained in eikonal Born series, Modified Glauber approximation, second Born, Glauber and first Born approximation. In addition, we have also calculated the generalised oscillator strength employing a variety of target wavefunctions. In this chapter we shall also report the results of resonance transition (2s-2p) of lithium atom in Modified Glauber approximation.

In Chapter 6, we present our results concerning molecular high energy electron and x-ray scattering intensities for ten electron systems (Ne, HF, H_2O, NH_3 and CH_4). The difference between the usual elastic intensities for electron and x-ray from nonvibrating but freely rotating molecules and the fully elastic intensities for scattering from the J=0 state are studied. The effect of molecular binding and various other trends and systematics in the intensities have been examined with the help of difference function computed between the present scattering intensities (total, elastic, inelastic) and that for the independent atom model (IAM).

Chapter 7 summarizes the work reported in the earlier chapters and contains some comments, pointing out the drawback and the suggestions for their improvement.

LIST OF PUBLICATIONS

1. Systematic approach for discrete excitation of helium in Coulomb-Born model (with Rajesh Srivastava and A.N. Tripathi), Phys.Rev.A31 652(1985),

2. 2^1S excitation of helium: A precise distorted wave approach (with Rajesh Srivastava and A.N.Tripathi), J.Chem.Phys. 82 1818(1985).

3. Study of e^+-He scattering: a distorted-wave approximation (with Rajesh Srivastava and A.N.Tripathi), J.Phys. B18 4169(1985).

4. Excitation of helium by positron:A distorted wave polarized orbital approach (with Rajesh Srivastava and A.N. Tripathi) J.Chem.Phys.Lett 192(1985) (in press).

5. Electron impact excitation of the 3s state of lithium at intermediate and high energies (with S.S. Tayal and A.N. Tripathi) J.Phys.B18 135(1985).

6. Scattering of high energy electron and x-rays from molecules. The ten electron series Ne, HF, H_2O, NH_3 and CH_4 (with A.N. Tripathi and V.H.Smith,Jr) Int.J.Quantum Chem.(1986) (in press).

7. An improved distorted wave polarized approach (with Rajesh Srivastava and A.N. Tripathi), Ninth International Conference on Atomic Physics, edited by Robert S.Van Dyck, Jr. E.Norval Fortson, Seattle, Washington 1984, p.A58.

8. Excitation of helium by e^+ and e^-: An improved approach (with Rajesh Srivastava and A.N. Tripathi) Proc. of Third International Workshop on positron (electron-gas scattering, Detroit, U.S.A.(1985), Edited by E.Kauppila, S.Stein and M.Wadehra, Published by World Scientific Co., Singapore.

9. Positron excitation of the 2^1S and 2^1P states of helium in distorted wave approximation (with Rajesh Srivastava and A.N. Tripathi) Proc. of Seventh International Conference on Positron annihilation, New Delhi, India (1985), edited by P.C.Jain, R.M.Singru and K.P. Gopinathan, Published by World Scientific Co. Singapore.

10. Scattering of high energy electron from molecules (with A.N. Tripathi and V.H.Smith, Jr) Fourteenth International Conference on the Physics of Electronic and Atomic Collisions, Edited by M.J.Coggiola, D.L. Huestis and R.P. Sayon, Palo Alto (1985) p.231.

11. A reliable calculation for 2^1S excitation of helium atom by positron impact (with Rajesh Srivastava and A.N. Tripathi) Fourteenth International Conference on the Physics of Electronic and Atomic Collisions, Edited by M.J. Coggiola, D.L. Huestis and R.P.Sayon, Palo Alto (1985), p.327, Edited by J.Eichler, W.Fritsch, I.V.Hertel, N.Stolterfoht and U.Wille, Berlin(1983), p.156.

12. Electron impact excitation of lithium 3s state in the intermediate energies (with S.S.Tayal and A.N.Tripathi) Thirteen International Conference on the Physics of Electronic and Atomic Collision,

13. Distorted wave polarized model: An improved approach (with Rajesh Srivastava and A.N. Tripathi) Fifth National Workshop on Atomic and Molecular Physics, Edited by S.K. Mitra, Tata Institute of Fundamental Research, Bombay, India (1984), p.66.

OTHER PUBLICATIONS

14. Double excitation of helium by electron impact :A distorted-wave polarized-orbital approach (with Rajesh Srivastava) Phys. Rev.A31 3639(1985).

15. Electron impact excitation of helium-like ions in Coulomb Glauber approximation-II (with S.N.Singh, A.N. Tripathi and M.K. Srivastava) Indian I.Phys.57B, 1(1983).

CONTENTS

Chapter Page

CHAPTER -1

I N T R O D U C T I O N

1.1 GENERAL REMARKS

The primary aim of Physics is to understand basic laws of nature. For the convenience, physics is divided into many branches which equip us with different information about these laws. The macroscopic aspect fails to explain the basic interaction between the colliding particles and radiations which arises due to electronic structure of atoms and molecules. The atomic and molecular physics specially 'collisional physics' provides the information about these phenomena. The theoretical study of electron, positron and photon collisions with atomic systems has attracted a considerable amount of interest in recent years because a number of theoretical and experimental techniques of atomic and molecular collision are available in literature. Such study of collision processes is very useful in the following diverse fields as radiation physics, electron spectroscopy, plasma physics, atmospheric physics, astrophysics, radiation chemistry, transport properties of gases, fusion process, chemical reactions, auroral phenomenon, solar corona, radiation biology and health physics etc. Most of the applications of the collision physics in the above fields need absolute cross-section over a wide range of energies, which can be obtained

either using the different theories or experimental techniques. At present, the most important use of cross-section is in designing the different types of gas lasers and tokamak.

Due to the above reasons, the collision physics is very wealthy field and have wide scope for further developments in both the theoretical and experimental sides. The main work of the workers in the experimental side is to develop the new techniques to get accurate information using the hi-fi electronic instruments. But on the theoretical side, they compute the absolute cross-sections with the use of different approximations (given in Section 1.2) and compare with the experimental data to check the trustworthiness of that method.

In a simple way the basic ideas which are required in the analysis of charged particle scattering by atoms and molecules, we assume that a well collimated beam of nearly monoenergetic particles is incident upon a target from a large distance and interact with it, after the collision with the target, the outgoing particles are detected by detector which are also located at a macroscopic distance from the target so that the whole system reaches in the stationary state and then their energy and angular distribution are measured. As the incident particles interact with the scatterer, a number of changes occur. Here we shall discuss only elastic and inelastic process. In the elastic scattering, particle simply scattered without any change

in the internal structure. If during the scattering, there is any transfer of energy of incident particle, in giving the internal motion of the target then the system undergoes a change of internal structure and the scattering is called inelastic scattering. But in both the cases, the total energy of the system is conserved. For illustration, we consider projectile as electron and target as hydrogen atom

$$\begin{aligned} e^- + H(1s) &\rightarrow e^- + H(1s) && : \text{elastic scattering} \\ &\rightarrow e^- + H^* && : \text{excitation} \\ &\rightarrow e^- + H^+ + e^- && : \text{ionization.} \end{aligned}$$

Each different initial or final state of the colliding system defines a reaction channel. For example, here we have three different channels. A channel is open if the corresponding collision is allowed by known conservation laws (energy conservation, charge conservation and angular momentum conservation), otherwise the channel is said to be closed. The situation is much more complicated if we are dealing with molecular systems because molecule possesses additional degrees of freedom like rotation and vibration. Thus the the electron molecule scattering, in addition to elastic scattering, may include the electronic excitation, rotational and vibrational excitations and molecular dissociation.

The theoretical formulation of electron atom or molecule scattering is a many body problem and the Schrödinger equation of the system is not exactly solvable. Even for the simplest system such as an electron and the hydrogen atom, one comes across a three body problem and as yet no exact solution is

known. So the theorists are forced to use the approximate methods. But there is no universal approximation, which gives entire information over a wide range of energy. However, the reliability and accuracy of an approximate method is assessed by comparing it with other theoretical methods and the available experimental data. In general, the study of the collision processes are carried out in three different energy regions namely, the low, intermediate and high energy regions.

Low energies:

The low energy region is the one where only a few states can be excited or equivalently, only a few states are open.

Intermediate energies:

This is one of the difficult energy range extending from the region where only a few channels are open to a few times the ionization threshold but below the region in which first Born approximation becomes accurate. The basic problem here is to allow in some average way for the infinite number of open channels including continuum, particularly when the convergence of the perturbation theory is poor.

High energies:

The applicable energy range extends from a few times the ionization threshold upwards. The region is characterised theoretically by the rapid convergence of perturbation theory and at sufficiently high energies, the first Born approximation

will usually, but not always, be applicable.

Recent reviews by Bransden and McDowell(30), Byron and Joachain(66), Callaway(77), Henry(141), Burke and Williams(122), Moiseiwitsch(31) and Walters(73) describe in detail about the various theoretical methods.

In the next section (1.2), we present a brief review of the theoretical methods and also discuss the underlying assumptions and the region of validity of the various approximations.

1.2 BRIEF REVIEW OF APPROXIMATE METHODS

Here we are concerned with the atomic system in which we assumed that the incident particle (electron) is interacting for a long time with the atom (hydrogen) so that the whole system has reached a stationary state. A non-relativistic collision between an electron and a hydrogen atom is described by Schrödinger equation

$$(H-E)\psi(\vec{r}_1, \vec{r}_2) = 0 \qquad \ldots (1.1)$$

where $\psi(\vec{r}_1, \vec{r}_2)$ is the wavefunction of the entire system, incident electron plus the atom with appropriate boundary condition, $\vec{r}_1$, $\vec{r}_2$ are the position vectors of incident particle and atomic electron with respect to the atomic nucleus (assumed to be infinitely heavy). H is the total Hamiltonian of the system and is given by (in atomic units, $h = m_e = e = 1$)

$$H = -\frac{1}{2}\nabla^2 + H_t(\vec{r}_2) + V(\vec{r}_1, \vec{r}_2) \qquad \ldots (1.2)$$

$$V = -\frac{1}{r_1} + \frac{1}{|\vec{r}_1 - \vec{r}_2|} \qquad \ldots (1.3)$$

In Eq. (1.2), $-\frac{1}{2}\nabla^2$ is the kinetic energy operator of the incident electron, H_t is the Hamiltonian of the target (hydrogen) and V is the interaction potential between the incident electron and target atom, E is the total energy of the system and is given by

$$E = \frac{1}{2}k_i^2 + \varepsilon_i = \frac{1}{2}k_f^2 + \varepsilon_f \qquad \ldots (1.4)$$

$\varepsilon_{i,f}$ are the target internal energies in the initial and final channels, given by

$$H_t \phi = \varepsilon \phi \qquad \ldots (1.5)$$

where ϕ is the eigenfunction of the target (hydrogen) and ε is the corresponding eigen energy of the incident electron in the initial and final channels respectively. Due to the indistinguishability of electrons, the total wavefunction of the system should be antisymmetric with respect to interchange of spin and space coordinates of the electron. The space wavefunction of the system is given by

$$\psi^{\pm}(\vec{r}_1, \vec{r}_2) = \frac{1}{\sqrt{2}} \left[\psi(\vec{r}_1, \vec{r}_2) \pm \psi(\vec{r}_2, \vec{r}_1) \right] \qquad \ldots (1.6)$$

where ψ^+ is for symmetric (singlet) and ψ^- is for antisymmetric (triplet) space wavefunction.

We assume, when the incident particle is at large distance from the target, it can be described by a plane wave $e^{i\vec{k}_i \cdot \vec{r}_1}$ and after the interaction with the target, the outgoing

scattering wavefunction $F(\vec{r}_1)$ is described as a superposition of the incident plane wave and outgoing spherical wave, we have

$$F(\vec{r}_1) \underset{r_1 \to \infty}{\simeq} \exp(\vec{k}_i \cdot \vec{r}_1)\delta_{if} + r_1^{-1} f_{if}(\theta,\phi)\exp(k_f r_1) \quad \ldots (1.7)$$

where $f_{if}(\theta,\phi)$ is the scattering amplitude for the transition, in which the target goes from the initial state i to any final state f. We can easily verify that for any function $f(\theta,\phi)$, the expression (1.7) satisfies equation (1.1) asymptotically through terms of order r_1^{-1} in the region where V can be neglected, if the potential vanishes faster than r_1^{-1} as $r_1 \to \infty$. Using the scattering amplitude $f(\theta,\phi)$, we can directly calculate the differential $(\frac{d\sigma}{d\Omega})$ and total scattering cross-sections

$$\frac{d\sigma(\theta,\phi)}{d\Omega} = \frac{k_f}{k_i} |f_{if}(\theta,\phi)|^2 \quad \ldots (1.8)$$

$$= \frac{k_f}{k_i} \int_0^{2\pi} \int_0^{\pi} |f_{if}(\theta,\phi)|^2 \sin\theta \, d\theta \, d\phi \quad \ldots (1.9)$$

for elastic scattering i=f

From this brief introduction, it is obvious that the basic quantity of interest, is the scattering amplitude and is contained in the asymptotic form of the total wavefunction. The evaluation of this quantity provides a meeting ground between theory and experiment. The calculation of scattering amplitude is not so straightforward. Now we shall discuss various approximation schemes employed for the evaluation of the wavefunction $\psi(\vec{r}_1, \vec{r}_2)$ in equation (1.1) and the scattering amplitude.

1.2.1 Eigen function expansion method

In this approximation, the total wavefunction of the system is expanded in terms of the target eigenfunctions ϕ_n

$$\Psi^{\pm}(\vec{r}_1,\vec{r}_2) = \frac{1}{\sqrt{2}} \sum_n \left[F_n^{\pm}(\vec{r}_1)\phi_n(\vec{r}_2) \pm F_n^{\pm}(\vec{r}_2)\phi_n(\vec{r}_1)\right] \quad \ldots (1.10)$$

where + sign refers to the singlet and -sign to the triplet spin case and $F_n^{\pm}(\vec{r})$ represent the scattering wave-function while $\phi_n(r)$ represent the eigenfunctions of the target. The sum over n, is over the the complete set of the target eigenfunctions, which includes an integration over continuum states of the target. If we solve equation (1.1) with the use of equation (1.10), an infinite set of coupled equations for $F_n^{\pm}(\vec{r})$ is obtained in the form

$$(\nabla^2 + k_n^2)F_n^{\pm}(\vec{r}_1) = 2\sum_m \left[V_{nm}(\vec{r}_1)F_m^{\pm}(\vec{r}_1) \pm \int W_{nm}(\vec{r}_1,\vec{r}_2) F_m^{\pm}(\vec{r}_2)d\vec{r}_2 \right] \quad \ldots (1.11)$$

where $V_{nm}(\vec{r})$ is the direct local potential

$$V_{nm} = \int \phi_n^{\otimes}(\vec{r}_2) V(\vec{r}_1,\vec{r}_2)\phi_m(\vec{r}_2)d\vec{r}_2 \quad \ldots (1.12)$$

and W_{nm} is the non-local exchange potential defined as

$$W_{nm} = \phi_n^{\otimes}(\vec{r}_2)[H-E]\phi_m(\vec{r}_1) \quad \ldots (1.13)$$

This infinite set of equations is just the original Schrödinger equation in a new basis and as such is not solvable. However, it can be made tractable and solvable if we adopt some approximation scheme. So, we now discuss about the approximations for solving this equation.

1.2.2 Low energy collision theory

(A) Partial wave analysis

The partial wave method is one of the methods used to solve the set of equations (1.11-1.13). This method is applicable for spherically symmetric potentials. In this approach it is possible to separate out the coupled equation (1.11) into its angular and radial variables. This is achieved by carrying out an expansion of $F(\vec{r}_1)$ and $\frac{1}{|\vec{r}_1-\vec{r}_2|}$ in terms of the Legendre polynomials i.e.,

$$F_n^{\pm}(\vec{r}_1) = r_1^{-1} \sum_{\ell=0}^{\infty} A_\ell \, f_{n\ell}^{\pm}(\vec{r}_1) P_\ell(\cos\theta) \qquad \ldots (1.14)$$

and

$$\frac{1}{|\vec{r}_1-\vec{r}_2|} = \sum_{\ell=0}^{\infty} \frac{r_<^\ell}{r_>^{\ell+1}} P_\ell(\hat{r}_1 . \hat{r}_2) \qquad \ldots (1.15)$$

where $r_<$ and $r_>$ are the lesser and greater of r_1, r_2 and θ is the polar angle of r_1, A_ℓ is normalisation constant. With the use of equations (1.14-1.15) in the equation (1.11) one gets the following radial equation

$$\left[\frac{d^2}{dr_1^2} + k_n^2 + \frac{\ell(\ell+1)}{r_1^2}\right] f_{n\ell}^{\pm}(\vec{r}_1)$$
$$= 2 \sum_m \left[V_{nm}(\vec{r}_1) f_{m\ell}^{\pm}(\vec{r}_1) \pm \int W_{nm}^{\ell}(\vec{r}_1, \vec{r}_2) f_{m\ell}^{\pm}(\vec{r}_2) d\vec{r}_2 \right] \qquad \ldots (1.16)$$

with

$$W_{nm}^{\ell}(\vec{r}_1, \vec{r}_2) = \frac{4\pi}{(2\ell+1)} r_1 r_2 \phi_m(\vec{r}_1) \phi_n^{*}(\vec{r}_2)$$
$$\left[z' \frac{r_<^\ell}{r_>^{\ell+1}} - \frac{1}{2}(E-\varepsilon_n-\varepsilon_m)\delta_{\ell 0} \right] \qquad \ldots (1.17)$$

z' represents the change on the incident particle.

The radial function $f^{\pm}_{n\ell}(\vec{r}_1)$ is known as ℓ^{th} partial wave with the following asymptotic form

$$f^{\pm}_{n\ell}(\vec{r}_1) \underset{r_1\to\infty}{\simeq} \frac{1}{k_n} \sin(k_n r_1 - \frac{\ell\pi}{2} + \eta^{\pm}_{n\ell}) \qquad \ldots (1.18)$$

where $\eta^{\pm}_{n\ell}$ is phase shift of ℓ^{th} order and is directly related with scattering amplitude as

$$f^{\pm}(\theta) = k_n^{-1} \sum_{\ell=0}^{\infty} (2\ell+1) \exp(i\eta^{\pm}_{n\ell}) \sin\eta^{\pm}_{n\ell} P_\ell(\cos\theta) \qquad \ldots (1.19)$$

This equation has been widely used to obtain the collisional cross-section in terms of phase shifts using partial wave method.

(B) Close-coupling approximation

The close coupling is one such method in which the situation can be handled easily. In this method the first few intermediate states in the infinite summation in equation (1.10) are retained while the effect of rest is neglected (130, 96), the order of the approximation depends on the fact that how many atomic states are retained in the expansion of the total wavefunction. This method is highly accurate if the coupling of neglected states is weak and is also very successful in predicting resonances but is less useful in treating excitation processes. Due to neglect of coupling with higher states and with continuum, this method suffers from the drawback that the long range

distortion of the target is not represented properly. While the 18.6% and 54.6% dipole polarizability of hydrogen and helium(124) respectively comes from the continuum states. So to remove this drawback, the present method is modified with the inclusion of neglected states in some way, like (i) second order potential (SOP) approach in which the effect of neglected states is accounted by inclusion of some effective potential(27,89,28) or (ii) using the pseudo-state approximation(79, 121, 123, 125, 127) in which higher excited and continuum states are replaced by pseudo states, chosen to be orthogonal to each other and to the first few atomic eigenstates included in the eigen function expansion method, such that they give rise to the exact polaria-ability of the atom. A large number of calculations have been done by various workers(86, 182, 168) using these approximations. Another equivalent method for solving the coupled equations for the radial functions $f_n^{\pm}(\vec{r}_1)$ has been introduced by Burke and Robb(127) and is called R-matrix approach in which, one expands the continuum orbital in each channel in a complete set of basis orbitals. A number of calculations based on this approach have been done by many workers(86, 182, 181, 170).

(c) Polarized orbital method

It is one of the most successful methods in which the effect of the polarisation of the target is taken into account by just adding a perturbing part representing the polariza-tion of the target to the unperturbed wavefunction of the target. Using the first order perturbation theory the perturbing part is obtained. This method was introduced by Temkin(19) and Temkin and Lamkin(20) by obtaining the

single integro-differential equation of the infinite set of equations (1.16). The adiabatic and nonadiabatic polarization potential is introduced by Labahn and Callaway(148) and Khare and Shobha(159). It is described in detail by Drachman and Temkin(140).

1.2.3 Intermediate and high energy collision theory

The low energy methods which we have discussed in the Section (1.2.2) are not suitable for intermediate and high energy regions. Because in this energy region, the low energy method become quite complicated as large number of channels become open for scattering and a great number of partial waves are to be computed. Since the intermediate energy region provides a link between low and high energies, there are two natural lines of attack, one from low energies and the other from the high energies. We adopt here, the second approach in which we start correcting the high energy approaches. In general, the corrections to the first order term of the multiple scattering is sought in various ways. To achieve this, we write equation (1.1) in the integral form (40) in place of differential equation. This integral form is highly useful in analysing the scattering problem in this region of energy. The integral form of Schrödinger equation (1.1) for two electron system is given as

$$\psi(\vec{r}_1,\vec{r}_2) = \exp(i\vec{k}_i.\vec{r}_1)\phi_i(\vec{r}_2) + 2\sum_m \int (\phi_m^*(\vec{r}_2)\phi_m(\vec{r}_2')G_m(\vec{r}_1,\vec{r}_1') \times V(\vec{r}_1,\vec{r}_2')\ (\vec{r}_1',\vec{r}_2')d\vec{r}_1\ d\vec{r}_2' \qquad \ldots (1.20)$$

where $G_m(\vec{r}_1,\vec{r}_1')$ is Green function and given by

$$G_m(\vec{r}_1, \vec{r}_1') = -\frac{1}{4\pi} \frac{\exp(ik_m(\vec{r}_1 - \vec{r}_1'))}{|\vec{r}_1 - \vec{r}_1'|} \qquad \ldots (1.21)$$

This equation shows summation over an infinite set of the target wavefunctions. The scattering amplitude for any initial state i to final state f is given by

$$f_{fi} = -\frac{1}{2\pi} \int \exp(-i\vec{k}_f.\vec{r}_1)\phi_f^{\otimes}(\vec{r}_2)V(\vec{r}_1, \vec{r}_2)\psi(\vec{r}_1, \vec{r}_2)d\vec{r}_1 d\vec{r}_2 \qquad \ldots (1.22)$$

The Born series for the scattering amplitude can be easily obtained by iterating the solution of equation (1.20). We expect that the Born series will converge if the incident particle has a high energy and (or) if the potential is weak enough.

(A) First Born approximation

Due to simplicity this approximation has been widely used(93, 109) in many scattering problems. The underlying assumption in this approximation is that the incident particle interacts slightly with the target so the wavefunction can be expressed as a plane wave which will be the correct function in the absence of all interaction. To obtain, the first Born expression only the first leading term is retained in series expansion. This is given as

$$f_{fi}^{(1)} = f_{B1} = -\frac{1}{2\pi} \int \exp(-i\vec{k}_f.\vec{r}_1)\phi_f^{\otimes}(\vec{r}_2)\, V(\vec{r}_1, \vec{r}_2) \exp(i\vec{k}_i.\vec{r}_1)\phi_i(\vec{r}_2)d\vec{r}_1\, d\vec{r}_2$$

$$= -\frac{1}{2\pi} \int \exp(i\vec{q}.\vec{r}_1)\, V_{fi}(\vec{r}_1)d\vec{r}_1 \qquad \ldots (1.23)$$

with $V_{fi}(r_1) = \int \phi_f^{*}(r_2)\left(\frac{1}{r_1} - \frac{1}{|\vec{r}_1-\vec{r}_2|}\right)\phi_i(r_2)d\vec{r}_2$.

where $\vec{q} = \vec{k}_i-\vec{k}_f$ is the momentum transfer vector. This approximation is valid if the velocity of incident particle is very large compared to the bound electron or energy of incident particle is high. It is well known that for the elastic scattering the first Born term (f_{B1}) dominates the Born-series both at small momentum transfer q and at very high energies. In the region of large q, it converges to the second Born term. However, for the inelastic scattering, because of the orthogonality of the initial and final bound state wavefunction, removes the electron nucleus interaction from the f_{B1}, as a result the first Born cross-section for high energy and large angle is of orders of magnitude too small.

(B) Second Born approximation

The first Born approximation (FBA) which completely neglects the effects due to the polarization of the target by the incident electron and the distortion of the incident wave. These effects are very important for intermediate energies. In order to include these effects of first Born approximation (FBA). We use the second Born approximation (SBA). The second Born amplitude is obtained by retaining the first and second term in the Born series. It is written as

$$f_{B2} = f_{fi}^{(1)} + f_{fi}^{(2)} \qquad \ldots \quad (1.24)$$

where $f_{fi}^{(2)}$ is the second term of the Born series and given by

$$f_{fi}^{(2)} = \frac{1}{\pi} \sum_{m} \int \exp(i\vec{k}_i.\vec{r}_1 - \vec{k}_f.\vec{r}_1) G_m(\vec{r}_1, \vec{r}_1') V_{fm}(\vec{r}_1) V_{mi}(\vec{r}_1') d\vec{r}_1 \, d\vec{r}_1' \quad \ldots (1.25)$$

Here the summation on m includes the sum over all bound and continuum states ϕ_m of the atom. Hence, its evaluation is quite difficult. This may be done by taking the energy of the intermediate states to be fixed at some average energy which is different from the ground state energy of the target and then performing the summation by the closure property(74) Holt and Moisewitsch(16) and Holt et al(17), have considered the first few target states explicitly and the effects of the rest is included by replacing the energies of the intermediate states by an average excitation energy.

(c) Third Born term

There has been no serious attempt made to evaluate the third Born term into a form which can be used in analysing the higher order correction to the Born series. One such attempt in recent past is due to Yates(4). His procedure parallels that of Glauber(139) and is very similar to the high energy small angle potential scattering analysis of Schiff(103).

As the strength of the potential increases, the inclusion of higher order term of the Born series is difficult and therefore, it is not possible to obtain the proper convergence of the series. Therefore, some high energy semi-classical and its related methods have been used to study

the scattering of electron by atomic targets.

(D) Eikonal approximation

It is a semi-classical approximation, which is applicable when the wavelength ($\lambda = \frac{1}{k_i}$) of a particle is sufficiently short compared with the distance over which the potential changes appreciably, then it is possible to define the particle trajectories which obey the laws of classical mechanise. If the potential V is of range a, the short wavelength condition requires

$$k_i \, a \gg 1$$

and the high energy condition requires

$$|V| \; / \; E \ll 1.$$

In this approximation, the scattering wavefunction is written as a product of the incident plane wave and a slowly varying function of r_1 which is a modulating factor to the incident wave and its departure from unity is a measure of the scattering effect of the potential and is given by

$$F(\vec{r}_1) = \exp\left[i\vec{k}_i.\vec{r}_1 - \frac{i}{k_i}\int_{-\infty}^{z} V(b,z')dz' \right] \quad \ldots (1.26)$$

where b is impact parameter and it is assumed here that the incident wave moves in the z-direction with constant speed v_i and $\vec{r}_1 = \vec{b}+z\hat{k}_i$. Using the equation (1.26) the scattering amplitude is

$$f_E = -\frac{1}{2\pi}\int \exp(i\vec{q}.\vec{r}_1)\, \phi_f^{\otimes}(\vec{r}_2) V(\vec{r}_1,\vec{r}_2)\phi_i(\vec{r}_2) \times \exp\left[-\frac{i}{k_i}\int_{-\infty}^{z} V(b,z')dz' \right] d\vec{r}_1 d\vec{r}_2 \quad \ldots (1.27)$$

Due to straight line trajectorie (66) the eikonal approximation is only reliable at small angles. For small angles, $\vec{q}$ is perpendicular to the incident direction but the actual phase of the scattering wavefunction should be evaluated along the curved trajectory.

(E) Glauber approximation

In 1959, Glauber(139) suggested an improvement in the wavefunction equation (1.26) can be achieved by performing the z-integration in the phase along a straight line parallel to the bisector of the scattering angle i.e. perpendicular to $\vec{q}$, because phase could not be obtained along the curved trajectory of the particle in semi-classical limit. The Glauber approximation is a special case of eikonal approximation having the usual conditions of eikonal approximation. The scattering amplitude may be written as

$$f_G = \frac{ik_i}{2\pi} \int \exp(i\vec{q}.\vec{b}) \phi_f^*(\vec{r}_2) \Gamma(\vec{b}, \vec{r}_2) \phi_i(\vec{r}_2) d^2b \, d\vec{r}_2 \quad \ldots (1.28)$$

where,

$$\Gamma(\vec{b}, \vec{r}_2) = 1 - \exp[i\chi(b, r_2)] \quad \ldots (1.29)$$

and $$\chi(\vec{b}, \vec{r}_2) = -\frac{1}{k_i} \int_{-\infty}^{\infty} V(\vec{r}_1, \vec{r}_2) dz$$

Here ϕ_i and ϕ_f are the target wavefunctions in the initial and final states respectively, $\vec{r}_1 = \vec{b} + z\hat{k}_i$ is the projectile coordinate and $\vec{r}_2 = \vec{s} + z\hat{k}_i$ is the coordinates of the target electron with respect to the nucleus of the target. The expansion of the exponential $e^{i\chi}$, gives the Glauber scattering amplitude in the form of an infinite series, referred as

Glauber eikonal series (GES)

$$f_{if}(\vec{q}, k_i) = \sum_{n=1}^{\infty} i^{n-1} f_{if}^{(n)}(\vec{q}, k_i) \qquad \ldots (1.30)$$

where

$$f_{Gn} = f_{if}^{n}(\vec{q}, k_i) = \frac{k_i}{2\pi n_t} \int d\vec{b}\, e^{i\vec{q}.\vec{b}} \langle \phi_f | \chi^n | \phi_i \rangle \qquad \ldots (1.31)$$

We note that $f_{B1} = f_{G1}$ because of our choice of z-axis. We also see that Glauber terms are alternately real or purely imaginary, while the Born terms for $n \geq 2$ are complex. Yates(3) and Singh and Tripathi (157) have analysed in detail the different terms of Glauber eikonal series for elastic and inelastic scattering of electrons by hydrogen and helium respectively. Before we point out some improvements made in the Glauber amplitude, we must point out some of the shortcomings with which this approximation suffers. The most important of which are the following.

(i) The logarithmic divergence of the imaginary part of the elastic amplitudes in the forward direction because of the long range electromagnetic forces.

(ii) The excitation cross-sections for states for which $(L_f - M_f) - (L_i + M_i)$ is an odd number, are identically zero whereas for even number, it enhances the cross-section (here L_f, M_f and L_i, M_i are the angular momentum quantum numbers of final and initial states respectively). The calculation of the orientation parameters λ and χ is therefore,

meaningless in this theory.

(iii) It does not distinguish between scattering of positve and negative particles.

These failures can be traced back to the neglect of the intermediate energy transfer in the derivation of Glauber amplitude. As a result, the first two shortcomings mentioned above can be removed by introducing an average excitation energy of finite value of the atom as its intermediate states. This has been worked out by Rosendorff(1) in a consistent way. The improved amplitude obtained by him resembles the conventional Glauber amplitude in character. It satisfies the unitarity theorem (to all orders of the perturbation expansions). However, still it does not distinguish the scattering of positive particles from that of negative particles. Further, the vanishing of real part of f_{G2} from the Glauber series is particularly disturbing as it amounts to the loss of the leading contribution from the target polarization.

(F) Eikonal-Born series method

We have seen that the Glauber terms are alternately real or purely imaginary, while the Born terms for $n \geq 2$ are complex i.e.

$$f_G = \bar{f}_{G1} + \text{Im } \bar{f}_{G2} + \text{Re } \bar{f}_{G3} \qquad \ldots (1.32)$$

$$f_B = \bar{f}_{B1} + [\text{ Re } \bar{f}_{B2} + \text{Im } \bar{f}_{B2}] + [\text{Re } \bar{f}_{B3} + \text{Im } \bar{f}_{B3}] \qquad \ldots (1.33)$$

Using the property of Glauber and Born series Byron and Joachain (67) introduced a new approach called Eikonal-Born

series(EBS). It basically combines the Born and Glauber series to get a consistent picture of the scattering amplitude through order k_i^{-2}. It is achieved as follows

$$f_{EBS} = f_{B1}+f_{B2}+f_{G3} \qquad \ldots (1.34)$$

where f_{B1} and f_{B2} are the first and second terms of Born series, f_{G3} is the third order Glauber term. It must be emphasized that for processes in which both the initial and final states are spherically symmetric, the Glauber term f_{Gn} gives in each order the loading piece of the corresponding Born term (for large k_i) at all momentum transfer, except in the second order. It has been established further on the basis of potential scattering that the third order Born term (expanded in powers of $1/k_i$) is almost identical to the third order Glauber term and can therefore be evaluated easily. This is the rational behind using the third Glauber term in EBS approach.

(G) Modified Glauber approximation

This approximation is apparently very similar to EBS, in which, the full Glauber amplitude is corrected for the missing second order real term by substituting the f_{B2} in place of f_{G2}. This modification was pointed out by Byron and Joachain (65) and elaborated by Gein(175), is called modified Glauber approximation(MG) and is given as

$$f_{MG} = f_G - f_{G2} + f_{B2} = f_{B1}+f_{B2}+f_{G3}+\sum_{n=4}^{\infty} f_{Gn}$$

$$= f_{EBS} + \sum_{n=4}^{\infty} f_{Gn} \qquad \ldots (1.35)$$

This approach, instead of working to order k_i^{-2} removes the logarithmic divergence of the Glauber amplitude in the forward direction and includes the polarization effect of the target. The modified Glauber amplitude is more accurate in the comparison of EBS amplitude because in MG we include the higher order Glauber terms. This inclusion of higher order terms play a significant role at large scattering angles. A detailed study, comparing the EBS and MG has been done by Tripathi and coworkers(163,164,165,166). Apart from the success of EBS and MG approach, recently Yates(4) has proposed a high energy higher order Born approximation. In this method he has evaluated all the Born terms on equal footing. Recently the EBS and MG approach has been unitarised (68,69) by using a method due to Wallace(152) and referred as UEBS. This method has been used recently by Byron and coworkers to study the elastic and inelastic scattering of electron from hydrogen. In this direction, Dewangan(50) has proposed a new theoretical model which fully incorporates the second Born amplitude under a closure approximation and in limit of high energy reduces to Glauber restricted approximation (82).

The recent review article by Gerjouy and Thomas(57), Byron and Joachain(66), Chain et al(63), Joachain and Quigg(38) and Tripathi(14) have dealt in detail about the various aspects of these theoretical approaches.

(H) Corrected static and its variants

We know that the static interaction (V_{st}) correctly reduces for small values of r to the Coulomb interaction acting between the projectile electron and the nucleus of the target. Therefore, we expect it to govern large angle direct elastic scattering. If one makes an expansion of the static scattering amplitude in powers of V_{st}, i.e.

$$f_{st} = -\frac{1}{2\pi}\langle k_f|V_{st}+V_{st}G+V_{st}+\ldots.|k_i\rangle$$
$$= f_{B1}+\sum_{n\geq 2} f_{Bn}(V_{st}) \qquad \ldots (1.36)$$

It contains the term $f_{Bn}(V_{st})$ of the Born series having the initial state (ground state here) as intermediate state. These terms correspond to virtual transition going through elastic intermediate states and dominate the direct scattering amplitude at large k_i and large q since the convergence of the Born series is slower at large q than at small q, it is therefore useful at large angles to perform an exact (partial wave) treatment of the potential V_{st} and thereby the resulting amplitude f_{st} sums the contribution of V_{st} to all orders of the perturbation theory.

For small values of q, however, the static approximation is poor. This is due to the inadequate treatment of f_{B2}, since the static potential is real and of short range and does not account for absorption and polarization effects which play an important role at small angles. So in order to improve this, we must add to the f_{B2} that part which lacks i.e. we now carry out an expansion of the static scattering

amplitude in powers of $\{(V-V_{st})+V_{st}\}$ giving rise to what is called corrected static approximation (f_{cs}) (74,25)

$$f_{cs} = f_{st} + [f_{B2}(V)-f_{B2}(V_{st})] \qquad \ldots (1.37)$$

This approach does not include the contribution from the non-static part of the third and higher order terms which may be quite important. In the case of elastic scattering from the 2s state of atomic hydrogen the real part of the scattering amplitude is found to be dominated by f_{G3} (third order Glauber term) in the intermediate and large angle region. The corrected static approximation may be improved upon by adding to it the contribution from the non-static parts of the third and higher order terms in (say) the Glauber approximation

$$f = f_{st}+(f_{B2}-f_{B2}^{st})+(f_{G1}-f_{G2}-f_{G}^{st}+f_{G2}^{st}) \qquad \ldots (1.38)$$

This equation should lead to an improvement over both the EBS and the CS approximation(112,116,163).

It can be easily seen here that the MG approximation can be obtained by dropping terms of order higher than two in f_{st} and its compensating term f_{G}^{st}.

$$f_{MG} = f_{G}+f_{B2}-f_{G2}$$

The EBS amplitude corresponds to further dropping the higher order Glauber terms G_4, G_5 ..... in a bid to obtain an expression correct to order $1/k_i^2$.

$$f_{EBS} = f_{B1}+f_{B2}+f_{G3}$$

All these approaches are basically high energy approaches and rely on convergence of the Born series. They do not work when applied at lower energies. At these energies the Born series have poor convergence and therefore, all the multiple scattering series should be evaluated on an equal footing rather than giving a special treatment to the second order Born term and ignoring/evaluating higher order terms in some other approximation. This will avoid disturbing delicate cancellations between various terms. If Glauber approximation for the higher order terms are used, then, the amplitude is given as

$$f = f_{st} + f_G - f_G^{st} \qquad \ldots (1.39)$$

This approach works quite well in the lower energy side of the intermediate energy region particularly for low polarizability targets.

(I) Two-potential methods

The basic idea of two-potential method is that the total projectile-target interaction, is broken up into two pseudo-potentials and the resulting two terms of the transition matrix are evaluated in different approximations. Generally one term of the broken part is treated exactly while the remaining part is evaluated approximately. Various choices of this break-up and the approximations have led to the various methods reported in the literature

(i) Distorted wave Born approximation,

(ii) Distorted wave eikonal approximation,

(iii) Two potential eikonal approximation,

(iv) Glauber distorted Born approximation,

(v) Coulomb projected Born approximation.

These methods have been used extensively. Ishihare and Chen(169) have treated the static part of the potential exactly and the remaining part is evaluated in the Glauber approximation, Madison and Shelton(47) and Culhaum et al(147) have applied the standard two potential formalism to obtain a systematic distorted wave model for electron impact excitation of atoms.

(J) Distorted wave method

As we have discussed that the Second Born approximation (SBA) makes partial allowance for the effect of distortion. But the distorted wave approximation provides better account of distortion. Due to their truthfulness, a large number of theoretical work is available in the literature (135, 160, 84, 145, 172, 161, 185, 47, 41, 30, 25, 169, 51, 90, 78). Basically, in this approximation we make a two state approximation involving just the initial state i, which we suppose to be the ground state of the atom and final state f, neglect coupling to all other state. This approximation has been used in different ways. A detailed account of the various distorted wave methods has been given in the review of Bransden and McDowell(30).

(a) Distorted wave first Born (DWBA) approximation

In the recent years, it has been applied by various authors. The philosophy here has been strictly speaking lies in the

choice of the distorting potentials. We can write the interaction V_i in two parts:

$$V_i = U_i + W_i \qquad \ldots (1.40a)$$

$$V_f = U_f + W_f \qquad \ldots (1.40b)$$

and we choose U_i and/or U_f as

$$V_i = \langle \phi_i | V_i | \phi_i \rangle = V_{st} \qquad \ldots (1.41)$$

so that

$$W_i = V_i - \langle \phi_i | V_i | \phi_i \rangle \qquad \ldots (1.42)$$

then the first term of the distorted wave Born series become

$$f_{fi}^{DWBA} = -\frac{1}{2\pi} \langle \chi_f^- | V_{fi} | \chi_i^+ \rangle \qquad \ldots (1.43)$$

where χ_c satisfies the equation

$$(\nabla^2 + k_c^2)\chi_c(r) = 2V_c\chi_c(r), \qquad c = (i \text{ or } f) \qquad \ldots (1.44)$$

The DWBA in this form has been applied by many authors to the study of excitation of hydrogen (47), helium(26).

(b) Distorted wave second Born (DWSBA) approximation

The sum of the first two terms of the distorted wave Born series gives the distorted wave second Born approximation to the scattering amplitude

$$f_{fi}^{DWSBA} = f_{fi}^{DWBA} - \frac{1}{2\pi} \langle \chi_f^- | \sum_{m=f \text{ or } i} V_{fm} G_m^+ V_{mi} | \chi_i^+ \rangle \qquad \ldots (1.45)$$

Its application is limited to the high energy region only if the closure approximation is used to perform the m summation.

The DWSBA offers a good basis for describing the e-atom excitation. Recently this approximation has been used by Dewangan and Walter's(51) to study the elastic scattering and Kingston and Walters and Winter(6,90) for electron-hydrogen excitation.

1.2.4 Exchange approximation

Due to indistinguishability of electron, in electron-atom scattering the exchange effect are really very important. So far we have not taken exchange into account in the described methods. It is obvious that exchange effect is not very important for high energy but for low and intermediate energies exchange effect play an important role, we see from equation (1.11) that in the high energy approximations the direct and exchange scattering amplitude are obtained separately and the total scattering amplitude is by combining these two according to symmetry requirement. In literature a large number of methods are available to calculate the exchange scattering amplitude, the most familiar methods are Born-Oppenheimer approximation (32) and Ochkur approximation(179).

1.3 PLAN OF THE THESIS

The primary aim of the present study is to investigate the scattering of charged particle (electron and positron) with atomic and molecular systems at intermediate and high energies using simple, accurate and computationally feasible quantum mechanical methods. The results obtained in the present

investigations are compared with available theoretical calculations and experimental data.

The whole work has been divided into three main categories. In the first category we have studied the inelastic scattering of electron by simple atoms like helium and lithium, under the second category we have studied the positron impact excitation of helium and in the last category we have calculated the elastic, inelastic, total high energy electron and x-ray scattering from the ten electron systems Ne, HF, H_2O, NH_3 and CH_4.

The first category deals with the following investigations

In general, the theoretical calculations suffer from two types of uncertainties (i) the basic nature of approximation employed for studying the collision process and (ii) use of the approximate wavefunction as input for evaluating the scattering amplitude within the framework of the scattering model. In the following two chapters, we have made an attempt so that the above mentioned uncertainties are best minimised.

(i) The study of electron impact excitation of helium for 1^1S-$2^1S, 2^1P$ transitions with the use of many parameter correlated wavefunctions in the Coulomb-Born (CB) model with the inclusion of exchange effect using Bonham-Ochkur approximation (see Chapter 2). The comparison of results with the experimental measurement of Suzukai and Takayanagi(75), Opal and Beaty(37) shows a better agreement compared to the

other theoretical calculations.

(ii) In Chapter 3, we studied the same problem using a distorted wave approximation (beyond Coulomb-Born model) employing the many parameter correlated wavefunctions. The effect of the distortion of incident electron, contribution due to polarization of the target and the exchange effect are appropriately taken in both the initial and final channels. The resulting radial Schrödinger equation was solved by a standard non-iterative procedure given by marriott and percival (Proc. Phys. Soc. 72, 121(1958)). The present results show all the possible features (near about) of experimental data.

(iii) The Chapter 5, presents our study of electron impact excitation of lithium for 2S-3S transition using the eikonal Born series, Modified Glauber approximation, second Born, Glauber and first Born approximation and a preliminary study ofor 2s-2p transition in Modified Glauber approach. In addition we have also calculated the generalised oscillator strength employing a variety of target wavefunction.

Second category presents our comparative study of positron impact excitation of helium atom for 1^1S-2^1S, 2^1P transitions using the same models which we have used in Chapters 2 and 3. The results are presented in Chapter 4. This study differs in two ways (i) No exchange effects are present (ii) the static distortion potential now bears a negative sign.

In the last category, Chapter 6, the elastic, inelastic and total x-ray and electron scattering from ten electron systems Ne, HF, H_2O, NH_3 and CH_4 have been calculated using SCF-MO wavefunctions obtained in double zeta quality basis of Gaussian contracted wavefunctions. The effect of molecular binding and various other trends and systematics in the intensities have been examined with the help of difference functions computed between the present scattering intensities and that for IAM.

The Chapter 7 contains a summary of the work presented in the earlier chapters and some comments.

CHAPTER -2

SYSTEMATIC APPROACH FOR ELECTRON IMPACT EXCITATION OF HELIUM IN COULOMB-BORN MODEL

2.1 INTRODUCTION

During the last few years the extensive study carried out on helium atom has provided a great deal of insight in understanding the behaviour of discrete excitation functions. Helium is the most suitable candidate to test any theoretical calculation, the presence of two electrons in helium permits interelectron repulsion. Recently, a number of measurements (105, 75, 37) of angular distribution for 1^1S-2^1S and 1^1S-2^1P have become available. On the theoretical side, the workers have widely used the various perturbative scattering model to study the 2^1S and 2^1P excitations of helium in intermediate energy region. Among them, the distorted wave approximation (47, 174, 95) and its variants, the second order optical model (28), the multichannel eikonal approximation (120), the many body Green's function (102) approach, close coupling calculations (90), eikonal Born series method (65, 39) and R-matrix method (180) are worth mentioning. The work of various workers both on the theoretical and experimental side upto 1978 has been well reviewed by Bransden and McDowell(30). The theoretical calculations in general suffer from two major sources of discrepancies in evaluating the scattering amplitudes. (i) The first is due

to the basic nature of the approximation employed for studying the scattering process and (ii) The second is the use of the approximate wavefunctions as input for explicit evaluation of the scattering amplitude within the frame work of the scattering model.

Among the scattering approximation, the first Born being the simplest one, can be computed (188,94) with ease by the use of accurate bound state wavefunctions both at Hartree-Fock and beyond Hartree-Fock levels. However, the use of accurate bound state wavefunction in evaluating the scattering amplitude in any other approximation is a rather difficult task. The problem has been recognised in part by many workers(119,44,24) at different places in scattering theories. The standard procedure to involve the use of accurate wavefunction in any scattering approximation is to take in matrix element the Fourier transform of the interaction potential which is sandwiched between the wavefunctions of the initial and final states of the target. Recently, Dillon and Inokuti(106) have successfully used this idea to calculate accurate differential scattering cross-sections for 2^1S and 3^1S excitations of helium in Coulomb-projected Born approximation (151), which essentially takes into account the distortion of the projectile electron wavefunction only in final channel. In fact, the above idea is easily applicable to S-S transitions, but for S-P transitions the analysis is not so straightforward. In this chapter in addition to S-S transition, we further demonstrate the

applicability of the above idea to a study of the discrete excitation of the 2^1P state of helium from its ground state in the Coulomb-Born model (34, 71). In this model, we have, thus considered the distortion due to nucleus of target in both the channels of ingoing wave and outgoing scattered wave of the electron. As is well known(42), the inclusion of distortion only in one channel can cause serious errors in the estimation of cross-sections (77, 95). Further, we have also used a very accurate many parameter correlated wavefunctions for the initial and final bound state of the target atom (helium).

We know that at intermediate energies the differential scattering cross-sections for discrete excitations decrease very steeply with the increase of scattering angle, and hence the main contribution to the total excitation cross-section, comes from the smaller angles. The total cross-section, therefore cannot be the main criteria of judging the suitability of a model where even the first Born results give fair agreement with the experiment while it fails to display the behaviour of angular distribution. We, therefore in this chapter, report our differential scattering cross-section only for 2^1S and 2^1P transition of helium at intermediate energies in the Coulomb-Born(CB) model. The effect of exchange is taken into account in the Bonham-Ochkur(134, 179) approximation. In the following section (2.2), we shall briefly outline the Coulomb-Born approximation and obtain the closed form expressions for the scattering amplitudes.

Section 2.3 contains our results and discussion for the 2^1S and 2^1P transitions of helium.

2.2 PROCEDURE

The scattering transition amplitude for the excitation of an atom from the initial state i to the final state f in the Coulomb-Born approximation is easily derived from the two potential formula(40) for the exact scattering amplitude. It is given as

$$T_{if} = -\frac{1}{2\pi}\left[\langle \chi_f^- | U_{if} | \vec{k}_i \rangle + \langle \chi_f^- | W_{if} | \chi_i^+ \rangle\right] \qquad \ldots (2.1)$$

The total interaction potential $V(\vec{r}_1, \vec{r}_2, \vec{r}_3)$ has been divided into two parts, viz. V=U+W such that the χ_f^- and χ_i^+ are respectively outgoing and ingoing distorted projectile electron waves (117) in the field of target nucleus with $\vec{k}_i$ and $\vec{k}_f$ as associated wave-vectors. U_{if} and W_{if} are expressed as

$$U_{if}(\vec{r}_1) = \langle \phi_f(\vec{r}_2, \vec{r}_3) | U | \phi_i(\vec{r}_2, \vec{r}_3) \rangle \qquad \ldots (2.2)$$

$$W_{if}(\vec{r}_1) = \langle \phi_f(\vec{r}_2, \vec{r}_3) | W | \phi_i(\vec{r}_2, \vec{r}_3) \rangle \qquad \ldots (2.3)$$

where ϕ_i and ϕ_f are the initial and final bound state of the target atom. $\vec{r}_1$, $\vec{r}_2$ and $\vec{r}_3$ stand respectively for the spatial coordinates of the incident and atomic electrons. z is the nuclear charge of the atom. The choice of the potentials U and W are arbitrary but are usually chosen as

$$U = -\frac{z}{\vec{r}_1} \qquad \ldots (2.4a)$$

$$W = \frac{1}{|\vec{r}_1-\vec{r}_2|} + \frac{1}{|\vec{r}_1-\vec{r}_3|} \qquad \ldots (2.4b)$$

so that for the inelastic scattering (excitation) in the present case, the equation (2.1) simplifies to the form

$$T_{if} = -\frac{1}{2\pi} \langle \chi_f^- | W_{if} | \chi_i^+ \rangle \qquad \ldots (2.5)$$

with

$$W_{if} = \int \phi_f^{\otimes}(\vec{r}_2, \vec{r}_3) W \phi_i(\vec{r}_2, \vec{r}_3) d\vec{r}_2 d\vec{r}_3 \qquad \ldots (2.6)$$

and the initial and final distorted waves are given as

$$\chi_i^+(\vec{r}_1) = \exp(\frac{\pi z}{2k_i}) \Gamma(1-a)\, e^{i\vec{k}_i.\vec{r}_1}\, {}_1F_1[a, 1; i(k_i r_1 - \vec{k}_i.\vec{r}_1)] \qquad \ldots (2.7a)$$

$$\chi_f^-(\vec{r}_1) = \exp(\frac{\pi z}{2k_f}) \Gamma(1-b)\, e^{i\vec{k}_f.\vec{r}_1}\, {}_1F_1[-b, 1; -i(k_f r_1 - \vec{k}_f.\vec{r}_1)] \qquad \ldots (2.7b)$$

where

$$a = \frac{iz}{k_i},$$

$$b = \frac{iz}{k_f}$$

Now with the help of Fourier transform of the interaction potential, we can express W_{if} as

$$W_{if} = \frac{1}{2\pi^2} \int d\vec{q}\, q^{-2} \exp(-i\vec{q}.\vec{r}_1) f_{if}(\vec{q}) \qquad \ldots (2.8)$$

$f_{if}(\vec{q})$ is the transition integral, which is defined as,

$$f_{if}(\vec{q}) = \int \phi_f^{\otimes}(\vec{r}_2, \vec{r}_3) \Big(\sum_{i=2}^{3} e^{i\vec{q}.\vec{r}_i} \Big) \phi_i(\vec{r}_2, \vec{r}_3) d\vec{r}_2\, d\vec{r}_3 \qquad \ldots (2.9)$$

2.2.1 Evaluation of the transition integral

To calculate $f_{if}(\vec{q})$ in equation (2.9), we have used the properly orthonormalized many parameter correlated (MPC) wavefunctions of Weiss(22) for both initial and final states of the target. The accurate generalized oscillator strength for various discrete transitions of helium have been calculated earlier by Kim and Inokuti(188) and Bell et al(94). These are recomputed here to generate the numerical numbers at different q-values in order to obtain an algebraic expression in the q-plane for $f_{if}(q)$, the structure of which may be well suited for easy evaluation of the distorted wave transition matrix element equation (2.5). In this respect, we have followed the prescription of Crothers and McEacharn(54) and Crothers(53). This method consists of locating all the four conjugate of paires of transition integral lying on the imaginary q-axis. In this procedure, one pair of the poles is the usual one proposed by Lassettre(58), but the other six poles arise due to the indistinguishability of the bound electrons(53). Following this procedure, the transition matrix element $f_{if}(\vec{q})$ which we require, have the following form

$$f(q)_{1^1S-2^1S} = \sum_{j=1}^{4} \frac{a_j}{(q^2+\alpha_j^2)^2} + \sum_{j=5}^{7} \frac{a_j q^2}{(q^2+\alpha_j^2)^3} \qquad \ldots (2.10)$$

$$f(\vec{q})_{1^1S-2^1P} = \left[\sum_{j=1}^{2} \frac{a_j}{(q^2+\alpha_j^2)^3} + \sum_{j=3}^{4} \frac{a_j q^2}{(q^2+\alpha_j^2)^4} + \sum_{j=5}^{6} \frac{a_j q^4}{(q^2+\alpha_j^2)^5} + \sum_{j=7}^{8} \frac{a_j q^6}{(q^2+\alpha_j^2)^6} \right] \vec{q} \qquad \ldots (2.11)$$

The fitted values are accurate to less than 1% even at high values of $q \lesssim 10$ a.u. The values of adjustable constants as needed in the equations (2.10-2.11) are given in table (2.1). The transition integral are also evaluated in q-plane in the closed form using the Hartree-Fock wavefunctions. These expressions in q are then directly used to calculate the distorted wave transition matrix element. The calculation using the bound state wavefunctions at Hartree-Fock level was done to see the effect of correlated wavefunctions in this model.

2.2.2 Analysis for 1^1S-2^1S transition

Using the equation (2.10) the matrix element in equation (2.8) can be easily evaluated. With the help of following two integrals

$$\int \frac{e^{-i\vec{q}.\vec{r}}}{(q^2+\alpha_j^2)} d\vec{q} = 2\pi^2 \frac{e^{-\alpha_j r}}{r} \qquad \ldots (2.12a)$$

and

$$\int \frac{e^{-i\vec{q}.\vec{r}}}{q^2(q^2+\alpha_j^2)} d\vec{q} = \frac{2\pi^2}{r\alpha_j^2}(1-e^{-\alpha_j r}) \qquad \ldots (2.12b)$$

$W_{if}(r_1)$ becomes i.e.

$$W_{if}(r_1) = \sum_{j=1}^{4} a_j \left(\frac{1-e^{-\alpha_j r_1}}{r_1 \alpha_j^4} - \frac{e^{-\alpha_j r_1}}{2\alpha_j^3}\right) + \sum_{j=5}^{7} a_j \frac{1}{8\alpha_j^2}\left(r_1 + \frac{1}{\alpha_j}\right)e^{-\alpha_j r_1} \qquad \ldots (2.13)$$

Thus using equation (2.13), the transition amplitude equation (2.5) can be put in the following closed form(12, 149, 33).

$$T_{if} = -\frac{1}{2\pi}\exp\left[\frac{\pi z}{2}\left(\frac{1}{k_i}+\frac{1}{k_f}\right)\right]\Gamma(1-a)\,\Gamma(1-b)$$
$$\times\left\{\sum_{j=1}^{4} a_j\left(\frac{\partial}{\partial\alpha_j^2}\right)\frac{1}{\alpha_j^2}\left[J(a,b;x=0)\right.\right.$$
$$\left.\left.-J(a,b;\ x=\alpha_j)\right]+\sum_{j=5}^{7}\frac{a_j}{2}\left(\frac{\partial}{\partial\alpha_j^2}\right)^2 J(a,b;\ x=\alpha_j)\right\} \qquad \ldots (2.14)$$

where,

$$J(a,b;x) = \int d\vec{r}\,\frac{e^{-xr+i\vec{k}_i.\vec{r}-i\vec{k}_f.\vec{r}}}{r}$$
$$\times\ {}_1F_1[a,1;\ i(k_i r-\vec{k}_i.\vec{r})]\times\ {}_1F_1[b;\ 1;i(k_f r+\vec{k}_f.\vec{r})] \qquad \ldots (2.15)$$

We have included the effect of exchange in the Bonham-Ochkur(134,179) approximation and transition amplitude for exchange is given by

$$T_{if}^{ex} = -\frac{1}{2\pi k_i^2}\exp\left[\frac{\pi z}{2}\left(\frac{1}{k_i}+\frac{1}{k_f}\right)\right]\Gamma(1-a)\,\Gamma(1-b)$$
$$\times\left[\sum_{j=1}^{4} a_j\left(\frac{\partial}{\partial\alpha_j^2}\right)J(a,b;\ x=\alpha_j)\right.$$
$$\left.+\sum_{j=5}^{7}\frac{a_j\alpha_j^2}{2}\left(\frac{\partial}{\partial\alpha_j^2}\right)^2 J(a,b;\ x=\alpha_j)\right] \qquad \ldots (2.16)$$

Finally, the differential cross-section may be written as

$$\left[\frac{d\sigma}{d\Omega}\right]_{1^1S-2^1S} = \frac{k_f}{k_i}\left|T_{if}-T_{if}^{ex}\right|^2 \qquad \ldots (2.17)$$

2.2.3 Analysis for 1^1S-2^1P transition

The analysis for this transition is not so straightforward as described in Section (2.2.2), because 2^1P state has the

$m=0,\pm1$ magnetic substates, thus the system is not spherically symmetric. Using the functional form of transition integral given by equation (2.11), we can write the equation (2.8), after some simplification in the following form,

$$W_{1^1S-2^1P}(\vec{r}_1) = \frac{1}{2\pi^2} D(\alpha_j^2)(i\vec{\nabla}_{r_1}) \int \frac{e^{-i\vec{q}\cdot\vec{r}_1}}{q^2(q^2+\alpha_j^2)} \qquad \ldots(2.18)$$

where the operator

$$D(\alpha_j^2) = \sum_{j=1}^{2} \frac{a_j}{2}\left(\frac{\partial}{\partial\alpha_j^2}\right)^2 + \sum_{j=3}^{4} \frac{a_j\alpha_j^2}{6}\left(\frac{\partial}{\partial\alpha_j^2}\right)^3 + \sum_{j=5}^{6} a_j\alpha_j^2\left[\left(\frac{\partial}{\partial\alpha_j^2}\right)^3 + \frac{\alpha_j^2}{24}\left(\frac{\partial}{\partial\alpha_j^2}\right)^4\right] + \sum_{j=7}^{8} a_j\alpha_j^2\left[\frac{1}{2}\left(\frac{\partial}{\partial\alpha_j^2}\right)^3 + \frac{\alpha_j^2}{8}\left(\frac{\partial}{\partial\alpha_j^2}\right)^4 + \frac{\alpha_j^4}{120}\left(\frac{\partial}{\partial\alpha_j^2}\right)^5\right] \qquad \ldots (2.19)$$

Now carrying $\vec{\nabla}_{r_1}$ operator and using the result of equation (2.12b), we get

$$W_{1^1S-2^1P}(\vec{r}_1) = -iD(\alpha_j^2)\frac{\vec{r}_1}{r_1}f(r_1) \qquad \ldots (2.20)$$

where

$$f(r_1) = \int_0^{r_1} r'' e^{-xr''} dr'' \qquad \ldots (2.20a)$$

The initial and final motion of the electron is described by an eigenstate of the Hamiltonian

$$H = T - \frac{Z}{r_1} \qquad \ldots (2.21)$$

where T is the kinetic energy term. The following commutator

relation holds (149).

$$\frac{\vec{r}_1}{r_1} = -\frac{1}{z}[H, \vec{\nabla}] \qquad \ldots (2.22)$$

This commutator allows to express the transition amplitudes for all the three magnetic substate as components of vectors

$$\vec{T}_{if} = -\frac{1}{2\pi z} D(\alpha_j^2)\ \vec{I} \qquad \ldots (2.23)$$

With

$$\vec{I} = \langle \chi_f^- | [H, \vec{\nabla}] f(r_1) | \chi_i^+ \rangle \qquad \ldots (2.24)$$

Reflection symmetry in the plane of $\vec{k}_i$ and $\vec{k}_f$ suggest that $\vec{I}$ has only two components in that plane and they are $\vec{I}.\vec{k}_i$ and $\vec{I}.\vec{k}_f$ respectively. Thus, the transition amplitude can alternatively be represented by two components along orthogonal directions, i.e. $(T_{if})_z$, a component along the direction of incident electron and $(T_{if})_x$, along an axis in the scattering plane,

$$\vec{T}_{if} = (T_{if})_z\ \hat{k}_i + (T_{if})_x\ \hat{x} \qquad \ldots (2.25)$$

where $(T_{if})_z$ and $(T_{if})_x$ can be written(149,33) as

$$(T_{if})_z = -\frac{1}{2\pi z} D(\alpha_j^2)(\vec{I}.\hat{k}_i) \qquad \ldots (2.26)$$

$$(T_{if})_x = -\frac{1}{2\pi z} D(\alpha_j^2)(\vec{I}.\hat{k}_f - \vec{I}.\hat{k}_i \cos\chi)/\sin\chi \qquad \ldots (2.27)$$

with

$\cos\chi = \hat{k}_i.\hat{k}_j$ as well as

$$\vec{I}.\hat{k}_i = \frac{1}{2}\exp\left(\frac{\pi z}{2k_i}\right) a\Big[(1-a)\Big\{\frac{k_i^2-k_f^2}{\alpha_j^2}\Big[J(a+1,\ b;\ x=0) - J(a,b;\ x=0) - J(a+1,b;\ x=\alpha_j) + J(a,b;\ x=\alpha_j)\Big] + J(a+1,b;x=\alpha_j) - J(a,b;\ x=\alpha_j) - \frac{2ik_i}{\alpha_j} J(a+1,b;\ x=\alpha_j)\Big| \quad \ldots (2.28)$$

and

$$\vec{I}.\hat{k}_f = \frac{1}{2}\exp\left(\frac{\pi z}{2k_f}\right) b\Big[(i-b)\Big\{\frac{k_i^2-k_f^2}{\alpha_j^2}\Big[J(a,b+1;\ x=0) - J(a,b;x=0) - J(a,b+1;\ x=\alpha_j) + J(a,b;\ x=\alpha_j)\Big] - J(a,b+1;\ x=\alpha_j) + J(a,b;\ x=\alpha_j) + \frac{2ik_f}{\alpha_j} J(a,b;\ x=\alpha_j)\Big| \quad \ldots (2.29)$$

Here also we have used the Ochkur-Bonham approximation to evaluate the exchange amplitude and same is given as,

$$(T_{if}^{ex})_z = -\frac{1}{2\pi z} D'(\alpha_j^2)\vec{I}.\hat{k}_i \quad \ldots (2.30)$$

$$(T_{if}^{ex})_x = -\frac{1}{2\pi z} D'(\alpha_j^2)(\vec{I}.\hat{k}_f - \vec{I}.\hat{k}_i\cos\chi)/\sin\chi \quad \ldots (2.31)$$

where

$$D'(\alpha_j^2) = \frac{1}{k_i^2}\Big\{\sum_{j=1}^{2}\frac{a_j}{2}\Big[2\Big(\frac{\partial}{\partial\alpha_j^2}\Big) + \alpha_j^2\Big(\frac{\partial}{\partial\alpha_j^2}\Big)^2\Big] + \sum_{j=3}^{4}\frac{a_j\alpha_j^2}{6}\Big[3\Big(\frac{\partial}{\partial\alpha_j^2}\Big)^2 + \alpha_j^2\Big(\frac{\partial}{\partial\alpha_j^2}\Big)^3\Big] + \sum_{j=5}^{6}\frac{a_j\alpha_j^2}{24}\Big[24\Big(\frac{\partial}{\partial\alpha_j^2}\Big)^2 + 12\alpha_j^2\Big(\frac{\partial}{\partial\alpha_j^2}\Big)^3 + \alpha_j^4\Big(\frac{\partial}{\partial\alpha_j^2}\Big)^4\Big] + \sum_{j=7}^{8}\frac{a_j\alpha_j^2}{120}\Big[180\Big(\frac{\partial}{\partial\alpha_j^2}\Big)^2 + 120\alpha_j^2\Big(\frac{\partial}{\partial\alpha_j^2}\Big)^3$$

$$+20\alpha_j^4\left(\frac{\partial}{\partial\alpha_j^2}\right)^4+\alpha_j^6\left(\frac{\partial}{\partial\alpha_j^2}\right)^5\Bigg]\Bigg\} \qquad \ldots (2.32)$$

The differential cross-section for m=0 and m=±1 are then given by the following two expressions, respectively

$$\left(\frac{d\sigma}{d\Omega}\right)_{1^1S-2^1P}=\frac{k_f}{k_i}\left|(T_{if})_z-(T_{if}^{ex})_z\right|^2 \qquad \text{for } m=0 \quad \ldots (2.33)$$

$$\left(\frac{d\sigma}{d\Omega}\right)_{1^1S-2^1P}=\frac{k_f}{2k_i}\left|(T_{if})_x-(T_{if}^{ex})_x\right|^2 \qquad \text{for } m=\pm 1 \quad \ldots (2.34)$$

2.3 RESULTS AND DISCUSSION

We have used the equations(2.17) and (2.33-2.34) for calculating the differential cross-sections (DCS) for 1^1S-2^1S and 2^1P excitations of helium. Our calculated values are shown in figures (2.1-2.4) at 100 and 200 eV. Our results in the energy region from 50-500 eV are shown in the tables (2.2-2.4). We have also carried this calculation with commonly used simple wavefunctions to see the changes in the cross-sections. For example, 1^1S and 2^1S are described by the Hartree-Fock(HF) wavefunctions of Byron and Joachain (64,65), while the wavefunction for 2^1P is taken from Morse et al(131). The results of these wavefunctions are also displayed in figures (2.1-2.4). In addition to the present results, on curves, we have shown various other results obtained in different models.

Before, we compare our results with other theoretical

calculations, it is worthwhile to compare first the present results obtained using two different wavefunctions for both transitions. For 2^1S transition, it is seen that there is not much difference between the two sets of results in the smaller angular region $\theta \leq 30^\circ$, but as the scattering angle increases ($\theta > 30^\circ$), the difference increases. The maximum deviation noticed in the region of larger scattering is about 12% at 100 eV and 5% at 200 eV. In the case of 2^1P excitation, the two different results differ in similar fashion as for 2^1S excitation except that at large angles the deviations are 13% at 100 eV and 10% at 200 eV.

2.3.1 1^1S-2^1S excitation

In figure (2.1), we present our results for 1^1S-2^1S excitation at 100 eV along with other available theoretical calculations and experimental data. It is seen that at low scattering angles $\theta \leq 30^\circ$, the first Born results falls off very slowly and thereafter it decreases very rapidly with the increase of scattering angle ($\theta > 30^\circ$). The reason for this behaviour is well known and obviously it is due to the dropping of the electron-nucleus interaction in the Born matrix element. In the smaller angular region $\theta \leq 30^\circ$, the results of the present calculations as well as those obtained from many other theoretical methods hardly differ among themselves. At large angles $\theta \geq 30^\circ$ the results from various models, show big improvement over the first Born results and approach to experimental results. The present results higher than the Coulomb-projected Born (CPB)(151) results. The distorted-wave polarized orbital (DWPO)(172) curve shows a clear minima at $\theta \simeq 50^\circ$ and increases again with the increase

in scattering angle upto 110° and after that it shows the same pattern as others. It is noted that the measurements of Opal and Beaty (37) and Suzuki and Takayanagi(75) differ significantly from each other. The R-matrix(180) method does predict the forward peak in the results but overestimate the results as compared to all the theoretical calculations at large scattering angles. The second-order potential (SOP) calculations of Bransden and Winter(28) are in fair accord with the measurements of Opal and Bealy (37) whereas the variable-charge Coulomb-projected Born (VCCPB) results of Singh et al(42) favour the Suzuki and Takayanagi(75) measurements. It is rather surprising that the magnitudes of DCS obtained in different models differ significantly among themselves, particularly in the large angular region of scattering. The figure (2.2) shows the behaviour of DCS at 200 eV. The variation of DCS shows the same pattern as in figure (2.1), but DWPO calculations of Scott and McDowell(172) does not show any minima but the cross-section curve still remains at the bottom. The present calculations follow closely the VCCPB results at the larger scattering angles. Our method overestimates the DCS in the region $\theta \lesssim 50^{\circ}$ and underestimates by an almost similar amount at large angles of scattering when compared to R-matrix results.

2.3.2 1^1S-2^1P excitation

The results for 1^1S-2^1P excitation of helium are shown in figures (2.3-2.4) at 100 and 200 eV respectively. It is

clearly seen that results for DCS from different models are in reasonably good agreement in the forward direction upto $\theta < 20^{\circ}$ and thereafter they decrease slowly and flatten out at large angles. The present method overestimates results as compared to the R-matrix results between the angles 30° and 90° and beyond ($\theta \geq 90^{\circ}$) the R-matrix results stand higher by a factor of 3. Recently, Madison and Winters(46) carried out a distorted wave calculation including higher order terms in the distorted wave series. Their second order results hardly show any improvement over the first order distorted wave results. Therefore, we have shown in the figures (2.3-2.4) only their first order results. The measurements of Suzuki and Takayanagi(75) are in reasonably good accord with the first-order distorted wave results, while the calculations of DWPO(172) underestimate the results at large scattering angles. At 200 eV (fig.2.4) the R-matrix (180) results are in better agreement with the measurements in the entire angular regions. The present results show a better improvement with experimental measurements in comparison with first-order distorted wave results in the angular region upto $\theta \simeq 80^{\circ}$. Beyond this angular region the present calculation underestimates the results.

2.4 CONCLUSION

The comparison of present results with other theoretical calculations and experimental data shows that the above methodology is highly accessible of yielding good results for excitation process over quite a wide energy range. At

low scattering angles most of the models, including ours along with the experimental results show very good agreement among themselves. At larger angles, however, the situation is different where almost all the theoretical results differ among themselves by a certain extent. The differences in the results among the distorted wave models can be obviously said to be due to the different choices of distortion potential, as well as their implementation in the channels. As can be seen from figures (2.3-2.4), for the 2^1P excitation (which Madison and Winters (46) also reported), results which took proper account of distortions in both channels, along with the use of accurate wavefunctions, produced a nice agreement with experimental data. The present model, except for taking the distortion by the fixed Coulomb field of the target, has all the precise feature required. However, it has other advantages, if 100% accurate results are not required, such as the model is easily approachable as the expressions for differential cross-sections are in closed form and do not require any numerical solution for generation of distorted wavefunctions. In the next chapter, we shall see how we can improve this calculation by taking into account the other physical effects (such as polarization and distortion effects) on a more sound basis.

Table 2.1- The expansion parameters of transition integral $f_{if}(q)$ for $1^1S - 2^1S$, 2^1P transitions.

j	$1^1S - 2^1S$		$1^1S - 2^1P$	
	a_j	α_j	a_j	α_j
1.	375.1315000	4.000000	-24249.400	1.841743
2.	-22.2950800	1.884728	156936.400	2.497592
3.	-105.6113000	2.540315	-21435.990	1.941743
4	355.0043000	3.344414	-14975.100	2.497592
5	-0.5141655	1.883720	-10745.440	1.841742
6	-146.7487000	2.540315	67675.780	2.497592
7	-416.7105000	3.344414	-4058.769	1.841743
8	-	-	-13288.230	2.497592

Table 2.2- Differential cross-sections $\frac{d\sigma}{d\Omega}(a_o^2 sr^{-1})$ for the 1^1S- 2^1S excitation of helium by electron impact.

Energy (eV)	Scattering Angles (deg) / Model	2	6	10	20	50	80	100	120	140
50	FB	1.26(-1)	1.21(-1)	1.13(-1)	8.01(-2)	1.28(-2)	1.68(-3)	5.44(-4)	2.25(-4)	1.20(-4)
	CB	5.23(-2)	5.06(-2)	4.75(-2)	3.70(-2)	1.90(-2)	1.20(-2)	8.74(-3)	6.64(-3)	5.42(-3)
	CBE	7.71(-2)	7.29(-2)	6.54(-2)	4.09(-2)	9.14(-3)	3.90(-3)	2.16(-3)	1.57(-3)	1.51(-3)
100	FB	1.71(-1)	1.56(-1)	1.31(-1)	6.11(-2)	2.07(-3)	1.05(-4)	2.40(-5)	8.08(-6)	3.83(-6)
	CB	9.85(-2)	9.04(-2)	7.70(-2)	4.17(-2)	8.62(-3)	2.80(-3)	1.52(-3)	9.52(-4)	6.84(-4)
	CBE	1.08(-1)	9.70(-2)	7.79(-2)	3.48(-2)	5.33(-3)	1.40(-3)	6.22(-3)	3.19(-4)	1.95(-4)
200	FB	1.92(-1)	1.58(-1)	1.09(-1)	2.59(-2)	1.59(-4)	4.22(-6)	8.06(-7)	2.44(-7)	1.08(-7)
	CB	1.41(-1)	1.17(-1)	8.26(-2)	2.50(-2)	2.00(-3)	4.30(-4)	2.09(-4)	1.24(-4)	8.72(-5)
	CBE	1.43(-1)	1.16(-1)	7.89(-2)	2.03(-2)	1.47(-3)	2.72(-4)	1.20(-4)	6.50(-5)	4.27(-5)
300	FB	1.97(-1)	1.47(-1)	8.50(-2)	1.15(-2)	2.77(-5)	5.77(-7)	1.02(-7)	2.92(-8)	1.25(-8)
	CB	1.59(-1)	1.19(-1)	7.12(-2)	1.38(-2)	6.96(-4)	1.32(-4)	6.32(-5)	3.74(-5)	2.63(-5)
	CBE	1.60(-1)	1.18(-1)	6.74(-2)	1.14(-2)	5.47(-4)	9.35(-5)	4.21(-5)	2.38(-5)	1.63(-5)
500	FB	1.98(-1)	1.21(-1)	5.11(-2)	2.99(-3)	2.61(-6)	4.27(-8)	6.85(-9)	1.84(-9)	7.56(-10)
	CB	1.73(-1)	1.07(-1)	4.73(-2)	4.90(-3)	1.63(-4)	2.89(-5)	1.38(-5)	8.23(-6)	5.82(-6)
	CBE	1.73(-1)	1.05(-1)	4.46(-2)	4.19(-3)	1.37(-4)	2.29(-5)	1.07(-5)	6.23(-6)	4.37(-6)

FB - first Born
CB - Coulomb-Born
CBE - Coulomb-Born with exchange
(-1) means 10^{-1}

Table 2.3 Differential cross-sections $\frac{d\sigma}{d\Omega}$ ($a_o^2 Sr^{-1}$) for the $1^1S - 2^1P(m=o)$ excitation of heliumoby electron impact.

Energy (eV)	Scattering angles (deg) → / Model ↓	2	6	10	20	50	80	100	120	140
50	FB	1.68	1.31	8.48(-1)	2.14(-1)	5.92(-3)	4.06(-4)	1.05(-4)	3.77(-5)	1.87(-5)
	CB	2.92(-1)	2.95(-1)	2.92(-1)	2.25(-1)	4.82(-2)	1.17(-2)	6.28(-3)	2.54(-3)	2.23(-3)
	CBE	3.04(-1)	2.98(-1)	2.78(-1)	1.87(-1)	3.85(-2)	8.92(-3)	3.35(-3)	6.11(-4)	7.14(-4)
100	FB	4.88	1.77	5.24(-1)	4.06(-2)	2.52(-4)	1.50(-5)	1.48(-6)	4.15(-7)	1.66(-7)
	CB	1.70	1.07	5.70(-1)	1.32(-1)	8.01(-3)	1.32(-3)	5.77(-4)	3.70(-4)	3.03(-4)
	CBE	1.71	1.05	5.42(-1)	1.20(-1)	7.13(-3)	1.04(-3)	3.95(-4)	2.26(-4)	1.70(-4)
200	FB	7.32	6.52(-1)	9.78(-2)	3.78(-3)	6.11(-6)	1.03(-7)	1.75(-8)	4.84(-9)	1.72(-9)
	CB	4.56	8.31(-1)	2.15(-1)	2.41(-2)	8.79(-4)	1.37(-4)	7.24(-4)	5.33(-5)	4.67(-5)
	CBF	4.55	8.15(-1)	2.08(-1)	2.30(-2)	8.06(-4)	1.67(-4)	5.90(-5)	4.20(-5)	3.60(-5)
300	FB	6.18	2.40(-1)	2.80(-2)	7.63(-4)	5.69(-7)	8.60(-9)	1.33(-9)	1.09(9)	8.79(-10)
	CB	5.02	3.98(-1)	7.89(-2)	7.19(-3)	2.24(-4)	3.71(-5)	2.18(-5)	1.74(-5)	1.62(-5)
	CBE	5.01	3.92(-1)	7.67(-2)	6.96(-3)	2.10(-4)	3.30(-5)	1.90(-5)	1.49(-5)	1.39(-5)
500	FB	3.02	5.39(-2)	5.00(-3)	7.74(-5)	2.43(-8)	7.11(-10)	6.73(-11)	2.84(-11)	-8.20(-12)
	CB	3.17	1.10(-1)	1.77(-2)	1.37(-3)	3.78(-5)	7.31(-6)	4.96(-6)	4.15(-6)	4.01(-6)
	CBE	3.16	1.08(-1)	1.73(-2)	1.34(-3)	3.60(-5)	6.81(-6)	4.56(-6)	3.79(-6)	3.66(-6)

Table 2.4 Differential cross-sections $\frac{d\sigma}{d\Omega}(a_o^2 sr^{-1})$ for the $1^1S-2^1P(m=\pm1)$ excitation of helium by electron impact.

Energy (eV)	Scattering angles (deg) → / Model ↓	2	6	10	20	50	80	100	120	140
50	FB	1.03(-2)	6.82(-2)	1.15(-1)	8.75(-2)	3.81(-3)	1.51(-4)	2.31(-5)	4.45(-6)	9.34(-7)
	CB	4.99(-3)	3.90(-2)	8.28(-2)	1.11(-1)	1.18(-2)	6.24(-4)	4.06(-4)	1.19(-4)	5.14(-5)
	CBE	5.20(-3)	3.99(-2)	8.11(-2)	9.10(-2)	5.05(-3)	2.14(-4)	2.69(-4)	2.55(-4)	3.82(-5)
100	FB	1.85(-1)	5.55(-1)	3.93(-1)	6.80(-2)	3.15(-4)	4.16(-6)	4.16(-7)	6.08(-8)	1.68(-8)
	CB	1.04(-1)	4.15(-1)	3.76(-1)	9.25(-2)	6.36(-4)	1.43(-5)	3.84(-5)	2.96(-5)	1.76(-5)
	CBE	1.04	4.09(-1)	3.57(-1)	7.50(-2)	2.72(-4)	3.10(-5)	4.28(-5)	2.78(-5)	1.56(-5)
200	FB	1.31	8.94(-1)	2.78(-1)	1.59(-2)	1.04(-5)	6.42(-8)	5.31(-9)	5.75(-10)	1.91(-10)
	CB	9.71(-1)	8.64(-1)	3.04(-1)	2.06(-2)	2.02(-5)	1.68(-5)	1.20(-5)	6.88(-6)	3.12(-6)
	CBE	9.69(-1)	8.46(-1)	2.87(-1)	1.69(-2)	1.80(-5)	1.72(-5)	1.11(-5)	6.10(-6)	2.73(-6)
300	FB	2.62	7.14(-1)	1.53(-1)	4.68(-3)	1.08(-6)	4.85(-9)	7.01(-10)	1.72(-11)	3.41(-10)
	CB	2.20	7.32(-1)	1.69(-1)	6.14(-3)	1.20(-5)	7.91(-6)	4.94(-6)	2.48(-6)	1.04(-6)
	CBE	2.19	7.17(-1)	1.60(-1)	5.11(-3)	1.31(-5)	7.62(-6)	4.58(-6)	2.24(-6)	9.32(-7)
500	FB	3.61	3.92(-1)	5.47(-2)	6.69(-4)	5.16(-8)	4.09(-10)	2.50(-11)	3.22(-11)	–
	CB	3.42	4.09(-1)	6.00(-2)	1.03(-3)	5.34(-6)	2.45(-6)	1.33(-6)	6.73(-7)	2.67(-7)
	CBE	3.41	4.01(-1)	5.66(-2)	8.81(-4)	5.46(-6)	2.35(-6)	1.26(-6)	6.30(-7)	2.47(-7)

2.5 FIGURE CAPTIONS

Figure 2.1 The differential scattering cross-section for the 1^1S-2^1S excitation of helium atom by electron impact at 100 eV.
Calculation: — : present results with MPC wavefunctions; O: present results with HF wavefunctions; - - - - : present results in first Born; —·—·— : results in VCCPB(42); —··— : results in CPB(151); —·x·—:results in DWPO(172); —x— : results in R-matrix(180); —xx— : results in SOP(28); ● :Experimental data of Suzuki and Takayanagi(75); ▲: Experimental data of Opal and Beaty(37).

Figure 2.2 Same as figure (2.1) but at 200 eV.

Figure 2.3 The differential scattering cross-section for the 1^1S-2^1P excitation of helium atom by electron impact at 100 eV. Same as figure 2.1, except —·—: results of Madison and Winter(46)

Figure 2.4 Same as figure 2.3 but at 200 eV.

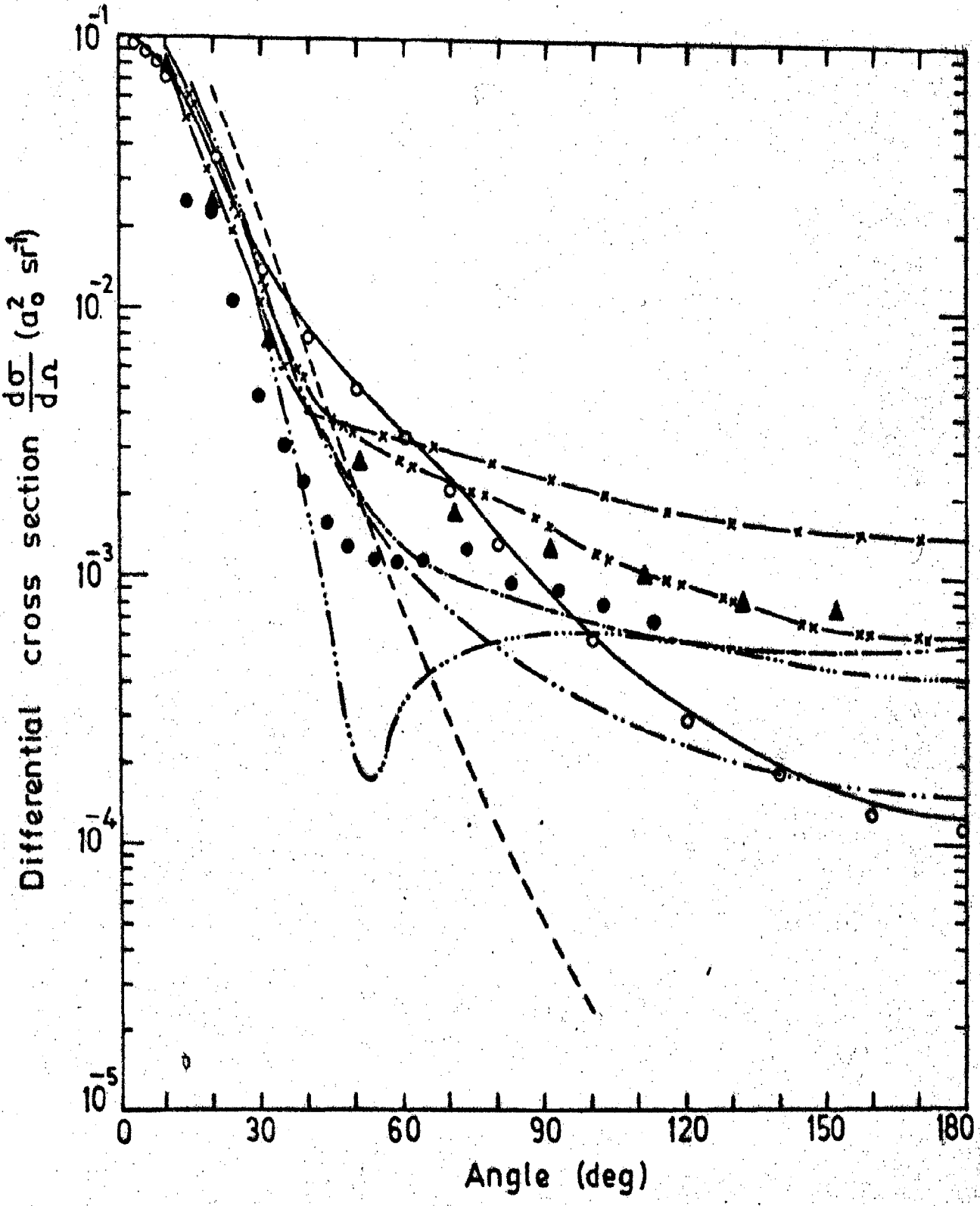
Differential cross section $\frac{d\sigma}{d\Omega}$ (a_0^2 sr^{-1})
10^{-1}
10^{-2}
10^{-3}
10^{-4}
10^{-5}
0
30
60
90
120
150
180
Angle (deg)

FIG. 2.1

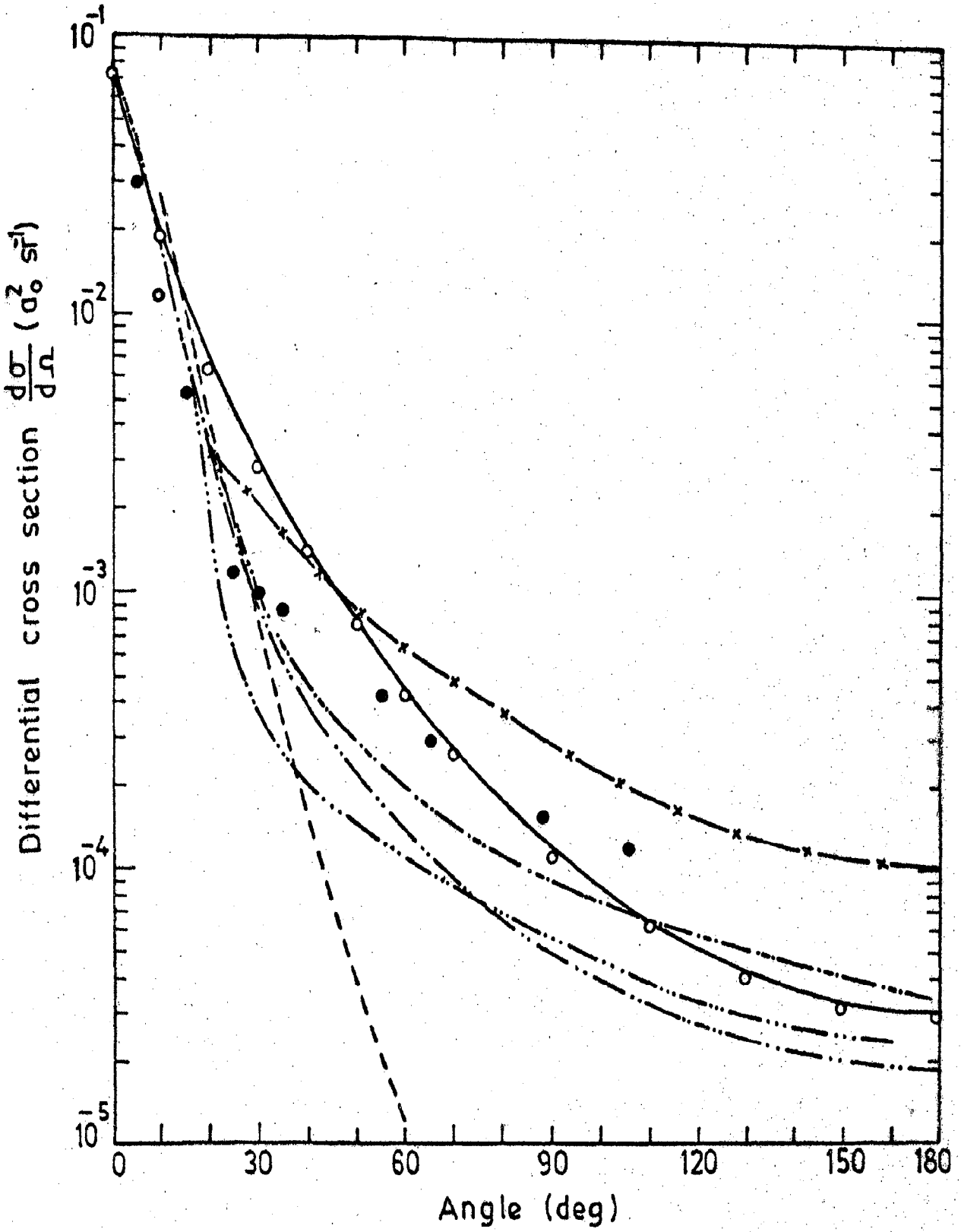
Differential cross section $\frac{d\sigma}{d\Omega}$ (a_0^2 sr^{-1})
10^{-1}
10^{-2}
10^{-3}
10^{-4}
10^{-5}
0
30
60
90
120
150
180
Angle (deg)

FIG. 2.2

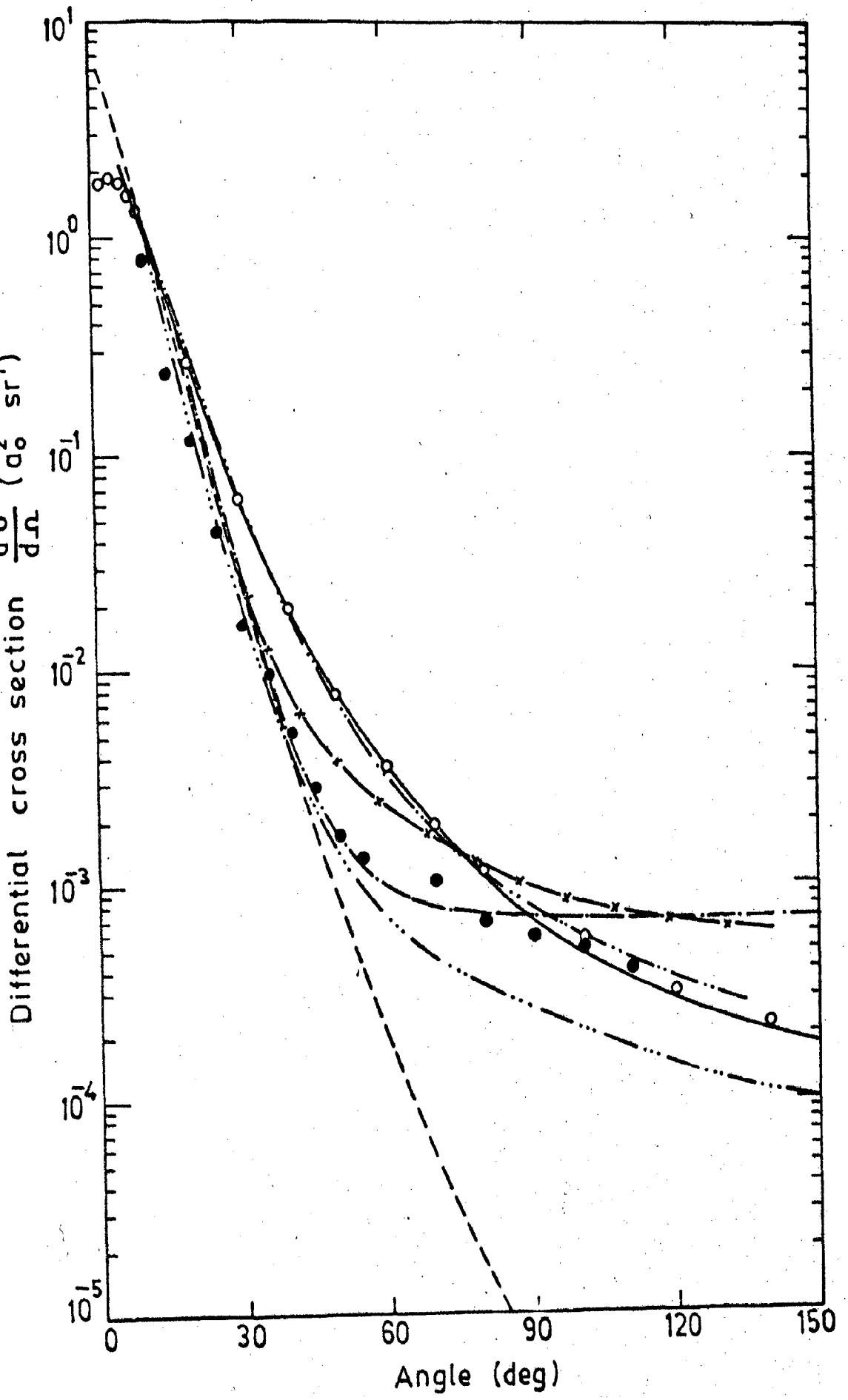
Differential cross section $\frac{d\sigma}{d\Omega}$ (a_0^2 sr^{-1})
10^1
10^0
10^{-1}
10^{-2}
10^{-3}
10^{-4}
10^{-5}
0
30
60
90
120
150
Angle (deg)

FIG. 2.3

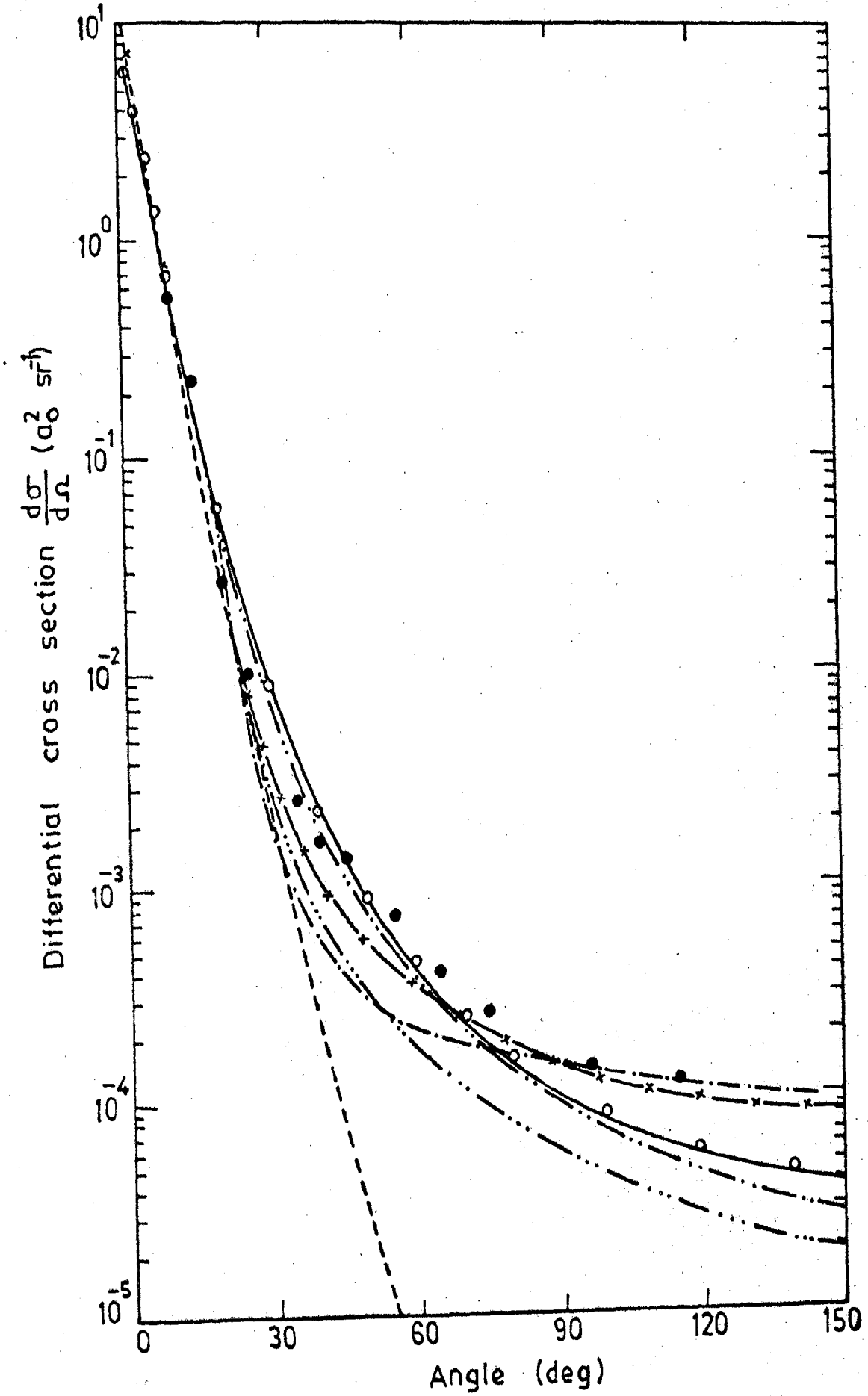
Differential cross section $\frac{d\sigma}{d\Omega}$ (a_0^2 sr^{-1})
10^{1}
10^{0}
10^{-1}
10^{-2}
10^{-3}
10^{-4}
10^{-5}
0
30
60
90
120
150
Angle (deg)

FIG. 2.4

work are given in Chapter 2. We, therefore, describe in Section 3.2, the theoretical procedure for 1^1S-2^1S, 2^1P transitions of helium and the results and discussion are presented in Section 3.3.

3.2 PROCEDURE

The transition matrix element for the electron impact excitation of helium atom from its initial state i to the final state f is expressed as (in atomic unit)

$$T_{if} = \langle \Psi_f^- | V | \Psi_i^+ \rangle \qquad \ldots (3.1)$$

where $V(\vec{r}_1, \vec{r}_2, \vec{r}_3) = -\frac{2}{\vec{r}_3} + \frac{1}{|\vec{r}_1 - \vec{r}_3|} + \frac{1}{|\vec{r}_2 - \vec{r}_3|}$ is the incident electron-helium interaction potential, $\vec{r}_1$ and $\vec{r}_2$ refer to the position vector of the atomic electrons relative to the center of mass to be fixed as the nucleus of helium. $\vec{r}_3$ is the position vector of incident electron. Ψ_i^+ is the total scattering wavefunction which we approximate in the present distorted wave model as

$$\Psi_i^+ = \left[\phi_i(\vec{r}_1, \vec{r}_2) + \phi_{pol}(\vec{r}_1, \vec{r}_2, \vec{r}_3)\right] F_1^+(k_i, \vec{r}_3) \pm \phi_i(\vec{r}_2, \vec{r}_3) F_i^+(k_i, \vec{r}_1) \qquad \ldots (3.2)$$

and similarly, the total wavefunction Ψ_f^- in the final channel is represented by

$$\Psi_f^- = \left[\phi_f(\vec{r}_1, \vec{r}_2) + \phi_{pol}(\vec{r}_1, \vec{r}_2, \vec{r}_3)\right] F_f^-(k_f, \vec{r}_3) \qquad \ldots (3.3)$$

where $F^+(k_i, \vec{r})$ and $F^-(k_f, \vec{r})$ are the ingoing and outgoing distorted waves with $\vec{k}_i$ and $\vec{k}_f$ as incident and scattered wave vectors, reppectively. ϕ_i and ϕ_f are the initial and

final unperturbed wavefunction of helium atom. ϕ_{pol} represent the polarization term of the target. In equation (3.2), we have neglected the exchange polarization term as the polarization contribution will be small at distances where exchange is importance. Further, representing the ground state wavefunction (100) to be expressible as separable Hartree-Fock wavefunction of the form (see Scott and McDowell(174, 118)).

$$\phi_i(\vec{r}_1, \vec{r}_2) = \phi_{1s}(\vec{r}_1)\, \phi_{1s}(\vec{r}_2) \qquad \ldots (3.4)$$

where $\phi_{1s}(\vec{r}) = R_{1s}(\vec{r})Y_{oo}(\hat{r})$. We can write then (20,10).

$$\phi_{pol}(\vec{r}_1, \vec{r}_2, \vec{r}_3) = \left[\phi_{pol}(\vec{r}_2, \vec{r}_3)\phi_{1s}(\vec{r}_1) + \phi_{pol}(\vec{r}_1, \vec{r}_3)\phi_{1s}(\vec{r}_2)\right] \qquad \ldots (3.5)$$

For $\phi_{pol}(\vec{r}, \vec{r}')$, we take in the dipole approximation the following expression (20, 10)

$$\phi_{pol} \simeq -\varepsilon(r, r')\phi_{1s}(\vec{r})\, \frac{1}{r'^2}\left(\frac{r^2}{2} + r\right)P_1(\hat{r}.\hat{r}') \qquad \ldots (3.6)$$

with step function

$$\begin{aligned} \varepsilon(r, r') &= 1 \qquad r' > r \\ &= 0 \qquad r' < r \end{aligned} \qquad \ldots (3.7)$$

Expanding $F^{\pm}(k, \vec{r})$ in spherical harmonics one gets

$$F^{\pm}(k, \vec{r}) = \frac{1}{\sqrt{k}} \sum_{\ell=0}^{\infty} (2\ell+1)(\pm i)^{\ell} \exp\left[\pm i\delta_{\ell}(k^2)\right] \times \frac{u_i^{\pm}(k, \vec{r})}{r} P_{\ell}(\cos\hat{k}.\hat{r}) \qquad \ldots (3.8)$$

δ_{ℓ} is the phase shift of the ℓ^{th} partial wave.

In order to obtain $u_{\ell}^{\pm}(k, \vec{r})$ we need to solve the following

two Schrödinger equations

$$H_i\psi_i^+ = E_i\psi_i^+$$

and

$$H_f\psi_f^- = E_f\psi_f^- \qquad \ldots (3.9)$$

Here H_i and H_f are the Hamiltonian corresponding to the initial and final channel of the system, respectively, E_i and E_f are the corresponding eigen energies. On substitution of ψ_i^+ and ψ_f^- in equation (3.9), we find that $u_\ell(k,\vec{r})$ satisfies the following radial equation

$$\left[\frac{d^2}{dr^2}+k^2-\frac{\ell(\ell+1)}{r^2}-2V_{st}(r)-2V_{pol}(r)\right] u_\ell(k,\vec{r}) = X_\ell(r) \qquad \ldots (3.10)$$

With

$$X_\ell(r) = (\varepsilon_{ls}-k^2)rR_{ls}(r)\delta_{\ell,o}\int_o^\infty r'R_{ls}(r')u_\ell(k,r')dr' - \frac{2}{(2\ell+1)}\, rR_{ls}(r)\int_o^\infty r'R_{ls}(r')u_\ell(k,r')\frac{r_<^\ell}{r_>^{\ell+1}}dr$$

for ingoing wave

and

$$X_\ell(r)=0, \text{ for outgoing wave}$$

subject to the following usual boundary conditions

$$u_\ell(k,r) \underset{r\to o}{=} 0$$

$$u_\ell(k,r) \underset{r\to\infty}{=} \frac{1}{\sqrt{k}}\sin\left(kr-\frac{\ell\pi}{2}+\delta_\ell\right) \qquad \ldots (3.11)$$

In Eq.(3.10) the static potential V_{st} and polarization potential V_{pol} are given by

$$V_{st}(r) = -\frac{2}{r} + \left\langle \phi_{1s}(\vec{r}') \left| \frac{2}{|\vec{r}-\vec{r}'|} \right| \phi_{1s}(\vec{r}') \right\rangle \qquad \ldots (3.12a)$$

and

$$V_{pol}(r) = \left\langle \phi_{1s}(\vec{r}') \left| \frac{2}{|\vec{r}-\vec{r}'|} \right| \phi_{pol}(\vec{r},\vec{r}') \right\rangle \qquad \ldots (3.12b)$$

Equation (3.10) reveals that we have taken the distortion effects in both the channels by the ground state (100) of helium. This choice is in justification with the fact that one can expect the passage time of the projectile to be much smaller than that required for the atom to make its transition to an excited state so that the projectile is always in the field of the ground state.

Further, the polarization terms appearing in the equations (3.2) and (3.3) for ψ_i^+ and ψ_f^- will be omitted in further evaluation of T_{if}, (Eq.(3.1)). We take therefore account of the polarization distortion of the target only in obtaining the scattering function $F^{\pm}(k,\vec{r})$, but neglect its further effect on the T-matrix element. There is no obvious justification of this additional approximation, but neglecting this term is consistent (30, 172, 113) with our neglect of exchange polarization term in equation (3.2).

3.2.1 Calculation for $1^1S - 2^1S$ transition

Using eqs. (3.2) and (3.3), we can write eq.(3.1) for 1^1S-2^1S excitation as,

$$T_{if} = T_{if}^{d} - T_{if}^{ex} \qquad \ldots (3.13)$$

where T_{if}^{d} is direct excitation term and T_{if}^{ex} is the exchange

term and the same will be given by

$$T_{if}^{d} = \langle F^{-}(k_f, \vec{r}_3)\phi_f(\vec{r}_1, \vec{r}_2) |V| \phi_i(\vec{r}_1, \vec{r}_2)F^{+}(k_i, \vec{r}_3)\rangle \ldots (3.14)$$

and

$$T_{if}^{ex} = \langle F^{-}(k_f, \vec{r}_3)\phi_f(\vec{r}_1, \vec{r}_2) |V| \phi_i(\vec{r}_2, \vec{r}_3)F^{+}(k_i, \vec{r}_1)\rangle \ldots (3.15)$$

First, we evaluate the T_{if}^{d} and write it alternatively as

$$T_{if}^{d} = \langle F^{-}(k_f, \vec{r}_3) |V_{if}(\vec{r}_3)| F^{+}(k_i, \vec{r}_3)\rangle \quad \ldots (3.16)$$

where,

$$V_{if}(\vec{r}_3) = \langle \phi_f(\vec{r}_1, \vec{r}_2) | V(\vec{r}_1, \vec{r}_2, \vec{r}_3) | \phi_i(\vec{r}_1, \vec{r}_2)\rangle \quad \ldots (3.17)$$

After taking Fourier transform of $V(\vec{r}_1, \vec{r}_2, \vec{r}_3)$ (the interaction potential), the above equation (3.17) reduces to

$$V_{if}(\vec{r}_3) = \frac{1}{2\pi^2} \int d\vec{q}\ \vec{q}^{-2} \exp(-i\vec{q}.\vec{r}_3)\ f_{if}(\vec{q}) \quad \ldots (3.18)$$

Alternatively $V_{if}(\vec{r})$ can also be obtained by first calculating the transition density $\rho_{if}(r)$ and then fitting it into some suitable polynomial of r so that the further use of integral form of Poisson's equation give a closed form expression for $V_{if}(\vec{r})$.

In equation (3.18), the $f_{if}(q)$ is the transition form factor given by

$$f_{if}(\vec{q}) = \langle \phi_f(\vec{r}_1, \vec{r}_2) | \sum_{j=1}^{2} \exp(i\vec{q}.\vec{r}_j) | \phi_i(\vec{r}_1, \vec{r}_2)\rangle \quad \ldots (3.19)$$

It is obtained by choosing, for both ϕ_i and ϕ_f the properly orthogonalized many parameter correlated (MPC) wavefunctions due to Weiss. The resulting expression for $f_{if}(q)$ is then

brought to an analytic form in q plane as discussed in the Chapter 2 (see Section 2.2.1) and the same is given by

$$f_{if}(q) = \sum_{j=1}^{4} \frac{a_j}{(q^2+\alpha_j^2)^2} + \sum_{j=5}^{7} \frac{a_j q^2}{(q^2+\alpha_j^2)^3} \qquad \ldots (3.20)$$

With the form as given in equation (3.20) and using equations (2.12a) and (2.12b) of the previous chapter, $V_{1^1S-2^1S}(r_1)$ becomes

$$V_{1^1S-2^1S}(r) = \sum_{j=1}^{4} a_j \left(\frac{1-e^{-\alpha_j r}}{r\,\alpha_j^4} - \frac{e^{-\alpha_j r}}{2\alpha_j^3}\right)$$

$$+ \sum_{j=5}^{7} a_j \frac{1}{8\alpha_j^2}\left(r + \frac{1}{\alpha_j}\right)e^{-\alpha_j r} \qquad \ldots (3.21)$$

With the help of equations (3.8) and (3.21), T_{if}^{d} can be written in the following form

$$T_{if}^{d} = \sum_{\ell=0}^{\infty} B_{\ell}^{d} P_{\ell}(\cos\hat{k}_i.\hat{k}_f) \qquad \ldots (3.22)$$

where,

$$B_{\ell}^{d} = \frac{4\pi(2\ell+1)}{\sqrt{k_i k_f}} \exp\left[i\delta_{\ell}(k_i^2)+i\delta_{\ell}(k_f^2)\right] I_A \qquad \ldots (3.23)$$

and

$$I_A = \int_0^{\infty} u_{\ell}^{+}(k_i, \vec{r}) u_{\ell}^{-}(k_f, \vec{r}) V_{if}(\vec{r}) d\vec{r} \qquad \ldots (3.24)$$

In the similar manner, using Bonham-Ochkur(134, 179, 47) approximation, Equation (3.15) for T_{if}^{ex} can be written as

$$T_{if}^{ex} = \langle F^{-}(k_f, \vec{r}_3) | V_{if}^{ex}(\vec{r}_3) | F^{+}(k_i, \vec{r}_3) \rangle \qquad \ldots (3.25)$$

$$V_{if}^{ex}(r_3) = \frac{1}{2\pi^2}\int d\vec{q}\; q^{-2}\; e^{-i\vec{q}.\vec{r}_3}\; f'_{if}(q) \qquad \ldots (3.26a)$$

where

$$f'_{if}(q) = \frac{q^2}{k_i^2} f_{if}(q)$$

$$= \frac{1}{k_i^2}\left[\sum_{j=1}^{4} \frac{a_j q^2}{(q^2+\alpha_j^2)^2} + \sum_{j=5}^{7} \frac{a_j q^4}{(q^2+\alpha_j^2)^3}\right]$$

$$= \frac{1}{k_i^2}\left[\sum_{j=1}^{4} \frac{a_j q^2}{(q^2+\alpha_j^2)^2} + \sum_{j=5}^{7} \frac{a_j q^2}{(q^2+\alpha_j^2)^2} - \sum_{j=5}^{7} \frac{a_j \alpha_j^2 q^2}{(q^2+\alpha_j^2)^3}\right] \qquad \ldots (3.26b)$$

Thus, using eq.(3.26b), eq.(3.26a) can be put in the form,

$$V_{if}^{ex}(r_3) = \frac{1}{k_i^2}\left[\sum_{j=1}^{7} a_j \frac{e^{-\alpha_j r}}{2\alpha_j} - \sum_{j=5}^{7} a_j \frac{1}{8}\left(r + \frac{1}{\alpha_j}\right)e^{-\alpha_j r}\right] \qquad \ldots (3.26c)$$

The values of a_j's and α_j's are given in table 2.1 of Chapter-2. Using eqs.(3.8) and (3.26c) the exchange matrix element of eq.(3.25), on simplication, becomes

$$T_{if}^{ex} = \sum_{\ell=0}^{\infty} B_\ell^{ex}\, P_l(\cos\hat{k}_i.\hat{k}_f) \qquad \ldots (3.27)$$

With

$$B_\ell^{ex} = \frac{4\pi(2\ell+1)}{\sqrt{k_i k_f}} \exp\left[i\delta_\ell(k_i^2)+i\delta_\ell(k_f^2)\right] I_B \qquad \ldots (3.28)$$

and

$$I_B = \int_0^{\infty} u_\ell^{+}(k_i, r)\; u_\ell^{-}(k_f, r) V_{if}^{ex}(r)dr \qquad \ldots (3.29)$$

Now combining equations (3.22) and (3.27), we get the final expression for T_{if} (equation 3.13),

$$T_{if} = B_\ell P_\ell(\cos\hat{k}_i.\hat{k}_f) \qquad \ldots (3.30)$$

where,

$$B_\ell = \frac{4\pi(2\ell+1)}{\sqrt{k_i k_f}} \exp\left[i\delta_\ell(k_i^2)+i\delta_\ell(k_f^2)\right] (I_A-I_B) \quad \ldots (3.31)$$

The differential cross-section $\frac{d\sigma}{d\Omega}$ and total cross-section σ can be expressed as

$$\frac{d\sigma}{d\Omega} = \frac{1}{4\pi^2}\frac{k_f}{k_i}\sum_{\ell=0}^{\infty}\sum_{\lambda=0}^{\infty} B_\ell B_\lambda \cos\left[\delta_\ell(k_i^2)+\delta_\ell(k_f^2) - \delta_\lambda(k_i^2)-\delta_\lambda(k_f^2)\right] P_\ell(\cos\hat{k}_i.\hat{k}_f)P_\lambda(\cos\hat{k}_i.\hat{k}_f) \quad \ldots (3.32)$$

and

$$\sigma = \frac{1}{\pi^2}\frac{k_f}{k_i}\frac{|B_\ell|^2}{(2\ell+1)}(\pi a_o^2) \quad \ldots (3.33)$$

3.2.2 Calculation for 1^1S-2^1P transition

To evaluate the transition matrix for 1^1S-2^1P transition of helium, we start with the equations (3.13), (3.15) and (3.16). Consider first the equation (3.16) for direct excitation. In In this equation V_{if} is given by

$$V_{if}(r) = \langle \phi_f(\vec{r}_1,\vec{r}_2) |V| \phi_i(\vec{r}_1,\vec{r}_2)\rangle \quad \ldots (3.34)$$

Following the procedure as outlined and discussed in the preceding Chapter 2 (Section 2.2.1, equation (2.11) and Section 2.2.3, equation (2.18)), the above expression for $V_{1^1S-2^1P}(\vec{r})$ can be put in the form,

$$V_{1^1S-2^1P}(\vec{r}) = -iD(\alpha_j^2)\frac{\vec{r}}{r^3}f(r) \quad \ldots (3.35)$$

Here $D(\alpha_j^2)$ is the operator as defined by equation (2.19). With the use of above equation, transition-matrix (3.16) for

1^1S–2^1P can be represented in three components as

$$T^d_{if} = T^d_x\hat{i} + T^d_y\hat{j} + T^d_z\hat{k} \qquad \ldots (3.36)$$

one can easily show that $T^d_{if}(m=o) = (T^d_{if})_z$ and

$$T^d_{if}(m=\pm 1) = \frac{1}{\sqrt{2}}\left[T^d_x \pm iT^d_y\right]$$

(A) Evaluation of $T^d_{if}(m=o)$

We can write,

$$z = r\cos\theta = r\sqrt{\frac{4\pi}{3}}Y_{10}(\hat{r})$$

Thus

$$(T^d_{if})_z = -iD(\alpha_j^2)\left\langle F_f^-(k_f,\vec{r})\left|\frac{z}{r^3}f(r)\right|F_i^+(k_i,\vec{r})\right\rangle$$
$$= -iD(\alpha_j^2)\left(\frac{4\pi}{3}\right)^{1/2}\left\langle F_f^-(k_f,\vec{r})\left|\frac{Y_{10}(r)}{r^2}f(r)\right|F_i^+(k_i,\vec{r})\right\rangle$$

Using equation (3.8), $(T^d_{if})_z$ can be finally expressed as

$$(T^d_{if})_z = \left(\frac{4\pi}{3k_ik_f}\right)^{1/2} i \sum_{\ell=o}^{\infty}\sum_{\ell'=o}^{\infty}(2\ell+1)(2\ell'+1)(i)^{\ell}(-i)^{\ell'}$$
$$\exp\left[i\delta_\ell(k_i^2)+i\delta_{\ell'}(k_f^2)\right]$$
$$\times\left[-D(\alpha_j^2)\right]\int_o^{\infty}u^+_\ell(k_i,r)\frac{f(r)}{r^2}u^-_{\ell'}(k_f,r)$$
$$\times\int P_\ell(\cos\hat{k}_i\cdot\hat{r})Y_{10}(\hat{r})\,P_{\ell'}(\cos\hat{k}_f\cdot\hat{r})d\vec{r}$$
$$\ldots (3.37)$$

The angular integration over the spherical part can be done using the addition theorem (108) and thus the above expression takes the form

$$(T^d_{if})_z = i\frac{(4\pi)^2}{\sqrt{k_i k_f}}\sum_{\ell=0}^{\infty}\sum_{\ell.=0}^{\infty}(2\ell+1)^{1/2}(2\ell+1)^{1/2}(i)^{\ell}(-i)^{\ell'}$$
$$\exp[i\delta_{\ell}(k_i^2)+i\delta_{\ell'}(k_f^2)]\; Y^{*}_{\ell',m'}(\hat{k}_f)Y_{\ell m}(\hat{k}_i)$$
$$\begin{pmatrix}\ell & 1 & \ell'\\ 0 & 0 & 0\end{pmatrix}\begin{pmatrix}\ell & 1 & \ell'\\ m & 0 & m'\end{pmatrix}\left[-D(\alpha_j^2)\right]\int_0^{\infty} u^{+}_{\ell}(k_i,r)\frac{f(r)}{r^2}u^{-}_{\ell'}(k_f,r)dr \qquad \ldots (3.38)$$

Using the angular momentum algebra (108), we can further write the above expression for transition matrix in which only one sum is left,

$$(T^d_{if})_z = T^d_{if}(m=o)$$
$$= \sum_{\ell=0}^{\infty} B^d_{\ell}(m=o)P_{\ell}(\cos\hat{k}_i.\hat{k}_f) \qquad \ldots (3.39)$$

where

$$B^d_{\ell}(m=o) = \frac{4\pi i}{\sqrt{k_i k_f}}\left[(\ell+1)e^{i\xi_{\ell,\ell+1}}K(\ell,\ell+1)-\ell\, e^{i\xi_{\ell,\ell-1}}K(\ell,\ell-1)\right] \qquad \ldots (3.40)$$

where,

$$K(\ell',\ell'') = -D(\alpha_j^2)\int_0^{\infty} u^{+}_{\ell'}(k_i,r)\frac{f(r)}{r^2}u^{-}_{\ell''}(k_f,r)dr$$

and $\xi_{\ell',\ell''} = \delta_{\ell'}(k_i^2)+\delta_{\ell''}(k_f^2)$

(B) Evaluation of T^d_{if} $(m=\pm 1)$

As we know that

$$(x+iy) = \mp\sqrt{\frac{8\pi}{3}}\,\varepsilon^{\pm i\phi}\,Y_{1,\pm 1}(\hat{r})$$

Hence

$$T^{d}_{if}(m=\pm1) = \frac{1}{\sqrt{2}}(T_x \pm iT_y)$$

$$= \frac{1}{\sqrt{2}}\left\langle F_f^-(k_f,\vec{r}) \left| \frac{x\pm iy}{r^3} \right| F_i^+(k_i,\vec{r}) \right\rangle$$

$$= \left[-iD(\alpha_j^2)\right]\sqrt{\frac{4\pi}{3}} \left\langle F_f^-(k_f,\vec{r}) \left| \frac{Y_{1,\pm1}\, e^{\pm i\phi}}{r^3} f(r) \right| F_i^+(k_i,\vec{r}) \right\rangle \qquad \ldots (3.41)$$

Using the same procedure as we have used for m=0, the matrix element $T^{d}_{if}(m=\pm1)$ can be expressed as

$$T^{d}_{if}(m=1) = \sum_{\ell=0}^{\infty} B^{d}_{\ell}(m=1) P_{\ell}(\cos \hat{k}_i.\hat{k}_f)\, e^{i\phi} \qquad \ldots (3.42)$$

in which

$$B^{d}_{\ell}(m=\pm1) = \frac{4\pi i}{\sqrt{2k_i k_f}} \left[e^{i\xi_{\ell,\ell+1}} K(\ell,\ell+1) + e^{i\xi_{\ell,\ell-1}} K(\ell,\ell-1) \right] \qquad \ldots (3.43)$$

C. Evaluation of T^{ex}_{if}

One can include the effect of exchange in the Bonham-Ochkur(134,179,49) approximation. Equation (3.15) for exchange amplitude is given as

$$T^{ex}_{if} = \left\langle F_f^-(k_f,\vec{r}) \left| V^{ex}_{if}(\vec{r}) \right| F_i^+(k_i,\vec{r}) \right\rangle \qquad \ldots (3.44)$$

in which, $V^{ex}_{if}(\vec{r})$ is expressed by the expression

$$V^{ex}_{if}(\vec{r}) = \frac{1}{2\pi^2} \int d\vec{q}\; q^{-2}\, e^{-i\vec{q}.\vec{r}}\, f'_{if}(\vec{q}) \qquad \ldots (3.45)$$

where,

$$f'_{if}(\vec{q}) = \frac{q^2}{k_i^2} f_{if}(\vec{q})$$

This expression for $V_{if}^{ex}(\vec{r})$ can be simplified in the same manner as explained earlier (Section (2.2.3), equation (2.18)). Thus, it can be brought to the form

$$V_{if}^{ex}(\vec{r}) = -iD'(\alpha_j^2)\,\frac{\vec{r}}{r^3} f(r) \qquad \ldots (3.46)$$

where $D'(\alpha_j^2)$ is an operator given in equation (2.32), and $f(r)$ is defined by the equation (2.20a). To evaluate the T_{if}^{ex} (m=o) and $T_{if}^{ex}(m=\pm 1)$, we follow the same procedure as we have used for T_{if}^{d}, thus,

$$T_{if}^{ex}(m=o) = \sum_{\ell=o}^{\infty} B_{\ell}^{ex}(m=o) P_{\ell}(\cos \hat{k}_i . \hat{k}_f) \qquad \ldots (3.47)$$

where,

$$B_{\ell}^{ex}(m=o) = \frac{4\pi i}{\sqrt{k_i k_f}} \left[(\ell+1) e^{i\xi_{\ell,\ell+1}} K'(\ell,\ell+1) - \ell\, e^{i\xi_{\ell,\ell-1}} K'(\ell,\ell-1)\right] \qquad \ldots (3.48)$$

and

$$T_{if}^{ex}(m=1) = \sum_{\ell=o}^{\infty} B_{\ell}^{ex}(m=\pm 1) P_{\ell}(\cos \hat{k}_i . \hat{k}_f) \qquad \ldots (3.49)$$

in which

$$B_{\ell}^{ex}(m=1) = \frac{-4\pi i}{\sqrt{2k_i k_f}} \left[e^{i\xi_{\ell,\ell+1}} K'(\ell,\ell+1) + e^{i\xi_{\ell,\ell-1}} K'(\ell,\ell-1)\right] \qquad \ldots (3.50)$$

with

$$\xi_{\ell',\ell''} = \delta_{\ell'}(k_i^2) + \delta_{\ell''}(k_f^2)$$

$$K'(\ell',\ell'') = \left[-D'(\alpha_j^2)\right] \int_o^{\infty} u_{\ell'}^{+}(k_i, \vec{r})\, \frac{f(r)}{r^2}\, u_{\ell''}^{-}(k_f, \vec{r})\, dr$$

Hence, finally

$$T_{if}(m=o) = \sum_{\ell=o}^{\infty} B_{\ell}(m=0) P_{\ell}(\cos \hat{k}_i . \hat{k}_f) \qquad \ldots (3.51)$$

where,

$$B_\ell(m=o) = \frac{4\pi i}{\sqrt{k_i\, k_f}} \Big[(\ell+1)e^{i\xi}\ell,\ell+1(K(\ell,\ell+1)-K'(\ell,\ell+1)) - \ell\ e^{i\xi}\ell,\ell-1\ (K(\ell,\ell-1)-K'(\ell,\ell-1))\Big] \quad \ldots (3.52)$$

and

$$T_{if}(m=1) = \sum_{\ell=o}^{\infty} B_\ell(m=1)P_\ell(\cos\hat{k}_i.\hat{k}_f)$$

where

$$B_\ell(m=1) = \frac{4\pi i}{\sqrt{2k_i k_f}}\Big[e^{i\xi}\ell,\ell+1\ (K(\ell,\ell+1)-K'(\ell,\ell-1)) + e^{i\xi}\ell,\ell-1\ (K(\ell,\ell-1)-K'(\ell,\ell-1))\Big] \quad \ldots (3.54)$$

The differential cross-section $\frac{d\sigma}{d\Omega}$ can be expressed as

$$\frac{d\sigma}{d\Omega} = \frac{1}{4\pi^2}\frac{k_f}{k_i}\Big[|T_{if}(m=o)|^2 + 2|T_{if}(m=1)|^2\Big] \quad .. (3.55)$$

The radial equation (3.10) for $u^{\pm}_\ell(k,r)$ was solved by a noniterative procedure (143) the normalization and the phase shifts were obtained by comparison with the JWKB solution(2). The numerical integration for I_A, $K(\ell',\ell'')$ and I_B, $K'(\ell',\ell'')$ was done accurately using Simpson's rule.

3.3 RESULTS AND DISCUSSIONS

We have calculated total and differential cross-sections for excitation of 2^1S and 2^1P in the energy range from threshold to 200 eV using many parameter correlated (MPC) as well as Hartree-Fock(HF) wavefunctions. Present results for total cross-sections are displayed along with others in figures 3.1 and 3.4 for 2^1S and 2^1P respectively. For a detailed comparison, the total 1^1S-2^1S and 1^1S-2^1P cross-sections for incident

electron energies 26.5-200 eV along with the results in other approximations are given in tables 3.1 and 3.2. Differential cross-sections at 100 and 200 eV are shown in figures 3.2, 3.3 for 1^1S-2^1S and 3.5 and 3.6 for 1^1S-2^1P respectively, where other results are available for comparison and also the present model is expected to give reliable results.

3.3.1 1^1S-2^1S excitation

(A) Total cross-section

In figure 3.1, our total cross-section results are shown for 1^1S-2^1S and compared with those of other theories [distorted wave models(172,91,42,28), R-matrix(180), close coupling(87) as well as first Born approximation] and with a recent experiment(60). Among different distorted wave models (172,91,42,28) the distorted waves are taken in initial and final channels in various ways. It is therefore, desirable to see how they differ from each other before their results are compared. Scott and McDowell(172,118) incorporated the distortion only in initial channel due to static interaction, the target polarization and exchange effects. Singh, Srivastava and Rai(42) took distortion due to static interaction only in the final channel. Winters(91, 28) implemented the distortions in both the channels in which the initial channel included distortions due to static interaction, polarization of target, absorption and exchange effects while the final channel included only distortion due

to the static interaction. The present model is similar to Winters and Bransden (28) and Winters(91), except that it included in addition to polarization in the final channel along with static interaction but exclude the absorption effects in the initial channel. Further, the present model as well as that of Scott and McDowell and Singh, Srivastava and Rai evaluated in addition to direct matrix element equation (3.15) for the calculation of cross-sections while that of Winters(91) and Bransden and Winters(28) only evaluated the direct matrix element equation (3.14). The present results with MPC wavefunctions are higher (within 5%) than that with HF wavefunction below 200 eV and at high energies almost coincide. At energies above 150 eV, all results are in agreement except the results of Scott and McDowell(172) which become in agreement with these at somewhat higher energies. Below 70 eV down to 300 eV, the experimental data lie in between present curve and that of Scott and McDowell(172) while the remaining curves diverge away from these estimates. The maximum value of the present cross-section is less than that of Scott and McDowell(172) value and also slightly displaced towards the lower energy side.

(B) Differential cross-section

The differential cross-sections(DCS) for this transition are displayed in figure (3.2) at 100 eV. We compare our results with distorted wave results, Scott and McDowell(172) results, R-matrix(180), FBA and experimental data(75). It is

seen that the present DCS obtained using HF wavefunctions follow very closely the results using MPC-wavefunctions. The results of Scott and McDowell(172) show a big dip in the DCS curve nearly at 50 eV which is not shown by any other model. Agreement of our curve with the experiment in contrast to that of Scott and McDowell(172) curve reflects the importance of inclusion of distortion effects in both the channels. We also observe that below 30°, all models give nearly same results. At higher angles, however, R-matrix and distorted wave method of Bransden and Winters overestimate the DCS as compared to ours and experiment. The difference in the results of Bransden and Winters(28) and the present reveal the importance of the polarization contribution. Further, it is also seen from the figure (see the results of Singh et al(42)) that the distortion included only by static potential in the outgoing final channels, also reproduces good results at this energy.

The figure 3.3, presents the comparison of different theoretical and experimental DCS results at 200 eV. Except the distorted wave results of Bransden and Winters which is not available, the rest theoretical calculations displayed in this figure (3.3) are same as in figure (3.1). It is again seen that the present results are in very good agreement with the experiment in the entire range of scattering angles. Scott and McDowell(172) results are greatly diverging from the experiment while results of Singh et al(42)

are in between the two. The R-matrix method is again seen to overestimate the results.

3.3.2 1^1S-2^1P excitation

(A) Total cross-section

The figure (3.4) shows our total cross-section for 1^1S-2^1P excitation at impact energies ranging from 20-200 eV. We have compared our results with the results of many other theories such as R-matrix(180), five state close-coupling(87), DWPO(172), first Born and with experiment of Suzuki and Tokyo-Tokyanagi(75). It is seen that the results of present calculations using the MPC wavefunction are always lower (within 4%.), than that with HF wavefunctions at all impact energies. The results obtained using R-matrix method are higher than the experimental values but are considerably lower than those of five static close coupling calculations. The DWPO results lie in between the present results and R-matrix results. Further the present calculations show a remarkably good agreement with the experimental measurement of Suzuki and Tayanagi(75). The above results therefore, suggest that for electron impact excitation of 1^1S-2^1P, the present version(as given in Section 3.3.1) of distorted wave model is quite successful.

(B) Differential cross-section

The 1^1S-2^1P transition is an optically allowed transition. This transition has been studied in quite detail both

experimentally and theoretically. In recent years various groups have measured the 1^1S-2^1P differential scattering cross-section (DCS). The experimental data obtained by Trajmar(87), Hall et al(87), Truhlar et al(87), Chutijian and Srivastava(87) are in the lower energy region i.e. <80eV, whereas the data of Suzuki and Takayanagi(75), Opal Beaty(37), Chamberlin et al(87) and Dillon and Lassettree are available in low as well as high energy regions.

The figures (3.5) and (3.6) display our calculated results of the DCS at 100 and 200 eV respectively. On each figures we have shown our earlier calculations in Coulomb-Born model (see Chapter 2) and first Born results. The results of Madison and Winter in second order distorted wave, the R-matrix calculations of Fon et al(180), DWPO results of Scatt and McDowell(172) along with the experimental measurements of Suzuki and Takayanagi(75) are shown in each curve. The experimental data of Opal and Beaty(37) is not shown here and Suzuki and Tayanagi(75) are in good accord with each other. Therefore, we have only shown the data of Suzuki and Tayakanagi on our curves. At 100 eV it is seen that the DCS as a function of electron scattering angle θ is sharply peaked in the forward direction, i.e. $\theta < 30^\circ$. With the increase in scattering angle particularly $30 \leq \theta \leq 60^\circ$, the DCS decreases slowly and thereafter i.e. $\theta > 60^\circ$, the DCS flattens out. The first Born approximation (FBA) results give an exceedingly small result for $\theta > 30^\circ$ as expected. In

the small angular region i.e. $\theta < 30^{\circ}$ the results in all the theoretical models as well as the present one are same. Beyond $\theta > 30^{\circ}$, the differences between the results of calculations obtained in different model become noticeable. The calculations of Winters, Scott and McDowell in DWPO approach show a rapid fall in the cross-section and thus underestimates the DCS at large angles. The R-matrix calculations remain higher in comparison with all the other theoretical calculations as well as experimental data in the intermediate and large scattering angles ($\theta > 30^{\circ}$). The present calculations agree well with the Madison and Winters results and experimental measurements upto $\theta \simeq 110^{\circ}$. Beyond $\theta > 110^{\circ}$, the calculations of Madison and Winters and R-matrix results overestimate the cross-section compared with the present calculations. The present results, remain higher, but still close to the experimental measurements.

At 200 eV, the general trend of variation of the DCS are very much similar as seen at 100 eV. The quantitative disagreement between the results of the different models and the present one (as seen at 100 eV) gradually narrow down with the increase of impact energy. This feature is clearly seen in figure (3.6). The present distorted wave results show a reasonably good agreement with the results of R-matrix and, the second order distorted wave results of Madison and Winters at all angles except at intermediate angles $30^{\circ} \lesssim \theta \lesssim 60^{\circ}$. On the other hand the present results are in excellent agreement with the experimental measurements (75)

in the entire angular region. The present (total and differential cross-section) results for the excitations at 100 and 200 eV are compiled in Tables (3.1-3.3).

3.4 CONCLUSION

From the foregoing analysis of the results we conclude that the distorted wave model is a promising and useful approximation to reproduce the differential and total cross-section results. Although in order to avoid the complexities, we have made a few approximations in the calculation procedure (as already mentioned in this chapter) which seems reasonable in view of final results. Further, we also conclude that the target correlation does not play a significant role on the final results as very small differences are observed in the two sets of results obtained using HF and MPC wave-functions. The comparison of different distorted wave models among themselves as well as with the present approach suggest that the inclusion of target polarization in both the channels and exchange contribution provide significant improvement in the results.

Table 3.1 Total cross-sections σ (πa_o^2) for $1^1S - 2^1S$ excitation of helium by electron impact.

Energy (eV)	Present result with MPC wave-functions	Present result with HF wave-functions	R-matrix (Ref.87)	Close coupling (Ref.87)	VCCPB (Ref.42)	DWPO (Ref.172)	Exp. (Ref.60)
26.5	0.0142	–	0.0591	–	–	0.0296	–
30.0	0.0242	0.0236	–	–	0.0466	0.0281	0.0248
40.0	0.0231	0.0221	–	0.0656	0.0390	0.0209	0.0222
50.0	0.0221	–	–	–	0.0333	0.0178	–
70.0	0.0200	0.1198	–	–	0.0272	0.0148	–
100.0	0.0178	0.0172	0.0236	0.0302	0.0212	0.0124	0.0146
150.0	0.0139	0.0127	0.0160	–	0.0148	0.0103	–
200.0	0.0106	0.0101	0.0125	–	0.0106	0.0090	–

Table 3.2 Total cross-sections $\sigma(\pi a_o^2)$ for $1^1S - 2^1P$ excitation of helium by electron impact.

ENERGY (eV)	Present result with MPC wave-functions	Present result with HF wave-functions	R-matrix (Ref.180)	Close-coupling (Ref.87)	DWPO (Ref.172)	Exp. (Ref.60)
26.5	-	-	0.0594	-	-	-
30.0	0.0710	-	-	-	-	-
40.0	0.0903	0.0971	-	0.169	0.0774	0.0751
50.0	0.1231	0.1381	-	-	0.1030	-
70.0	0.1241	0.1384	-	-	-	-
100.0	0.1261	0.1299	0.1490	0.1630	0.1220	0.1148
150.0	0.1065	0.1091	0.1260	-	0.1080	0.1044
200.0	0.0851	0.0872	0.1090	-	0.0947	0.0944

Table 3.3- Differential cross-sections $\frac{d\sigma}{d\Omega}(a_o^2 Sr^{-1})$ for 1^1S-2^1S, 2^1P excitations of helium by electron impact.

Scattering angles (deg)	ENERGY (eV)			
	1^1S-2^1S		1^1S-$2^2P_{\pm}$	
	100	200	100	200
5	1.42(-1)	1.52(-1)	3.41	3.05
10	7.43(-2)	9.02(-2)	1.09	9.31(-1)
20	3.62(-2)	2.07(-2)	1.18(-1)	3.25(-2)
30	1.20(-2)	2.35(-3)	1.48(-2)	6.41(-3)
50	8.32(-4)	6.72(-4)	1.35(-3)	9.35(-4)
70	9.48(-4)	3.54(-4)	9.00(-4)	3.05(-4)
80	8.32(-4)	2.68(-4)	8.01(-4)	1.72(-4)
100	7.18(-4)	1.57(-4)	5.81(-4)	1.15(-4)
120	6.00(-4)	1.18(-4)	4.43(-4)	1.05(-4)
150	4.61(-4)	9.51(-5)	3.27(-4)	9.41(-5)
160	4.41(-4)	9.41(-5)	3.05(-4)	9.07(-5)

3.5 FIGURE CAPTIONS

Figur 3.1 Total excitation cross-sections for 1^1S-2^1S transition of the helium atom by electron impact. Calculations: ——, present results with MPC functions; ▲, present results with HP functions; - x -, results in R-matrix (180); —·—; variable charge Coulomb-projected Born results (VCCPB)(42); - - - - -, present results in first Born; O, results in close-coupling(87); — ···—results in DWPO (172); ....; second order potential results (28); ●, experimental data of deHeer and Jansen(60).

Figure 3.2 Differential cross-sections for 1^1S-2^1S excitation of helium by electron impact at 100 eV. Calculations: ——, present results with MPC functions; ▲, present results with HF functions; -x-, results in R-matrix (180); —·—, variable charge Coulomb projected Born results (VCCPB(42); —··—, results in DWPO(172); -xx- , results in SOP(28); ●, Experimental data of Suzuki and Takayangi (75).

Figure 3.3 Same as figure 3.2 but at 200 eV.

Figure 3.4 Total excitation cross-section for 1^1S-2^1P transition of the helium atom by electron impact. Calculations: —— , present results with MPC functions, ▲, present results with HF functions; -x-, R-matrix results (180); -·-, close coupling results (87) - - - -, first Born results; —··—, results in DWPO(171); ●, experimental data (60).

Figure 3.5 Differential cross-sections for 1^1S-2^1P excitation of the helium atom by electron impact at 100 eV.

Calculations: ——, present results with MPC wavefunctions; ....., CB results of Mukesh et al(113);

-x-, R-matrix results (180); -•-, variable charge Coulomb-projected Born (VCCPB)(42); -•••-, results in DWPO(172), - - - -, first Born results; ●, Experimental data (75).

Figure 3.6 Same as figure 3.5 but at 200 eV.

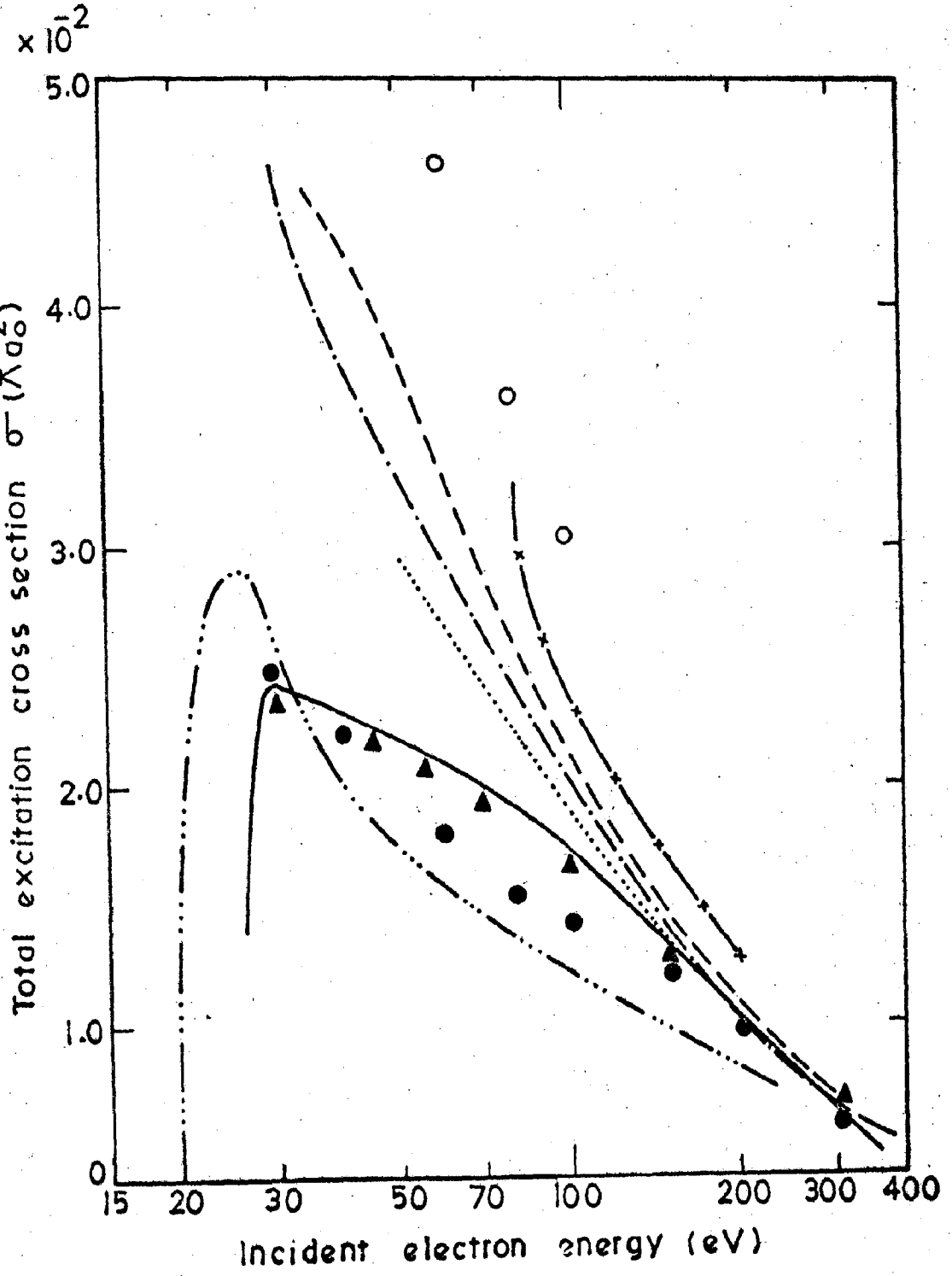
x 10^-2
5.0
4.0
3.0
2.0
1.0
0
Total excitation cross section σ (πa0^2)
15
20
30
50
70
100
200
300
400
Incident electron energy (eV)

Figure 3.1

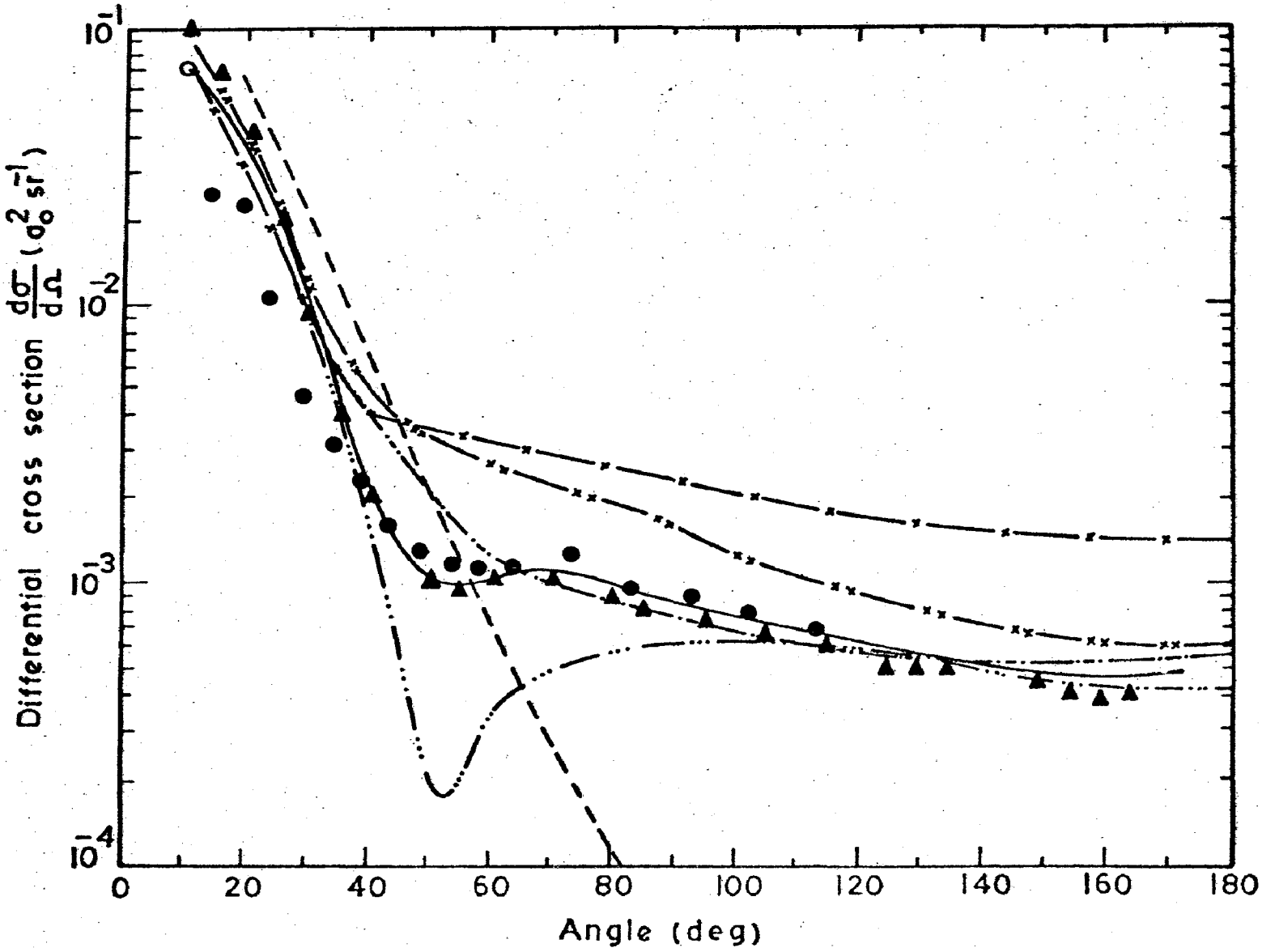
Differential cross section $\frac{d\sigma}{d\Omega}$ (a_0^2 sr^{-1})
10^{-1}
10^{-2}
10^{-3}
10^{-4}
0
20
40
60
80
100
120
140
160
180
Angle (deg)

Figure 3.2

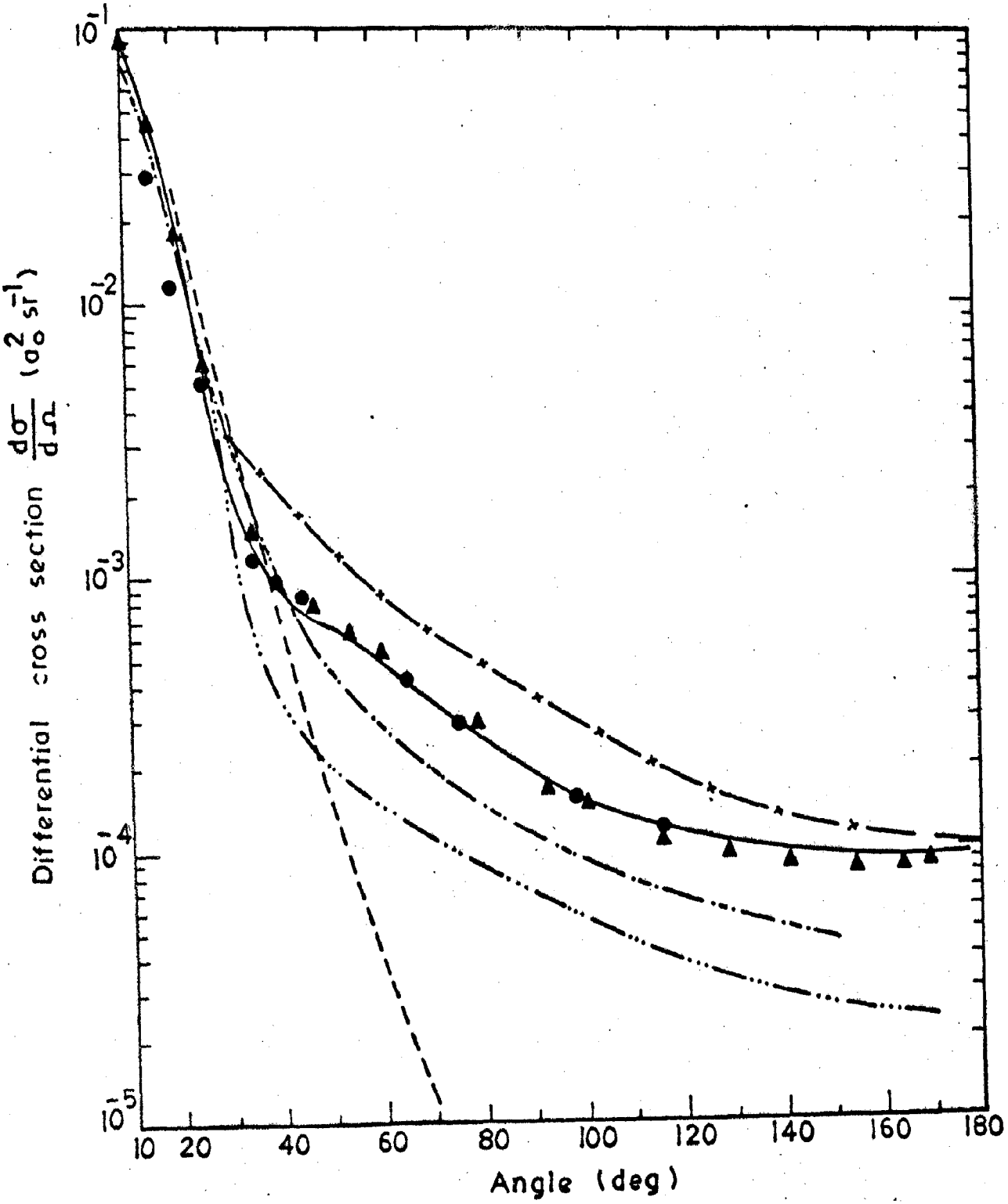
Differential cross section $\frac{d\sigma}{d\Omega}$ (a_0^2 sr^{-1})
10^{-1}
10^{-2}
10^{-3}
10^{-4}
10^{-5}
10
20
40
60
80
100
120
140
160
180
Angle (deg)

Figure 3.3

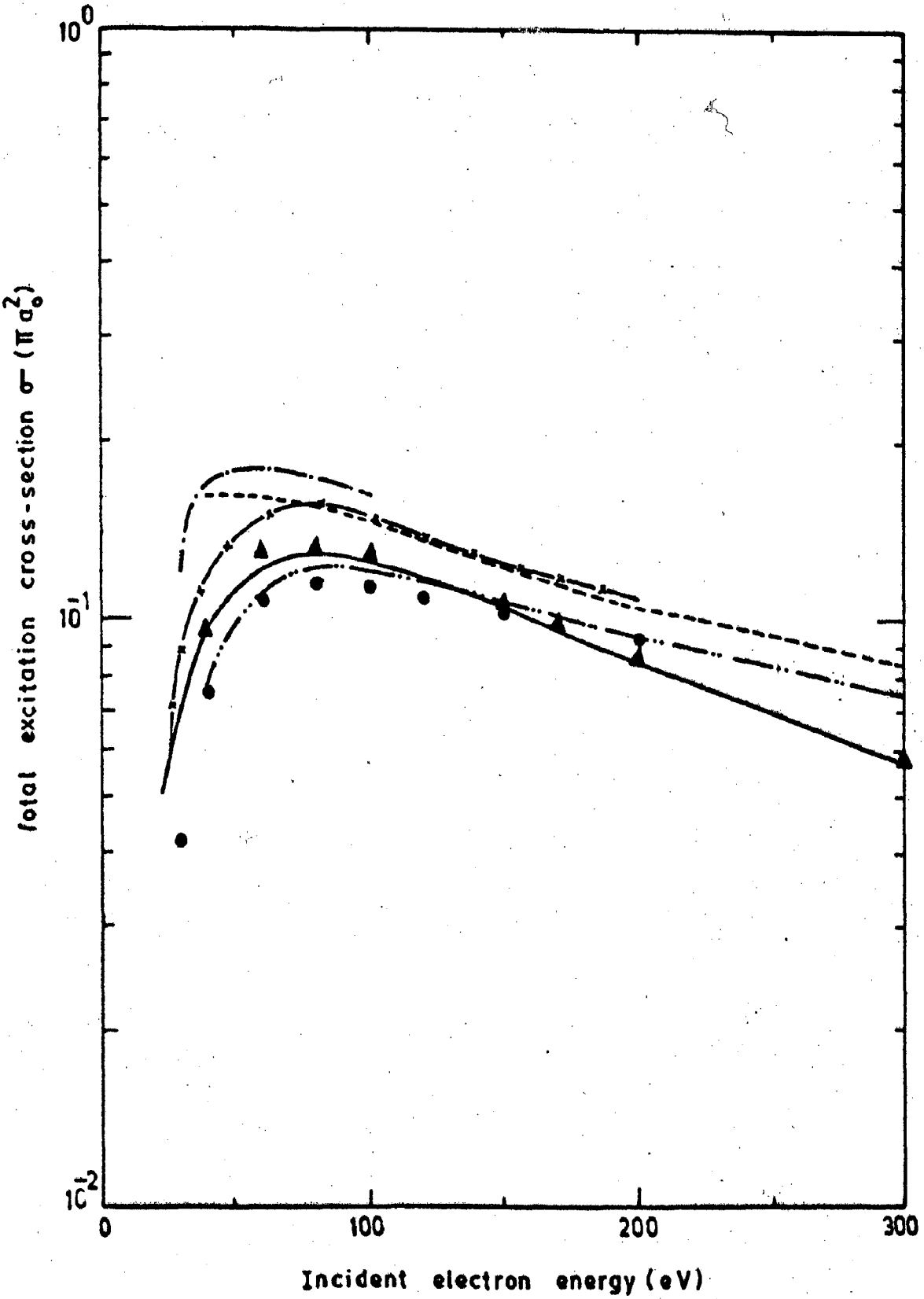
10^0
10^{-1}
10^{-2}
fotal excitation cross-section σ (πa_0^2)
0
100
200
300
Incident electron energy (eV)

FIG. 3.4

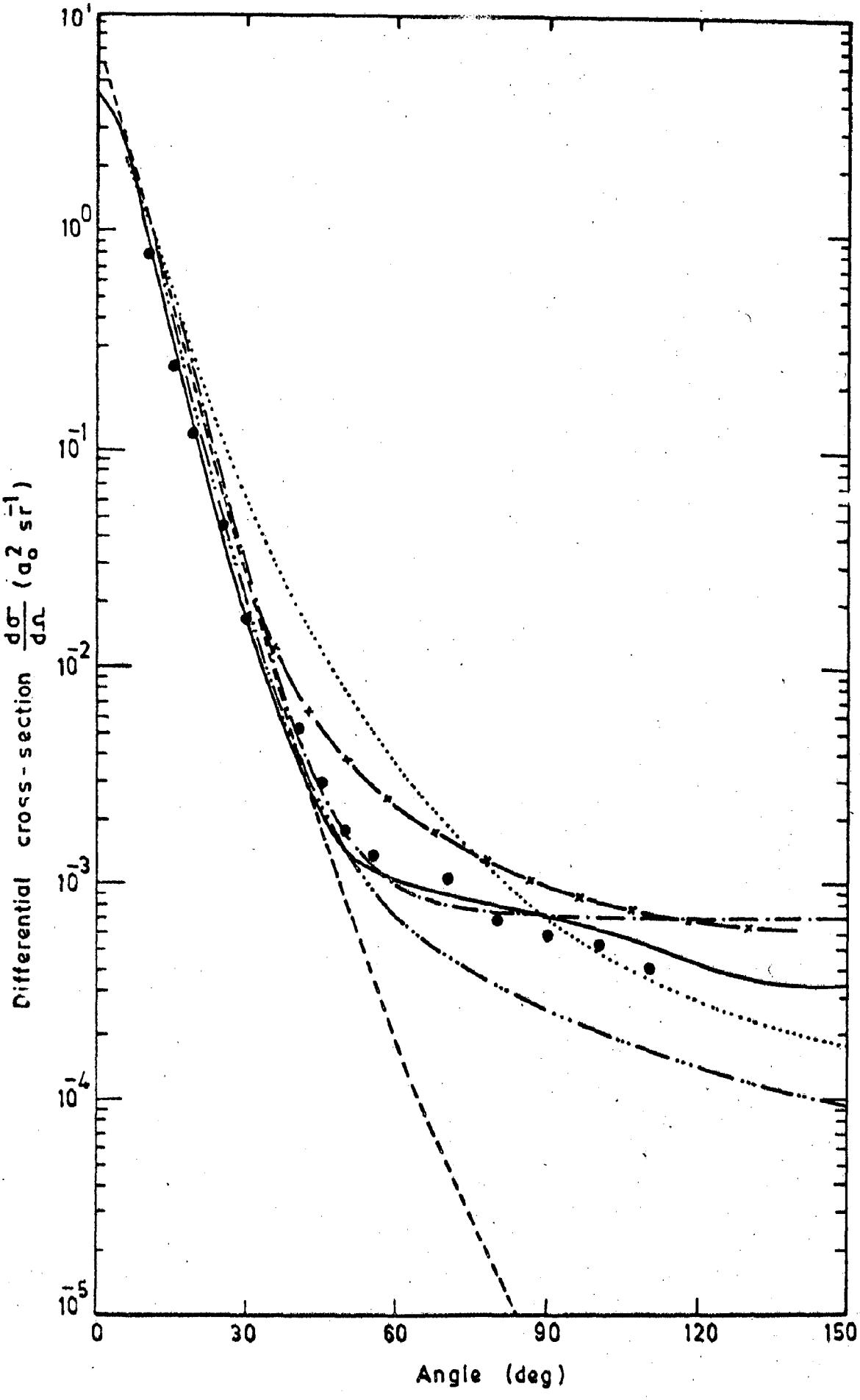
Differential cross-section $\frac{d\sigma}{d\Omega}$ (a_0^2 sr^{-1})
10^{1}
10^{0}
10^{-1}
10^{-2}
10^{-3}
10^{-4}
10^{-5}
0
30
60
90
120
150
Angle (deg)

FIG. 3.5

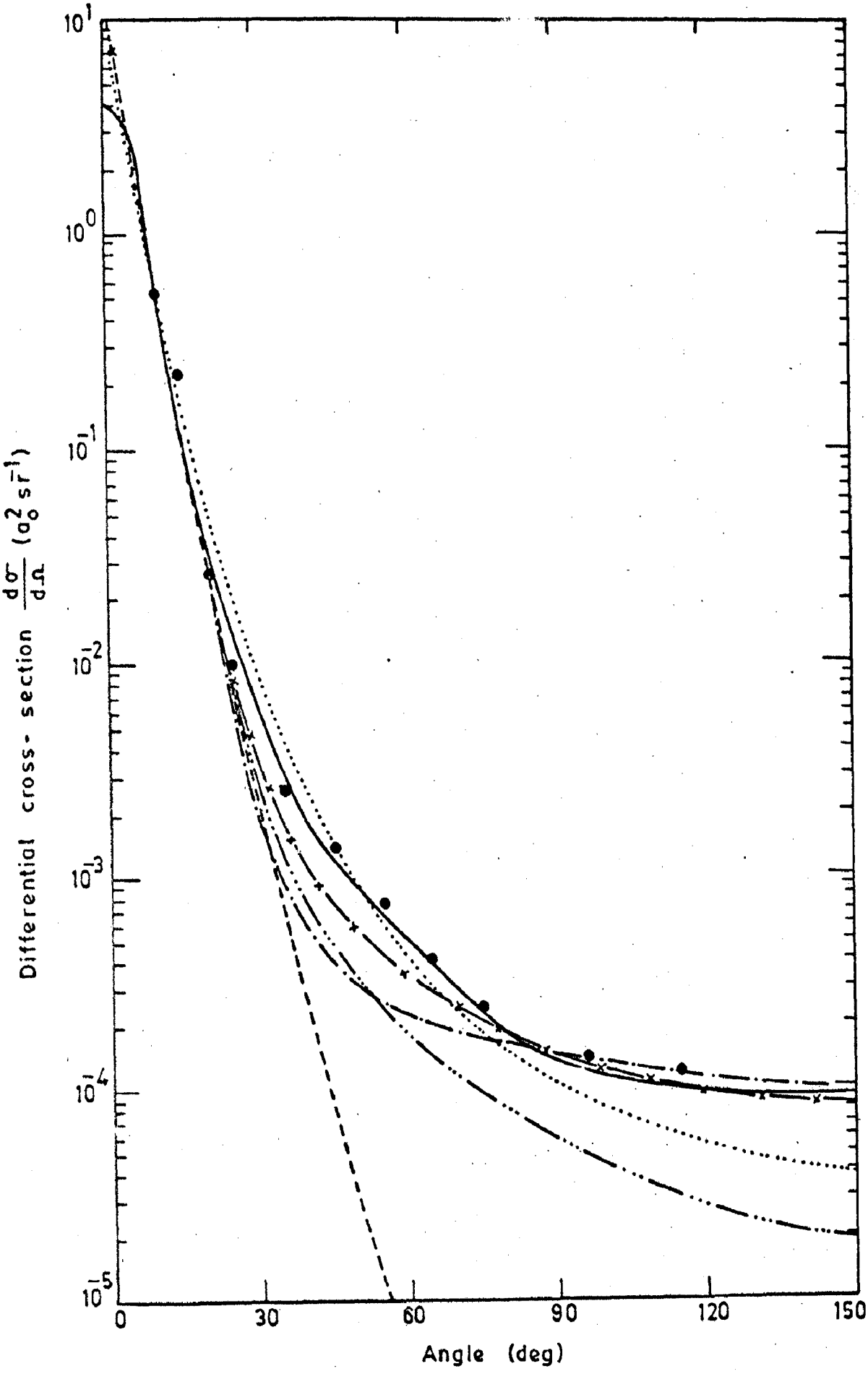

FIG. 3.6

CHAPTER -4

A COMPARATIVE STUDY OF e^+-He SCATTERING

4.1 INTRODUCTION

The study of positron gas scattering with atoms has become an active area of experimental and theoretical research during the last decade. Experimental investigations of Stein and Kaupplia(173) measuring cross-sections for individual transitions were mostly confined to total cross-sections. However, recently several groups have started measuring the cross-sections for some elastic and inelastic processes, such as positronium formation, atomic excitation and ionisation etc, separately. Amongst the atomic excitation measurements, Coleman and McNutt(130) and Coleman et al(129) have measured the total cross-section for positron impact elastic scattering of argon and helium atoms for the 1^1S-2^1S transition respectively. For helium they considered positron energies just above the threshold, i.e. 22-30 eV. In view of the promising progress of positron beam experiments of Canter and Mills (61), it is expected that these will provide us with data not only for total cross-sections but also for the differential cross-sections which display real scattering behaviour. Consequently, a lot of attention has been focused on similar theoretical investigations in recent years. In particular, for helium,

a few theoretical attempts(156,161,99,46) have been made. These calculations have been performed using eikonal Born series (EBS), modified Glauber approximations (MG), the close-coupling approximation(CC), the distorted wave approximation and its variants. Except for the CC calculations of Willis et al(156) for the 2^1S and 2^1P excitations and that of Madison and Winters(46) for the 2^1P excitation, the other authors report results only for 2^1S excitation. Among the various versions of the distorted-wave approximation, Saxena et al(161) employed distortion in both the channels by the Coulomb potential, Willis et al(156) used a distorted-wave Born model in which the distortions in both channels were taken in the field of static and polarisation potentials of the target ground state, Parcell et al(99) used distortion by static potential incorporating various polarisation potentials in the final channel and Madison and Winters used a distorted-wave Born series approach, retaining the second-order term in the series and using in place of the second-order potential a local second potential evaluated in the closure approximation. In most of the approaches outlined above, the representations of the bound-state wavefunctions of the target were at Hartree-Fock level.

As we have discussed in Chapters 2 and 3, that the theoretical calculations for cross-section suffer from the errors caused due to two main uncertainties, namely (i) the first is adoptation of an approximate model within the framework of which the calculation is carried out

(ii) the second is the choice of different simpler analytic wavefunctions to represent the initial and final states of the atomic target, as input to evaluate the scattering amplitude in that particular model.

We have made an attempt to minimise the above errors in the best possible way. For example, in the chosen theoretical description (i.e. model), the second source of error can be handled and the uncertainties in the results can be minimised with the use of available accurate generalised oscillator strengths for a specific transition. The minimisation of the above errors is the present effort having the following salient features (i) to include electron correlation effect with the use of many parameter correlated (MPC) wavefunctions (ii) Use of distorted wave approximation in particular Coulomb-Born model and distorted wave polarised orbital approach. The effect of electron correlation is included through the use of available accurate generalised oscillator strength for a specific transition. These generalised oscillator strengths are obtained with the use of accurate many parameter correlated atomic wavefunctions. Such ideas have been well recognised by earlier workers in different contents (119, 24). In this way, in any theoretical description (i.e. model), the second source of errors as pointed out above, can be handled and the uncertainties in the results can be minimised. Recently, Dillon and Inokuti (106) have implemented similar ideas for

electron impact excitation of the helium atom and performed the calculations using the Coulomb-projected Born (CPB) approximation only. The situation with S-P transitions is however not so straightforward.

The distorted-wave first Born model in its various versions of Bransden and McDowell(29) and Winters(90) has proved to be a useful model of electron-atom excitation at intermediate energies. Similar studies can also be considered for positron impact on atomic systems. The study of positron-atom scattering can be used as a first step and it would be worth exploring the effect of utilisation of accurate wave-functions in one of the distorted-wave approximation method itself. To begin with the attraction is naturally for positron impact studies on the helium atom, namely for excitations where other theoretical calculations for relative comparisons are already available. Further, since positron differ from electron only by a sign of the electric charge and so its study differs from that of electron in two ways. (i) The static interaction (arising from the Coulomb field of the undistorted atoms) which was attractive for electron scattering will now be repulsive for positrons, while the polarization interaction (resulting from the polarization of an atom by a passing charged particle) remains attractive for both positrons and electrons. (ii) Another important interaction i.e. exchange (arising from the indistinguish-ability of projectile electrons from electrons in the target) will be absent for positrons. In this chapter, we therefore

present our study for positron impact excitation of the 2^1S and 2^1P state of helium in Coulomb-Born(114) and distorted wave polarised orbital approach. Using an accurate generalised oscillator strength. In the Section (4.2), we present our complete study in Coulomb-Born model and Section (4.3), deal our calculations for the same exitations in distorted wave polarised orbital approach. These calculations are also performed using the Hartree-Fock(HF) wave-functions.

4.2 CALCULATION FOR 1^1S-2^1S, 2^1P TRANSITIONS IN COULOMB-BORN APPROACH

The transition amplitude for the excitation of the helium atom from its initial state i to the final state f by positron impact (having $\vec{k}_i$ and $\vec{k}_f$ as incident and scattered final wavevectors) in the Coulomb-Born approximation is given by

$$T_{if} = -\frac{1}{2\pi}\left\langle \chi_f^-(\vec{r}_1)\middle| U_{if}(\vec{r}_1)\middle|\chi_i^+(\vec{r}_1)\right\rangle \qquad \ldots (4.1)$$

In equation (4.1), χ_{if}^{+}, the distorted incident (scattered) wave is chosen to be a Coulomb wave in the screened charge ($z^{\boxtimes}$=-1.4) of the target helium atom. The justification and utility of such a choice of distorted waves have already been exemplified in the literature (161, 106). These have the following form

$$\chi_i^+(\vec{r}_1) = \exp\left(\frac{\pi z^{\boxtimes}}{2k_i}\right)\Gamma(1-a)\exp(i\vec{k}_i.\vec{r}_1)\ {}_1F_1(a,1,i(k_i r_1-\vec{k}_i.\vec{r}_1)) \qquad \ldots (4.2a)$$

$$\chi_f^-(\vec{r}_1) = \exp(\frac{\pi z^{\boxtimes}}{2k_f})\Gamma(1-b)\exp(i\vec{k}_f.\vec{r}_1)\,{}_1F_1(-b,1,-i(k_f r_1+\vec{k}_f.\vec{r}_1) \quad \ldots (4.2b)$$

with $a = \frac{iz^{\boxtimes}}{k_i}$ and $b = \frac{iz^{\boxtimes}}{k_f}$

With the use of Fourier transform of the interaction potential between the positron and the helium target atom, the expression for $U_{if}(\vec{r}_1)$ is given by

$$U_{if}(\vec{r}_1) = \frac{1}{2\pi^2}\int d\vec{q}\; q^{-2}\exp(i\vec{q}.\vec{r}_1)f_{if}(\vec{q}) \quad \ldots (4.3)$$

The form factors $f_{if}(\vec{q})$ for 1^1S-2^1S and 1^1S-2^1P transitions are evaluated using the same procedure as discussed in Chapter 2 (see equation (2.10–2.11). Using these forms of form factor and equations (4.2(a-b), we can directly obtain the transition amplitude as discussed in Chapter 2. So finally, using equations (2.10–2.15 and 2.18 –2.29), we can write the differential cross-sections for the two separate processes in which z equal to $z^{\boxtimes}(-1.4)$

$$\left(\frac{d\sigma}{d\Omega}\right)_{1^1S-2^1S} = \frac{k_f}{k_i}\left|T_{1^1S-2^1S}\right|^2 \quad \ldots (4.4a)$$

$$\left(\frac{d\sigma}{d\Omega}\right)_{1^1S-2^1P} = \frac{k_f}{k_i}\left\{\left|T_{1^1S-2^1P}(m=o)\right|^2+2\left|T_{1^1S-2^1P}(m=1)\right|^2\right\} \quad \ldots (4.4b)$$

In order to assess (in the present model) the effect of a many-parameter correlated wavefunction (MPC) compared with the commonly used Hartree-Forck(HF) wavefunction (156), the calculations are also performed using the HF wavefunction. We have used the accurate HF wavefunction due to Byron and

Joachain(64,65) for 1^1S and 2^1S states and that of Morse et al(131) for 2^1P state.

4.2.1 Results and discussion

We have used equations (4.4a and 4.4b) to calculate the differential cross-sections (DCS) for 2^1S and 2^1P excitations in helium at positron impact energies of 100 and 200eV. Most of the other theoretical predictions exist at these energies and also the present model is expected to produce the best results. The present results obtained using the MPC and HF wavefunctions along with others are displayed in figures (4.1-4.4) for each of the transitions at above two impact energies. Before we present the details of our results, it would be meaningful to examine the differences noticed in the results obtained using (i)MPC and (ii) HF wavefunctions. For the 2^1S excitation, there are no significant differences between the two sets of calculations in the small angular region but this difference is appreciable at larger scattering angles (approximately within 6% at 100 eV and 3% at 200 eV). For 2^1P, the situation is similar at smaller angles but at larger angles, the deviation (approximately within 13% at 100 eV and almost the same at 200 eV) is, on average, large.

Figure (4.1) shows DCS at 100 eV for 1^1S-2^1S excitation. It is apparent that the first Born approximation (FBA) yields very small results for $\theta \gtrsim 30^o$. This behaviour is not

surprising as it is well known that the FBA does not provide the leading term of the Born multiple scattering series for large momentum transfer (66). The present calculation underestimates the results in the near forward direction by almost the same amount as they are overestimated by the close-coupling (CC) and modified Glauber (MG) approximation methods(156) compared with other theoretical results. Except for the modified Glauber approximation (which is referred to the EBS in the paper of Willis et al(156)), no models show secondary maxima. Our model overestimates the results at larger angles of scattering (50° or more) while close-coupling and MG methods underestimate them for $\theta \gtrsim 120^{\circ}$ with respect to other results. Figure (4.2) shows the DCS results for 2^1S excitation again, but at 200 eV positron impact energy. The general trend of the results as displayed in figure (4.1) is followed in a similar manner in this case also. However, the general agreement among all the results including ours has improved considerably and the secondary maximum in the MG cross-section curve has now disappeared.

In figure (4.3), we display the results for the differential cross-section at 100 eV for the 1^1S-2^1P transition. Among the available results of Madison and Winter(46) as well as close-coupling results due to Willis et al(156). It is seen for $\theta \gtrsim 30^{\circ}$ that the close-coupling and first-order DWBA results agree closely while second order results lie closer to our results. For scattering angle $\theta \lesssim 30^{\circ}$, except

in the forward direction all approximation results are nearly the same. Figure (4.4) shows similar results for 2^1P excitation at 200 eV positron energy. In this figure however, first-order DWBA results due to Madison and Winters (46) are not available. Agreement at this energy seems much better as all the three curves are bunched relatively closer. Upto $\theta \simeq 60^\circ$, we see a similar trend to that in figure (4.3) but above this angle upto $\theta \simeq 100^\circ$, the second order DWBA results coincide with ours and then become higher than ours. The situation with FBA results in figures (4.3) and (4.4) remaining the same as figures (4.1) and (4.2). We have calculated the differential cross-sections for positron-impact energy in the range of 50-500 eV and the same are given in a tabular form in the tables (4.1-4.3).

4.3 CALCULATION FOR 1^1S-2^1S AND 2^1P TRANSITIONS IN DISTORTED WAVE POLARIZED ORBITAL APPROACH

We have seen in Chapter 3, that our consistent version of distorted wave Born approximation (DWBA) for electron impact 2^1S and 2^1P excitation of helium, gives results which are more accurate than any other modified Born calculations. The method also requires less computational effort as compared to any close coupling approximation (CCA). Exactly, the same DWBA method with only slight modification (needed for positron scattering) is therefore used for present calculation. Without going in detail of the model (for which see the Chapter 3), we give here simply its salient features. In our

distorted wave model(145), the distortions effects are incorporated in both the ingoing and outgoing positron distorted waves due to static and polarization effects. Further, instead of using prevalent used Hartree-Fock(HF) wavefunctions for target helium, we use for the first time many parameter correlated wavefunctions (MPC)(22). The polarization effects are incorporated using dipole approximation method(20). The positron impact studies as mentioned earlier differ from its counterpart study (145) by electron in two ways (i) No exchange effects are present, (ii) the static distortion potential now bears a negative sign while the polarization interaction remain the same as for electron study. Our approach is different from other distorted wave approaches i.e. of Parcell et al(99) who took distortions due to static potential in both channels but polarization contribution only in final channel and also the bound states of the helium target were taken at Hartree Fock(HF) level. To avoid repetition, we refer our chapter (3) for details regarding our DWBA model and calculation procedure. Like previous all approaches, we have also neglected presently the contribution of positronium formation. In the preceding section (4.2) we have also reported the discrete excitation of helium by positron impact in a relatively simpler approach using Coulomb-Born model in which the distortion were taken by Coulomb-potential of the target but the target wavefunctions were represented both by many parameter correlated and by Hartree-Fock wavefunctions separately. We have calculated total and

differential cross-sections (DCS) for 1^1S-2^1S and 1^1S-2^1P transitions in helium for positron energies from threshold to 200 eV. The comparison of the present results with other available theoretical and experimental results are shown in the figures (4.5-4.10).

4.3.1 Results and discussion

(A) 1^1S-2^1S excitation

Total cross-section

In order to assess the effect of using MPC wavefunctions, we have repeated our calculations and obtained results with the commonly used accurate HF wavefunctions also. Separate results are also obtained using polarization effect only in initial or final channel to see the effectiveness of polarization contribution in each case. Total cross-sections are shown in figure 4.5. In this figure we have displayed our various total cross-section results along with others and experimental data. First Born approximation (FBA) calculations (obtained using the same HF functions as we used) are due to Buckley and Walters. The other DWBA results are of Parcell et al who used self-generated HF function and took distortions by static potential in both the channels while incorporated polarization effect in final channel by scaled Dalgarno-Lynn potential. Three state close coupling (CC) results of Willis et al used the basis consisting of the 1^1S, 2^1S and 2^1P states, represented by Slater type orbitals. From this figure, various interesting features emerge on comparing different

into account in our model as its contribution slightly enhances the cross-section just near threshold energy region (183). We also realize that the experimental measurements in higher energy range ($\gtrsim$40 eV) are desired to see the further suitability of any model.

(b) Differential scattering cross-section

In figure 4.6, we present our differential scattering cross-section for 1^1S–2^1S excitation of helium by positron impact at 100 eV. The present results are compared with other available theoretical results. Among them the results of Willis et al(156) obtained in various perturbative approaches, Parcell et al(99) in distorted wave Born method and those of Mukesh et al(114) in Coulomb-Born model are worth mentioning. It is seen that all other results including ours in distorted wave polarized approach follow the same trend of variation over the entire angular region. The MG and CC results overestimate all the other results upto $\theta \lesssim 20^\circ$ while the present Coulomb-Born results underestimate upto $\theta \lesssim 30^\circ$. Further, for the scattering angles $\theta \gtrsim 30^\circ$, the present calculations are very different than that of Coulomb-Born results. In this angular region, the present calculations compared well with the results of other theoretical calculations in particular with the results of Parcell et al(99). It shows that the inclusion of distorted waves in both channels due to static and polarization effect is in right direction. Since there are no experimental measurements for

results among themselves. Our results with MPC wavefunctions are higher (within 10%.) with that we obtained using HF function (in the energy range from 70 eV to 200 eV). In contrast, similar comparison with electron impact results(145) (figure (3.1)) shows that cross-sections with MPC functions are lower (within 5%.) below 70 eV energy than that obtained using HF functions (64,65). Thus, for positron scattering, correlation effects seems to be of more importance. Further, the comparison of our two results with polarization taken only in initial or final channel suggests that polarization effects are more effective in final channel. One can recall that the same is argued by Parcell et al(99). On overall observation, we find that FBA and CC methods overestimates.the cross-sections as compared to DWBA. Also, except CC results, all DWBA results for high energies as expected. Willis et al(156) have themselves attributed this divergent behaviour in their CC results as due to inclusion of 2^1P state in the basis set. They converge to FBA. However, similar divergence in the results with the inclusion of more states in CC method is also seen in e^+–H scattering (98). Further, the differences in the DWBA results of ours and that of Parcell et al(99) can be said to be due to basically the different choices of both the wavefunctions and polarization potentials. Our(results below 40 eV) compare favourably with experiment(129) while that of Parcel et al seems to be in error near threshold energies. We feel that a better agreement of ours with experiment might be obtained if effect of positronium formation is also taken

DCS, except a few theoretical results, we therefore, prefered to give in detail our DCS results in a tabular form. These results might be useful for comparison purposes in case new measurements become available. The figure (4.7), present our DCS at 200 eV. The trend of variation is very similar as noticed at 100 eV in figure (4.6).

B. 1^1S-2^1P excitation

(a) Total cross-section

In figure (4.8), we have shown our results of total cross-section results for 1^1S-2^1P excitation of helium by positron impact in distorted wave polarized orbital approach. The present results both using the HF and MPC are compared with three state close-coupling calculation of Willis et al(156) in the energy range 20-200 eV. The calculation peaks around 60 eV and thereafter show a relatively rapid fall compared to CC results with the increase of incident energies. The present results obtained using HF wavefunction differs by about 5% in comparison with the results obtained using MPC wavefunctions (see table 4.4 for 1^1S-2^1S and 1^1S-2^1P transitions).

(b) Differential cross-section

In figure (4.9) display our differential cross-section results for 1^1S-2^1P excitation of helium at 100 eV. The present results in distorted wave polarized orbital method are compared only with the theoretical results of Kumar et al

in Coulomb-Born along with the first and second order DWBA result of Madison and Winters(46) and close-coupling results of Willis et al(156). All results show similar behaviour upto $\theta \simeq 30^{\circ}$, after that the first Born results as usual fall off rapidly. The first order distorted wave results of Madison and Winters(46) and CC calculations of Willis, et al(156) compare well among themselves upto $\theta \simeq 110^{\circ}$ and thereafter the CC results overestimates the first order results of Madison and Winters(46). The present calculation too show a rapid fall upto 60° and thereafter it underestimates both the first and second order distorted wave calculations of Madison and Winters upto $\theta \simeq 140^{\circ}$ beyond which it overestimate the first order and approach to second order distorted wave calculations. The disagreement between the present calculation and the second order distorted wave calculation of Madison and Winters(46) narrows down with the increase in the impact energy, as can be seen from the figure (4.10) at 200 eV. Details of our total and differential cross-sections are given in the tables (4.4-4.6).

4.4 CONCLUSION

It is clearly seen (through figures 4.1-4.10) that, in general, all the theoretical models(with which we compared our results) including ours (both) show nearly the same behaviour for DCS at low scattering angles. The latter differences in the behaviour of the different cross-section curves seen to narrow down as the impact energies of the positrons are

increased. Further, the present work demonstrates the use of accurate transition form factors in the evaluation of scattering amplitude in both the models. The results we obtained thus are closed-form expressions for monopole and dipole transitions in Coulomb-Born model as well as being free from conflicting assumptions (which usually arise) due to choice of simple target wavefunctions. Again, one of the attractions of our Coulomb-Born approach is its simplicity for obtaining reasonable results. In addition, the results obtained in distorted wave polarised orbital method are as reliable as those obtained by other DWBA calculations(156, 99, 46) at high impact energies. Of course, the adaptability of any model remains subject to comparison with the expected very demanding experimental data which is not yet available.

Table 4.1- Differential cross-sections $\frac{d\sigma}{d\Omega}$ ($a_o^2 Sr^{-1}$) for the 1^1S-2^1S excitation of helium by positron impact in Coulomb-Born model.

Energy (eV)	Scattering angles (deg) → / Model ↓	2	6	10	20	50	80	100	120	140
50	FB	1.26(-1)	1.21(-1)	1.13(-1)	8.01(-2)	1.28(-2)	1.68(-3)	5.44(-4)	2.25(-4)	1.21(-4)
	CB	8.77(-3)	8.59(-3)	8.24(-3)	6.98(-3)	3.82(-3)	2.35(-3)	1.77(-3)	1.41(-3)	1.19(-3)
100	FB	1.71(-1)	1.56(-1)	1.31(-1)	6.11(-2)	2.07(-3)	1.05(-4)	2.40(-5)	8.08(-6)	3.83(-6)
	CB	5.92(-2)	5.50(-2)	4.79(-2)	2.76(-2)	4.88(-3)	1.57(-3)	9.19(-4)	6.17(-4)	4.70(-4)
200	FB	1.92(-1)	1.58(-1)	1.09(-1)	2.56(-2)	1.59(-4)	4.22(-6)	8.06(-7)	2.44(-7)	1.08(-7)
	CB	1.19(-1)	1.00(-1)	7.26(-2)	2.23(-2)	1.29(-3)	2.86(-4)	1.48(-4)	9.27(-5)	6.77(-5)
300	FB	1.97(-1)	1.47(-1)	8.50(-2)	1.15(-2)	2.77(-5)	5.77(-7)	1.02(-7)	2.92(-8)	1.25(-8)
	CB	1.46(-1)	1.11(-1)	6.73(-2)	1.26(-2)	4.38(-4)	8.65(-5)	4.34(-5)	2.67(-5)	1.94(-5)
500	FB	1.98(-1)	1.21(-1)	5.11(-2)	2.99(-3)	2.61(-5)	4.27(-8)	6.85(-9)	1.84(-9)	7.56(-10)
	CB	1.66(-1)	1.04(-1)	4.64(-2)	4.26(-3)	9.73(-5)	1.79(-5)	8.85(-6)	5.41(-6)	3.90(-6)

Table 4.4- Total cross-sections σ (πa_o^2) of helium by positron impact in distorted wave polarized orbital approach.

Energy (eV)	Transitions			
	1^1S-2^1S		1^1S-2^1P	
	Present (MPC)	Present (HF)	Present (MPC)	Present (HF)
23	2.81(-2)	2.45(-2)	1.21(-1)	1.32(-1)
26	3.14(-2)	3.15(-2)	1.23(-1)	1.28(-1)
28	3.33(-2)	3.35(-2)	1.26(-1)	1.30(-1)
30	3.44(-2)	3.43(-2)	1.28(-1)	1.32(-1)
40	3.41(-2)	3.45(-2)	1.47(-1)	1.53(-1)
60	2.83(-2)	2.83(-2)	1.55(-1)	1.62(-1)
80	2.35(-2)	2.40(-2)	1.50(-1)	1.55(-1)
100	1.87(-2)	2.15(-2)	1.41(-1)	1.45(-1)
150	1.43(-2)	1.53(-2)	1.18(-1)	1.19(-1)
200	1.10(-2)	1.17(-2)	9.01(-2)	9.03(-2)

Table 4.2- Differential cross-sections $\frac{d\sigma}{d\Omega}$ ($a_o^2 Sr^{-1}$) for the $1^1S-2^1P(m=o)$ excitation of helium by positron impact in Coulomb-Born model.

Energy (eV)	Scattering angles (deg) → / Model ↓	2	6	10	20	50	80	100	120	140
50	FB	1.68	1.31	8.48(-1)	2.14(-1)	5.92(-3)	4.06(-4)	1.05(-4)	3.77(-5)	1.87(-5)
	CB	1.74(-1)	1.59(-1)	1.35(-1)	7.87(-2)	1.58(-2)	5.08(-3)	3.31(-3)	1.90(-3)	1.42(-3)
100	FB	4.88	1.77	5.24(-1)	4.06(-2)	2.52(-4)	1.50(-5)	1.48(-6)	4.15(-7)	1.66(-7)
	CB	1.98	9.89(-1)	4.33(-1)	8.25(-2)	5.34(-3)	1.16(-3)	5.84(-4)	3.68(-4)	2.77(-4)
200	FB	7.32	6.52(-1)	9.78(-2)	3.78(-3)	6.11(-6)	1.03(-7)	1.75(-8)	4.84(-9)	1.72(-9)
	CB	5.17	7.05(-1)	1.58(-1)	1.57(-2)	6.15(-4)	1.14(-4)	5.98(-5)	4.10(-5)	3.37(-5)
300	FB	6.18	2.40(-1)	2.80(-2)	7.63(-4)	5.69(-7)	8.60(-9)	1.33(-9)	1.09(-9)	8.79(-10)
	CB	5.28	3.18(-1)	5.59(-2)	4.53(-3)	1.48(-4)	2.78(-5)	1.56(-5)	1.16(-5)	1.01(-5)
500	FB	3.02	5.39(-2)	5.00(-3)	7.74(-5)	2.43(-8)	7.11(-10)	6.73(-11)	2.84(-11)	8.20(-12)
	CB	3.04	8.33(-2)	1.20(-2)	8.31(-4)	2.29(-5)	4.79(-6)	3.06(-6)	2.51(-6)	2.25(-6)

Table 4.3- Differential cross-sections $\frac{d\sigma}{d\Omega}(a_o^2 sr^{-1})$ for the $1^1S-2^1P(m=\pm1)$ excitation of helium by positron impact in Coulomb-Born model.

Energy (eV)	Scattering angles (deg)→ / Model↓	2	6	10	20	50	80	100	120	140
50	FB	1.02(-2)	6.82(-2)	1.15(-1)	8.75(-2)	3.81(-3)	1.51(-4)	2.31(-5)	4.45(-6)	9.34(-7)
	CB	1.97(-3)	1.47(-2)	2.90(-2)	3.50(-2)	6.76(-3)	1.34(-3)	5.01(-4)	1.99(-4)	7.01(-5)
100	FB	1.85(-1)	5.55(-1)	3.93(-1)	6.80(-2)	3.15(-4)	4.16(-6)	4.16(-7)	6.08(-8)	1.68(-8)
	CB	9.97(-2)	3.48(-1)	2.94(-1)	7.88(-2)	2.51(-3)	2.89(-4)	1.04(-4)	4.05(-5)	1.42(-5)
200	FB	1.31	8.94(-1)	2.78(-1)	1.59(-2)	1.04(-5)	6.42(-8)	5.31(-9)	5.75(-10)	1.91(-10)
	CB	1.01	8.16(-1)	2.89(-1)	2.54(-2)	2.60(-4)	3.04(-5)	1.23(-5)	5.35(-6)	1.97(-6)
300	FB	2.62	7.14(-1)	1.53(-1)	4.68(-3)	1.08(-6)	4.85(-9)	7.01(-10)	1.72(-11)	3.41(-10)
	CB	2.26	7.11(-1)	1.71(-1)	8.61(-3)	5.93(-5)	8.27(-6)	3.67(-6)	1.67(-6)	6.48(-7)
500	FB	3.61	3.92(-1)	5.47(-2)	6.69(-4)	5.16(-8)	4.09(-10)	2.50(-11)	3.22(-11)	-
	CB	3.43	4.08(-1)	6.39(-2)	1.56(-3)	9.33(-6)	1.73(-6)	8.17(-7)	3.61(-7)	1.57(-7)

Table 4.5- Differential cross-sections $\frac{d\sigma}{d\Omega}(a_o^2 Sr^{-1})$ for the 2^1S-2^1S excitation of helium by positron impact in distorted wave polarized orbital approach.

Angle (deg)	Energy (eV)						
	22	26	30	50	100	150	200
0	1.465(-3)	3.504(-2)	5.413(-2)	1.039(-1)	1.499(-1)	1.601(-1)	1.705(-1)
10	1.489(-3)	3.390(-2)	5.141(-2)	9.225(-2)	1.147(-1)	1.087(-1)	1.005(-1)
20	1.563(-3)	3.071(-2)	4.409(-2)	6.485(-2)	5.260(-2)	3.463(-2)	2.190(-2)
30	1.696(-3)	2.607(-2)	3.432(-2)	3.677(-2)	1.614(-2)	6.584(-3)	3.305(-3)
40	1.904(-3)	2.079(-2)	2.447(-2)	1.760(-2)	4.553(-3)	1.778(-3)	1.038(-3)
50	2.204(-3)	1.565(-2)	1.623(-2)	7.812(-3)	1.7321(-3)	8.978(-4)	5.771(-4)
60	2.614(-3)	1.122(-2)	1.026(-2)	3.688(-3)	9.780(-4)	6.450(-4)	4.190(-4)
70	3.151(-3)	7.765(-3)	6.385(-3)	2.076(-3)	7.742(-4)	5.018(-4)	2.955(-4)
80	3.825(-3)	5.312(-3)	4.049(-3)	1.439(-3)	6.573(-4)	3.705(-4)	2.340(-4)
90	4.635(-3)	3.694(-3)	2.694(-3)	1.197(-3)	5.531(-4)	3.092(-4)	1.595(-4)
100	5.567(-3)	2.686(-3)	1.913(-3)	1.106(-3)	4.823(-4)	2.464(-4)	1.246(-4)
110	6.590(-3)	2.07(-3)	1.460(-3)	1.045(-3)	4.098(-4)	1.771(-4)	1.101(-4)
120	7.658(-3)	1.685(-3)	1.202(-3)	9.812(-4)	3.364(-4)	1.612(-4)	7.538(-5)
130	8.713(-3)	1.412(-3)	1.065(-3)	9.283(-4)	3.005(-4)	1.505(-4)	7.426(-5)
140	9.691(-3)	1.192(-3)	1.001(-3)	8.942(-4)	2.837(-4)	1.092(-4)	6.709(-5)
150	1.053(-2)	1.007(-3)	9.751(-4)	8.648(-4)	2.459(-4)	1.049(-4)	4.779(-5)
160	1.117(-2)	8.630(-4)	9.666(-4)	8.238(-4)	2.198(-4)	1.247(-4)	6.314(-5)
170	1.158(-2)	7.722(-4)	9.648(-4)	7.834(-4)	2.385(-4)	8.712(-5)	4.892(-5)
180	1.172(-2)	7.413(-4)	9.647(-4)	7.671(-4)	2.630(-4)	6.216(-5)	2.800(-5)

Table 4.6- Differential cross-sections $\frac{d\sigma}{d\Omega}(a_o^2 Sr^{-1})$ for the $1^1S-2^1P_{0,\pm1}$ excitation of helium by positron impact in distorted wave polarized orbital approach.

Angles (deg)	Energy(eV)			
	80	100	150	200
0	3.24	4.21	4.52	3.91
10	1.48	1.52	1.27	9.83(-1)
20	2.38(-1)	1.58(-1)	7.42(-2)	4.38(-3)
30	5.04(-2)	2.78(-2)	4.31(-3)	5.83(-3)
40	1.21(-2)	7.48(-3)	3.52(-3)	1.88(-3)
50	2.78(-3)	1.28(-3)	7.90(-4)	9.21(-4)
60	1.78(-3)	1.01(-3)	3.75(-4)	4.42(-4)
70	8.28(-4)	7.89(-4)	3.65(-4)	2.73(-4)
80	6.42(-4)	6.00(-4)	3.08(-4)	1.78(-4)
90	5.85(-4)	4.43(-4)	1.60(-4)	1.15(-4)
100	3.65(-4)	3.38(-4)	1.52(-4)	8.49(-5)
110	3.48(-4)	2.87(-4)	1.40(-4)	6.53(-5)
120	3.12(-4)	2.43(-4)	1.43(-4)	5.21(-5)
130	2.26(-4)	2.11(-4)	1.92(-4)	4.31(-5)
140	2.19(-4)	1.92(-4)	1.34(-4)	4.01(-5)
150	1.99(-4)	1.90(-4)	1.50(-4)	3.90(-5)
160	1.64(-4)	2.00(-4)	1.31(-4)	3.81(-5)
170	1.64(-4)	2.20(-4)	1.37(-4)	3.73(-5)
180	1.65(-4)	2.50(-4)	1.38(-4)	3.43(-5)

4.5 FIGURE CAPTIONS

Figure 4.1 The differential scattering cross-sections for 1^1S-2^1S excitation of helium atom by positron impact at 100 eV in Coulomb-Born model.
Calculation: ——, present calculations with MPC wave-functions; O, present calculations with HF wave-functions; - - - -, present calculations in first Born approximation; — x —, results in the MG approximation(156); — xx —, results in the close-coupling approximation(156); —··—, results in the DWBA approximation(156); —·—, results of Parcell et al(99).

Figure 4.2 Same as figure 4.1 but at 200 eV.

Figure 4.3 The differential scattering cross-sections for the 1^1S-2^1P excitation of the helium atom by positron impcat at 100 eV in Coulomb-Born model.

Same as figure 4.1 except: —··—, distorted wave results of Madison and Winters(46) in second order; ——···——, distorted wave results of Madison and Winters(46) in first order.

Figure 4.4 Same as figure 4.3 but at 200 eV

Figure 4.5 The total scattering cross-sections for the 1^1S-2^1S excitation of the helium atom by positron impact distorted wave polarized orbital approach.
Calculation: ——;present results with CF wave-functions; O, present result with HF wavefunctions; — xx —, results in the close-coupling approximation (156); - - - , results in the first Born approximat-ion(25);—·—, distorted wave results of Parcell et al(99); x, present results with polarization effect in final channel; ⊙, present results with polariza-tion effect in initial channel; $\bar{\Phi}$, experimental data of Coleman et al(129).

Figure 4.6 The differential scattering cross-sections for the 1^1S-2^1S excitation of the helium atom by positron impact at 100 eV in distorted wave polarised orbital approach.
Calculation: same as figure 4.1, except,...,CB results of Mukesh et al(114),---, present results with MPC wavefunctions; O, present results with HF wavefunctions.

Figure 4.7 Same as figure 4.6 but at 200 eV.

Figure 4.8 The total cross-sections for the 1^1S-2^1P excitation of the helium atom by positron impact in distorted wave polarized orbital approach.
Calculation: Same as figure 4.5, -- xx --,three state close-coupling results of Willis et al(156).

Figure 4.9 The differential scattering cross-sections for the 1^1S-2^1P excitation of the helium atom by positron impact in distorted wave polarized orbital approach.
Calculation: Same as figure 4.3,...., CB results of Mukesh et al(114), -- , present results with MPC wavefunctions.

Figure 4.10 Same as figure 4.9 but at 200 eV.

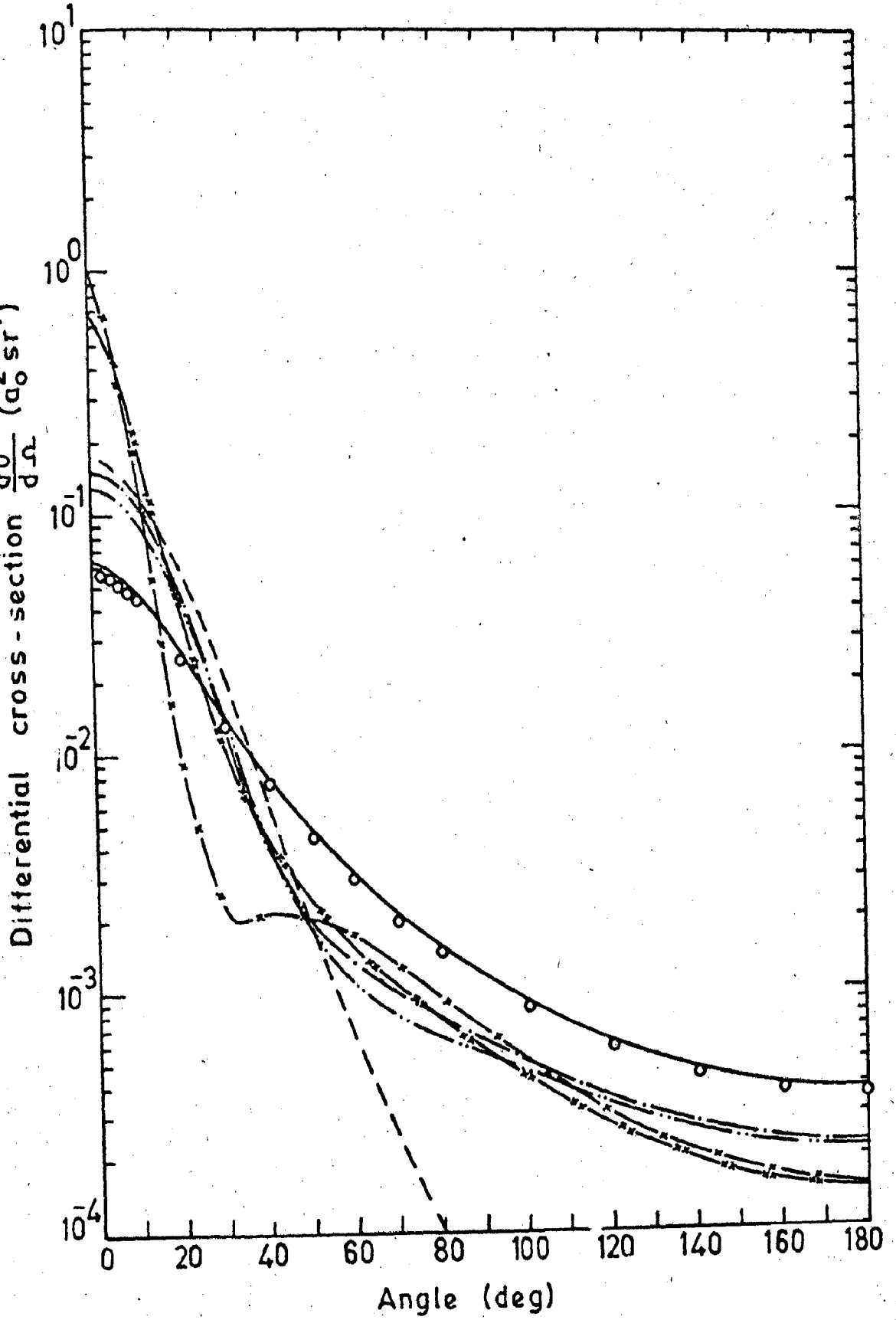
Differential cross-section $\frac{d\sigma}{d\Omega}$ ($a_0^2\,sr^{-1}$)
10^{1}
10^{0}
10^{-1}
10^{-2}
10^{-3}
10^{-4}
0
20
40
60
80
100
120
140
160
180
Angle (deg)

FIG. 4-1

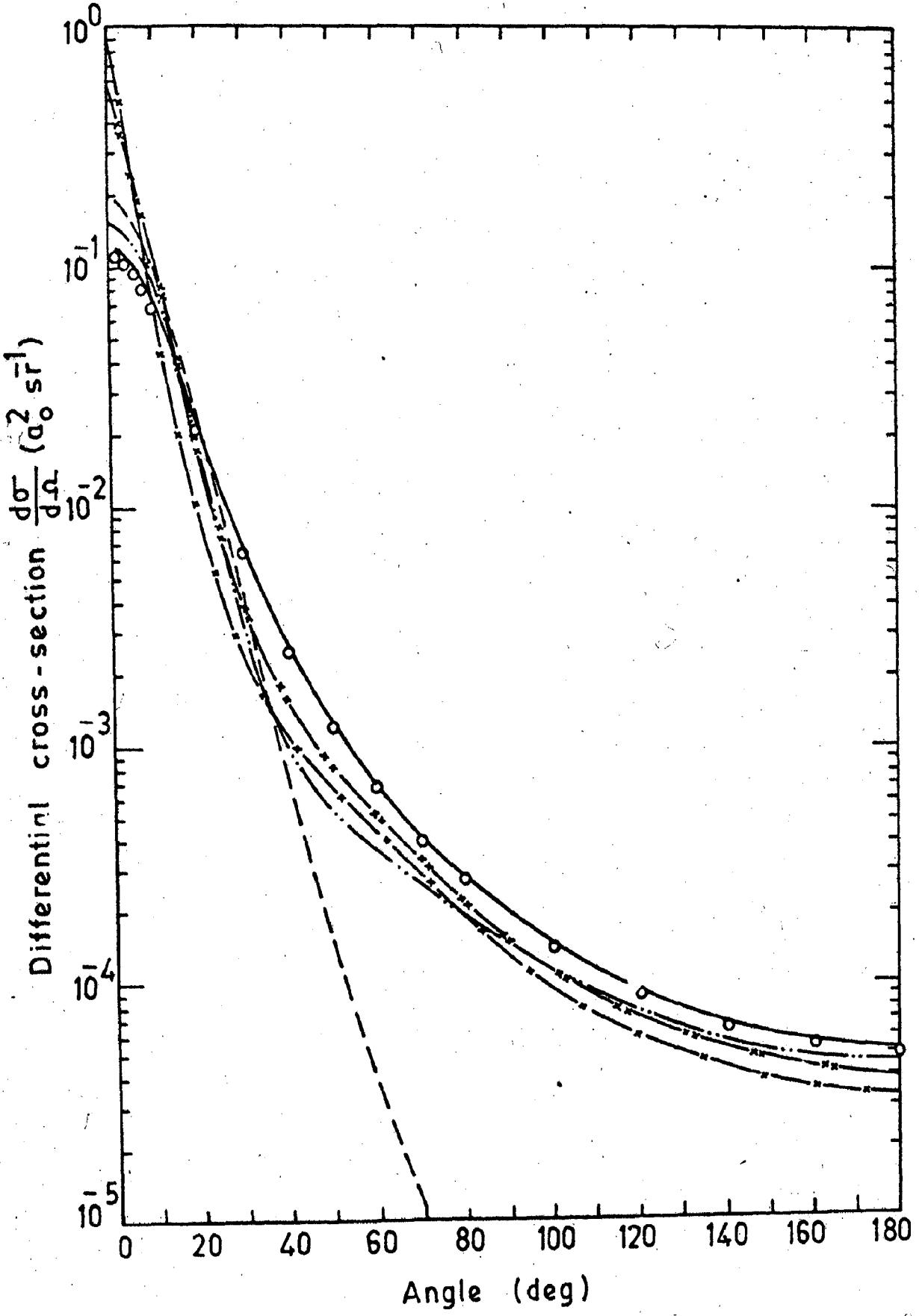
Differential cross-section $\frac{d\sigma}{d\Omega}$ (a_o^2 sr^{-1})
10^0
10^{-1}
10^{-2}
10^{-3}
10^{-4}
10^{-5}
0
20
40
60
80
100
120
140
160
180
Angle (deg)

FIG. 4·2

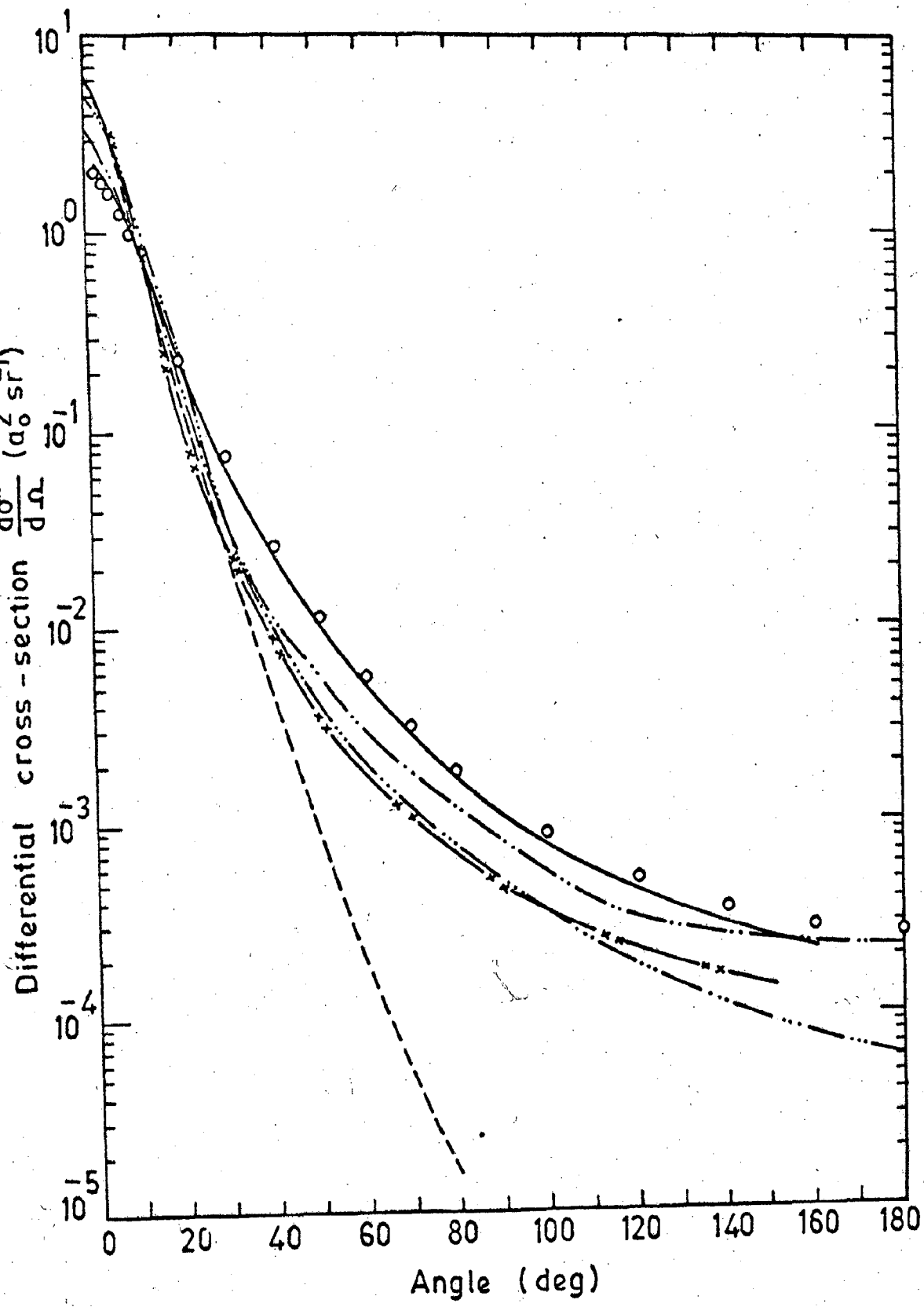
Differential cross-section $\frac{d\sigma}{d\Omega}$ (a_0^2 sr^{-1})
10^1
10^0
10^{-1}
10^{-2}
10^{-3}
10^{-4}
10^{-5}
0
20
40
60
80
100
120
140
160
180
Angle (deg)

FIG. 4·3

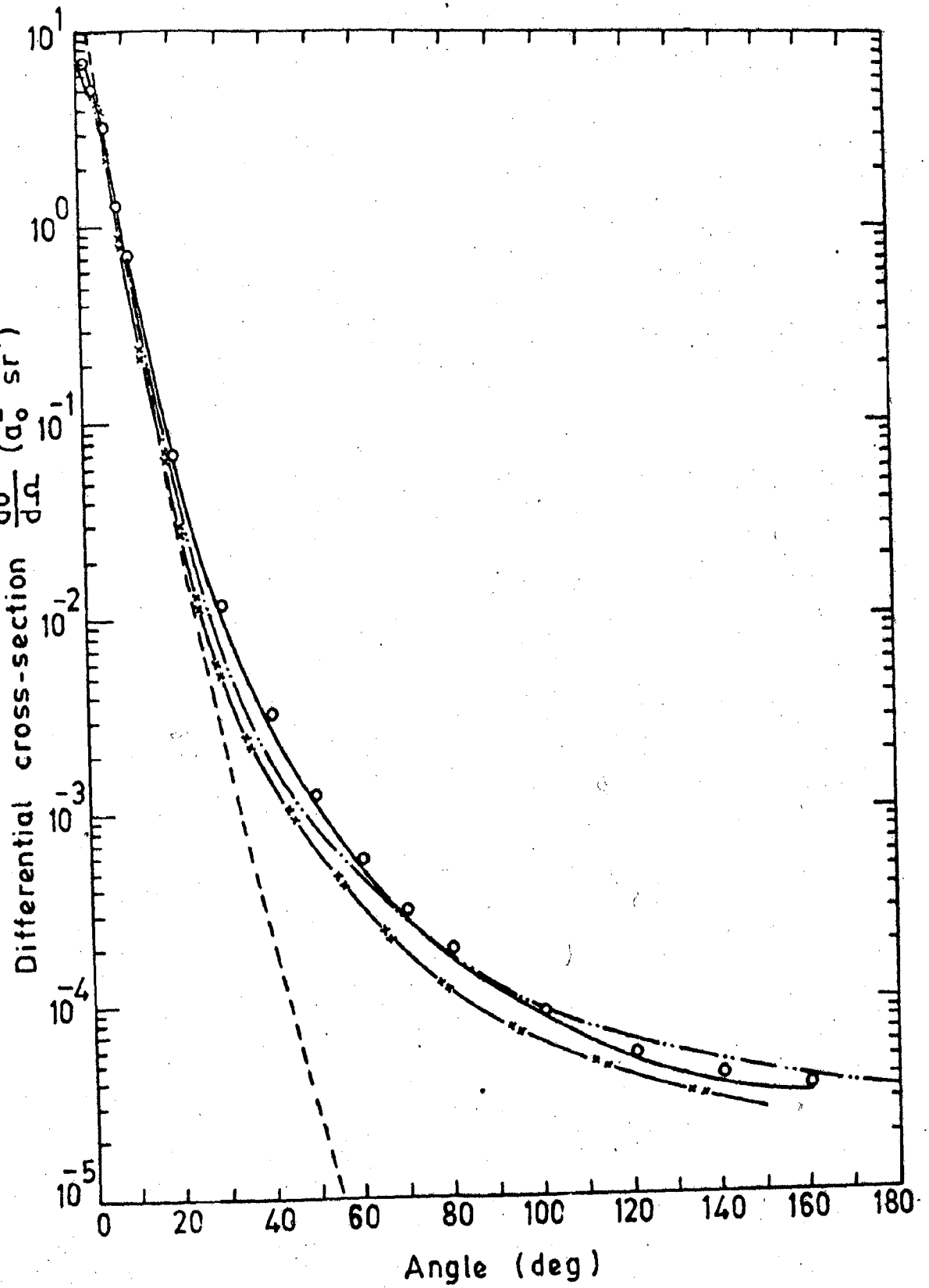
Differential cross-section $\frac{d\sigma}{d\Omega}$ (a_0^2 sr^{-1})
10^1
10^0
10^{-1}
10^{-2}
10^{-3}
10^{-4}
10^{-5}
0
20
40
60
80
100
120
140
160
180
Angle (deg)

FIG. 4·4

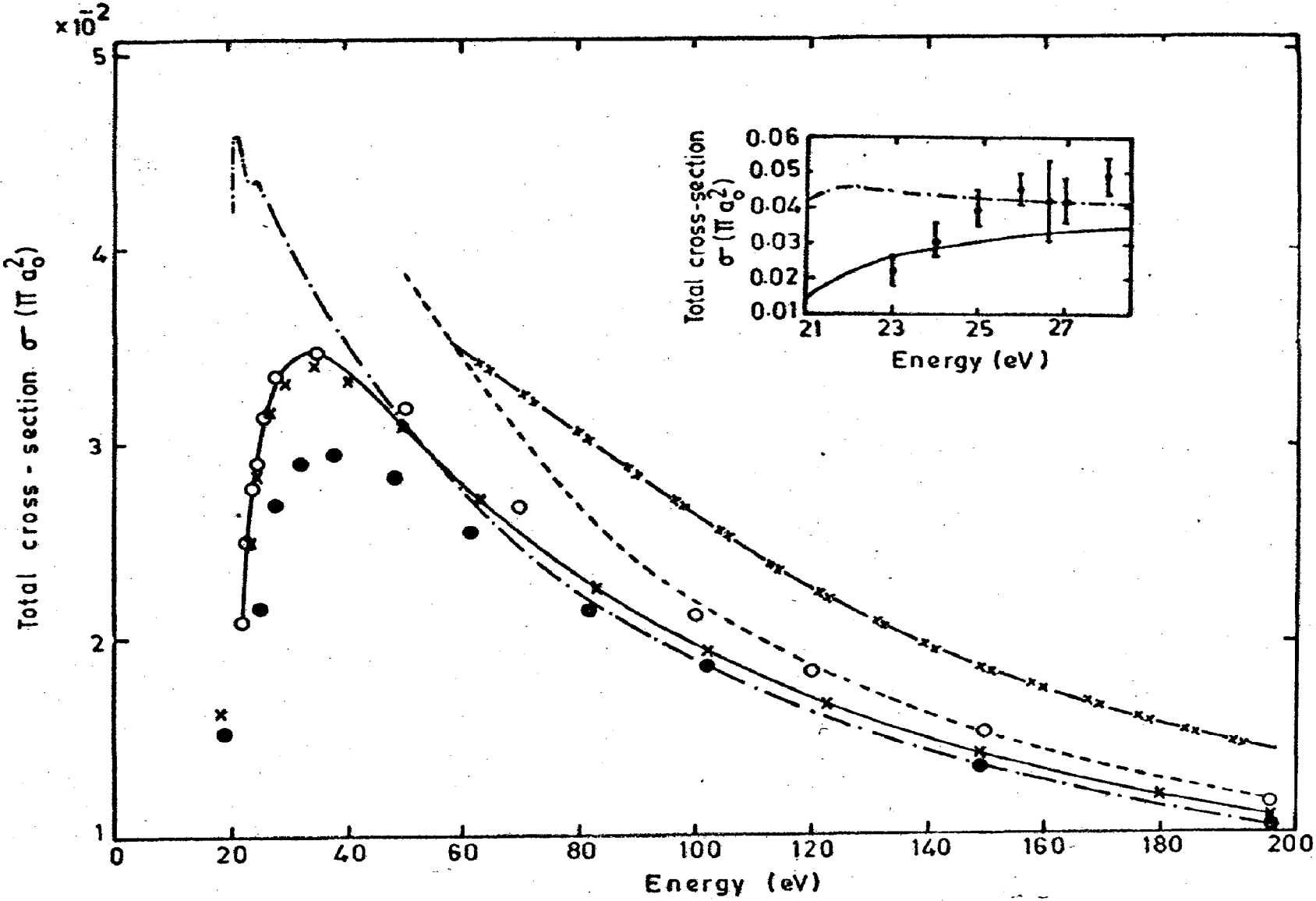
x 10^-2
5
4
3
2
1
Total cross - section σ (π a_o^2)
0
20
40
60
80
100
120
140
160
180
200
Energy (eV)
Total cross-section σ (π a_o^2)
0.06
0.05
0.04
0.03
0.02
0.01
21
23
25
27
Energy (eV)

Fig. 4·5

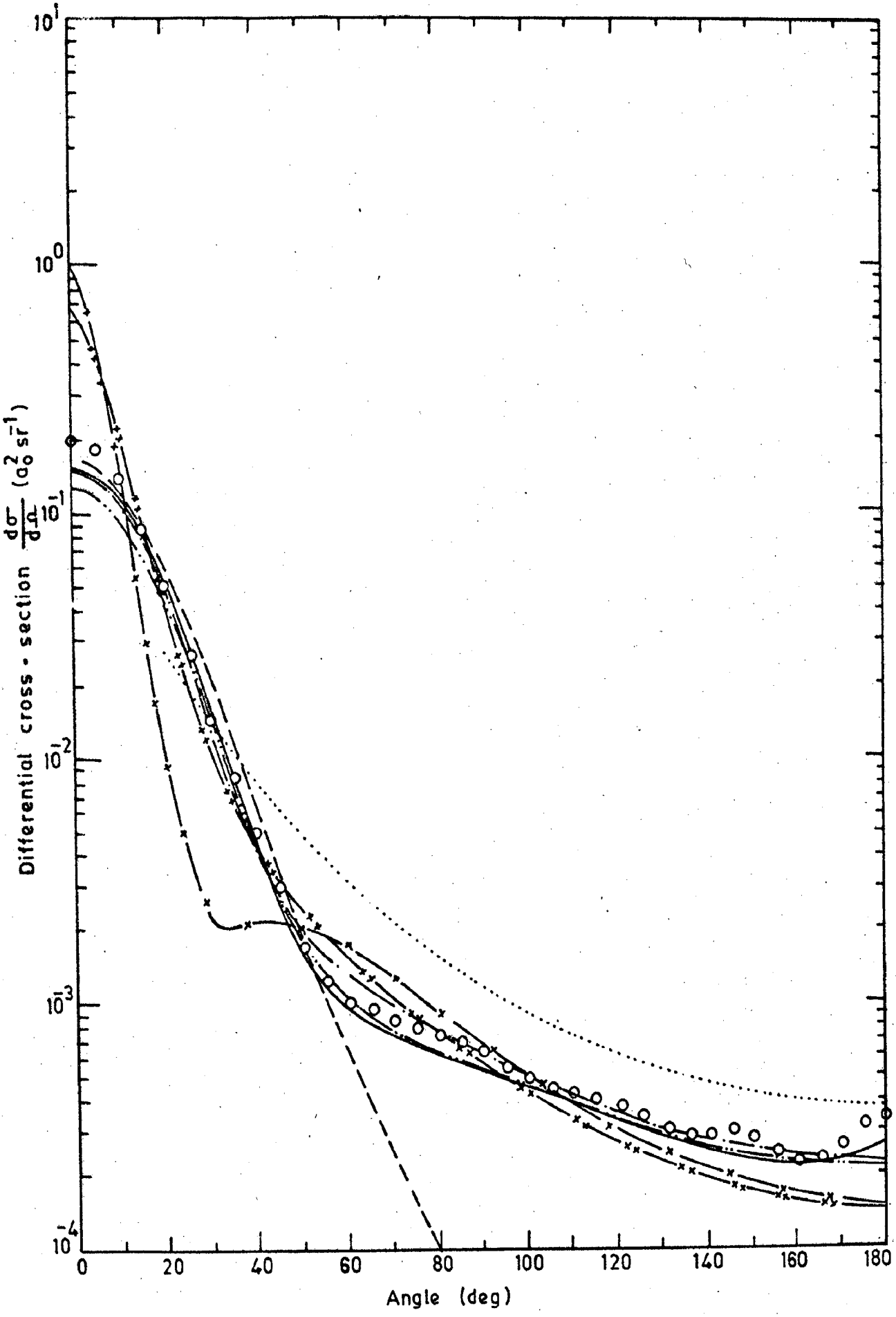
Differential cross - section $\frac{d\sigma}{d\Omega}$ ($a_0^2\,sr^{-1}$)
10^1
10^0
10^{-1}
10^{-2}
10^{-3}
10^{-4}
0
20
40
60
80
100
120
140
160
180
Angle (deg)

Fig. 4.6

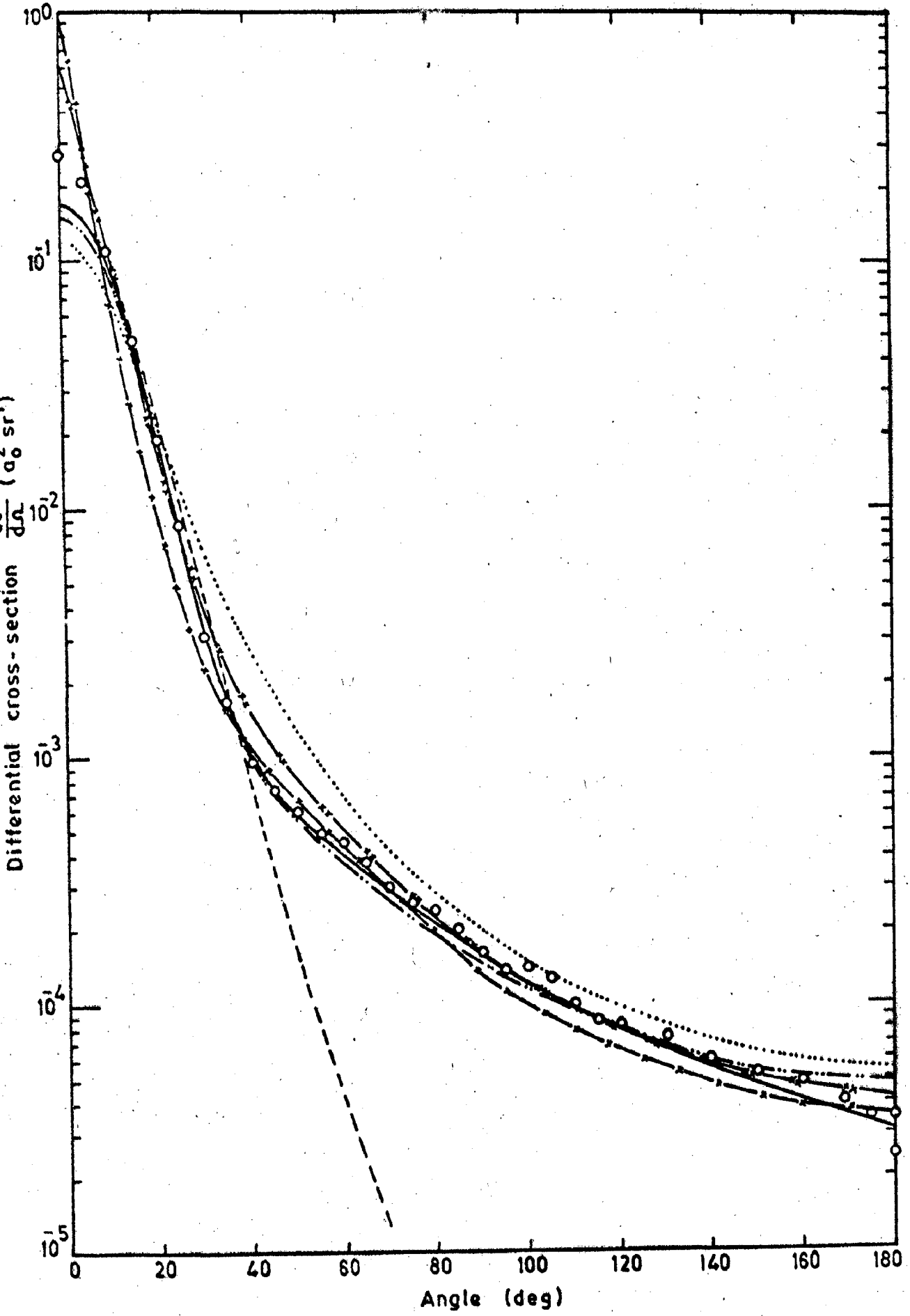
100
10⁻¹
10⁻²
10⁻³
10⁻⁴
10⁻⁵
Differential cross-section dσ/dΩ (a₀² sr⁻¹)
0
20
40
60
80
100
120
140
160
180
Angle (deg)

FIG. 4·7

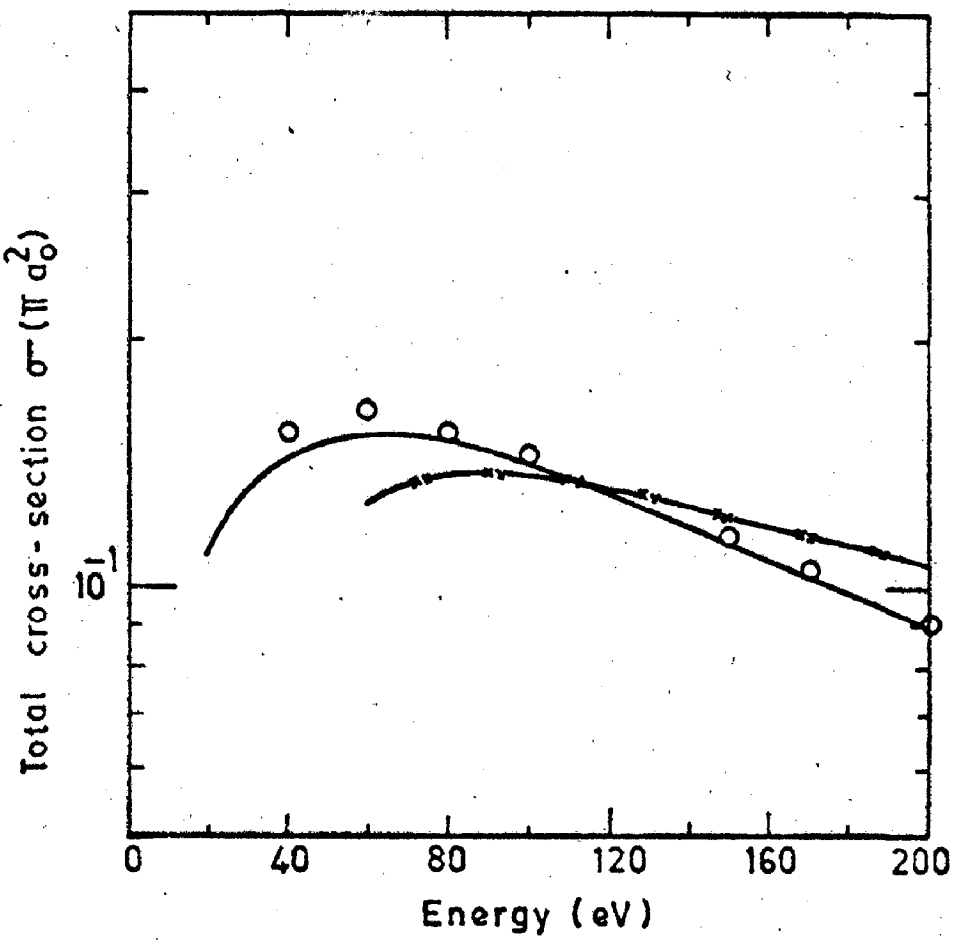

Fig. 4.8

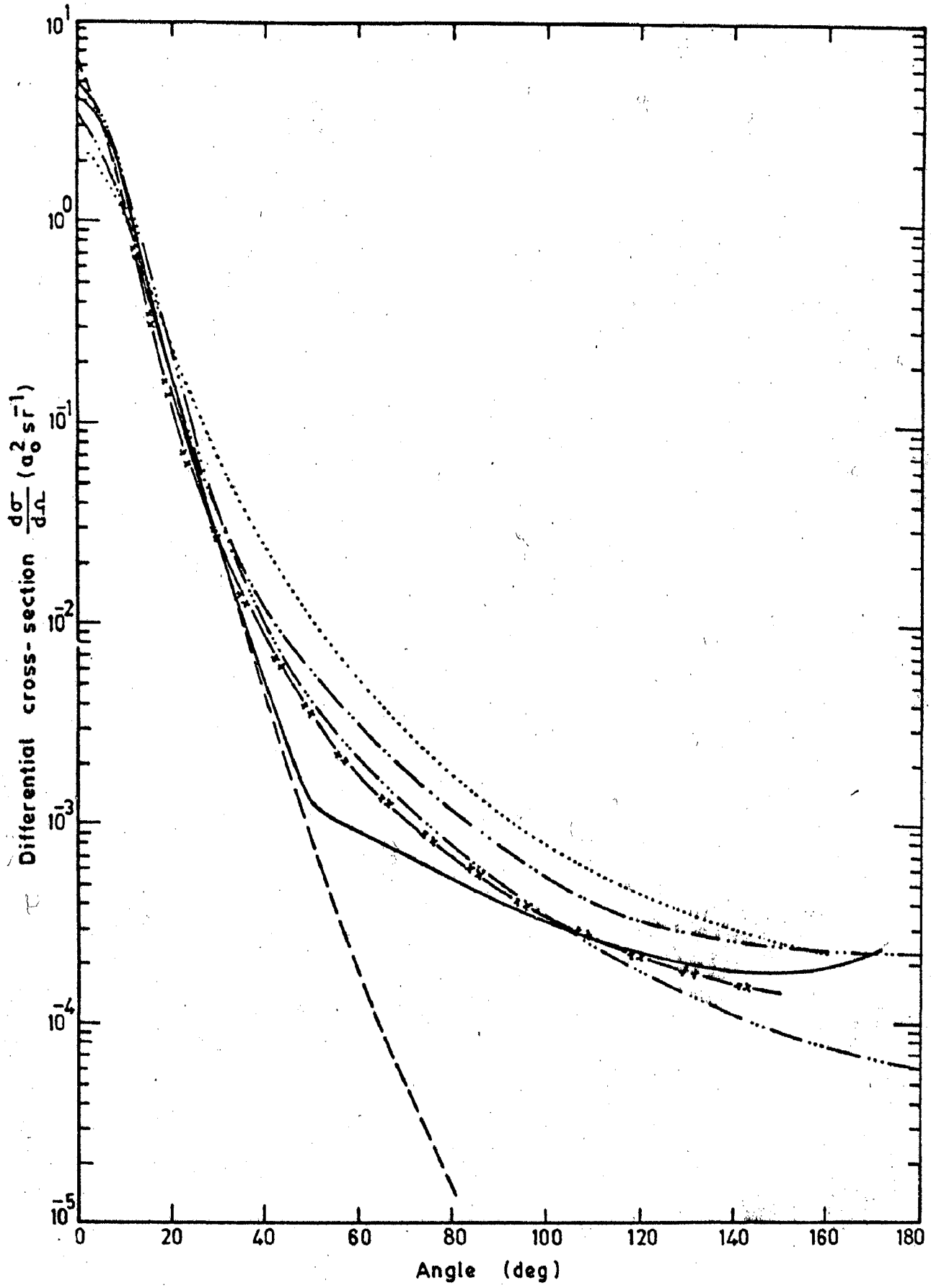
Differential cross-section $\frac{d\sigma}{d\Omega}$ (a_0^2 sr^{-1})
10^{1}
10^{0}
10^{-1}
10^{-2}
10^{-3}
10^{-4}
10^{-5}
0
20
40
60
80
100
120
140
160
180
Angle (deg)

Fig. 4·9

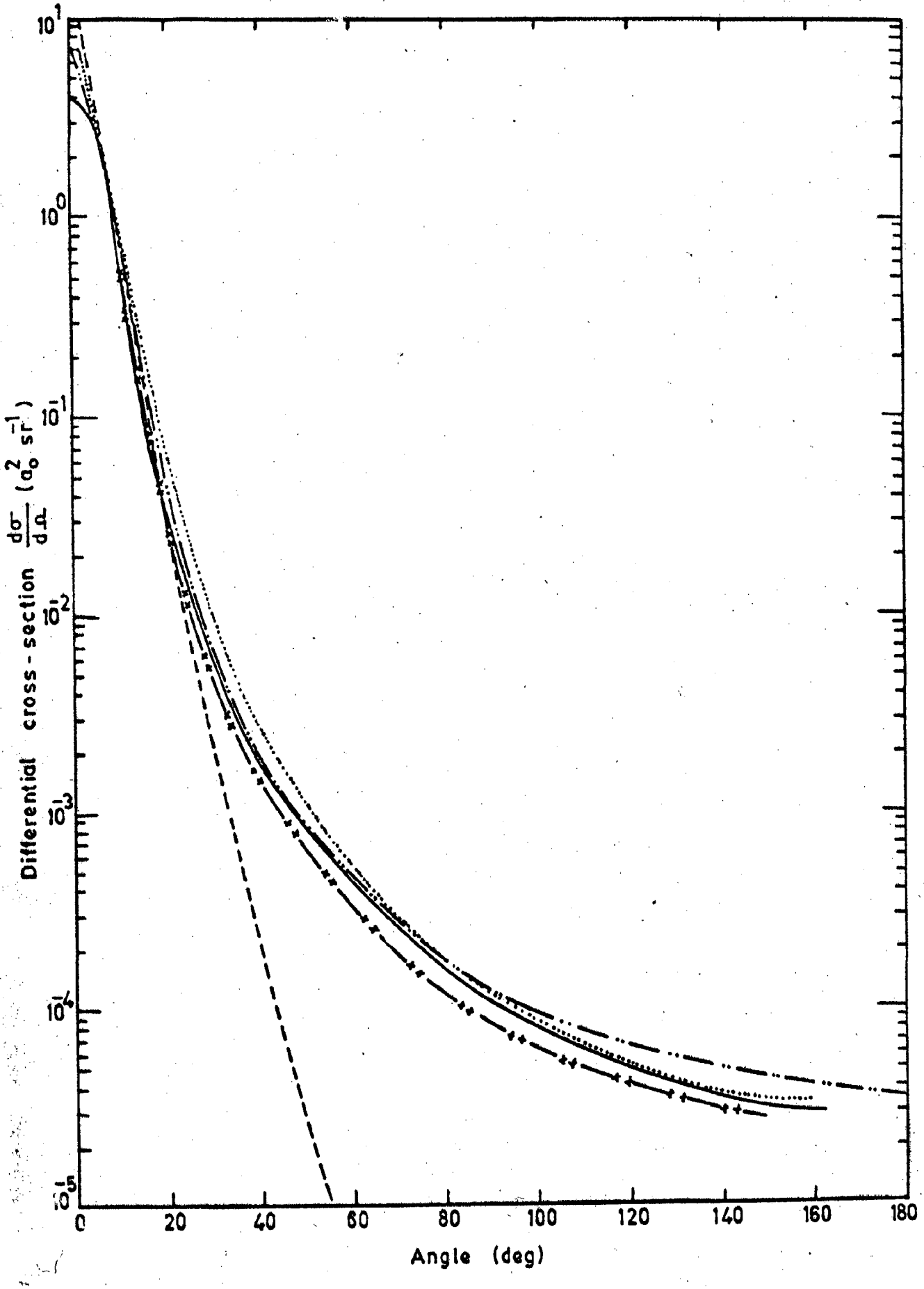
Differential cross-section $\frac{d\sigma}{d\Omega}$ (a_0^2 sr^{-1})
10^{1}
10^{0}
10^{-1}
10^{-2}
10^{-3}
10^{-4}
10^{-5}
0
20
40
60
80
100
120
140
160
180
Angle (deg)

Fig. 4·10

CHAPTER-5

ELECTRON IMPACT EXCITATION OF THE 3s AND 2p STATES OF LITHIUM ATOM AT INTERMEDIATE AND HIGH ENERGIES

5.1 INTRODUCTION

Recently the scattering of electrons by lithium atom has received a good deal of attention by various authors. This process is interesting from the theoretical as well as experimental point of view because it offers the simple test of electron atom collision processes. The extensive studies carried out on helium have already provided enough information for us to understand the behaviour of discrete excitation functions. Therefore in order to obtain more quantitative information on excitation, the lithium atom, having, spectra of a one electron nature, is perhaps the most suitable candidate. There exist many studies (Srivastava and Vuskovic(153), Phelps et al(83)) of electron impact excitation of sodium, potassium and caesium alkalie-metal atoms at intermediate and high energies but relatively few such studies are available for the lithium atom. The resonance transition(2s-2p) has been subjected to more studies(30) compared to s-s and other higher excited transitions in lithium. On the experimental side Williams et al(187) were the first to report the differential scattering cross-section measurements on a number of discrete excitations of lithium in the energy range 10-60 eV.

Zajonc and Gallagher(23) and Shuttleworth et al(171) have reported the total electron impact excitation cross-section for higher excited states (3s, 4s, 3d, 4d) of the lithium atom. The electron impact excitation of the resonance transition (2 s-2 p) in lithium has also been studied earlier by Zapesochnyi et al(76) and Leep and Gallagher(48). Recently Vuskovic et al(104) have measured the differential and total cross-sections for this (2 s-2 p) transition in the energy range of 10-200 eV.

On the theoretical side, a number of workers have reported their differential and total cross-sections using the different approximations for 2s-3s and 2s-2p transition of lithium atom. Recently, Tripathi(13) and Tayal and Tripathi(167) have studied many higher excited states of lithium in addition to 2s-3s, 2p transitions using Born and Glauber approximations. The 2s-3s has been studied by Sharma et al(142) using the two potential modified Born approximation (TPMB) and very extensively by Winters and Vanderpoorten (92) using the distorted wave Born approximation(DWBA) in the intermediate energy range 10-60 eV. Recently, Moorse(49) has reported a five state close-coupling calculation with correlation for the differential and total excitation cross-section for different discrete transition in lithium. However, he has considered energies only upto 10 eV, which is outside the energy range considered in the present study. Apart from the several calculations reported earlier for the resonance transition, Kennedy et al(84) have carried out an extensive calculation for total, differential

cross-section and coincidence parameters using a unitarised distorted wave polarised orbital method (UDWPO) in the energy range 5-100 eV. Very recently, Saxena et al(158, 159, 160) obtained the differential scattering cross-sections and angular parameters for 2s-2p transition and the differential cross-section for 2s-3s transition using a two potential approach in the energy range 10-60 eV. There is a wide variety of methods which describe this energy region and recent reviews by Bransden and McDowell(29) and Callaway(77) deal with them very exhaustively. A common feature to all the intermediate energy methods is that they all pay attention to the second order term of the mutliple scattering series and attempt to treat it as accurately as possible.

The failure of the first Born approximation to predict the large momentum transfer inelastic scattering cross-section is due to elimination of the electron-nuclear interaction term arising out of the orthogonality of initial and final state wavefunctions. However, this term is present in the second Born approximation (i.e. second term of the Born series), via coupling to the elastic channel in the intermediate states and consequently the second Born term will dominate at wide angles. Byron and Latour(70) have shown that 1s-ns transitions, the second Born term (f_{B2}) falls of like $k_i^{-2}q^{-2}$ for a large q whereas the first Born term (f_{B1}) falls like q^{-6}, where $\vec{q} = \vec{k}_i - \vec{k}_f$ is the momentum transfer and $\vec{k}_i, \vec{k}_f$ are wave numbers of the incident and scattered electrons respectively.

The scattering amplitude in the simplified second Born approximation (SSBA) is defined as

$$f = f_{B1} + f_{B2} \qquad \ldots (5.1)$$

where f_{B2} is the second Born term, obtained in closure approximation. Here it may be pointed out that the SSBA is not consistent through order k_i^{-2}. In fact a consistent calculation through order k_i^{-2}, referred as eikonal Born series (EBS) amplitude (as suggested by Byron and Joachain(65) discussed in detail in the first Chapter Section (1.2.3) is achieved as follows,

$$f_{EBS} = f_{B1} + f_{B2} + f_{G3} \qquad \ldots (5.2)$$

where f_{G3} is the third order Glauber term. Byron and Joachain(65) also proposed a modified version of EBS approximation which was subsequently suggested by Gein(175) and referred to as the modified Glauber approximation(175). In this approximation the full Glauber amplitude f_G is corrected for the missing second real term f_{G2} by substituting the second order Born term for the second order Glauber term i.e.,

$$\begin{aligned} f_{MG} &= f_G - f_{G2} + f_{B2} \\ &= f_{EBS} + \sum_{n=4}^{\infty} f_{Gn} \end{aligned} \qquad \ldots (5.3)$$

This approach, instead of working to order k_i^{-2} removes the logarithmic divergence of the Glauber amplitude in the forward direction and accounts for the target polarization effects.

It is found to be better than EBS. The EBS scattering amplitude is different from the MG one, in the sense that the former ignores the Glauber terms of order higher than k_i^{-2}. These perturbative approaches, developed to analyse the elastic scattering of electrons by hydrogen, helium and lithium atoms(67, 163, 175), are extended to study the inelastic scattering as well. In particular, these approaches have been very successfully applied to study electron impact excitation of s-s and s-p type transition in hydrogen(70, 175) and helium(65, 39) atoms. We therefore, in this chapter report our study of the differential and total cross-section for excitation of the 2s-3s transition in lithium by electron impact using EBS, MG along with the SSBA, first Born and Glauber approximation in the energy range of 20-200 eV. In this chapter, we have also included our preliminary study by electron impact of the lithium to its resonance transition (2s-2p) using only MG approximation. We report our study at 100 eV.

In section 5.2, we outline in brief the theoretical procedure to obtain the various term needed to evaluate the scattering amplitude in SSBA, EBS and MG approximation for 2s-3s transition of lithium and also discuss the results of these calculation in comparison to other theoretical and experimental results. Section 5.3 is devoted to study the excitation of 2s-2p transition of lithium in MG approximation.

5.2 EXCITATION OF 2s-3s TRANSITION IN LITHIUM BY ELECTRONS

5.2.1 Calculation

The wavefunction of the lithium atom is expressed as a determinant of one electron spin orbital function as

$$\Psi_i = \frac{1}{\sqrt{6}} \beta_1\alpha_1\alpha_2\phi_{1s}(1)\left[\phi_i(2)\,\phi_{1s}(3)-\phi_i(3)\,\phi_{1s}(2)\right] \quad \ldots (5.4)$$

where ϕ is the spatial part of the spin orbital, α and β are the components of the spin part. These orbitals are expanded in terms of one electron slater type orbital(STO) basis functions. We have used the simple Hartree-Fock wavefunctions for the one electron orbitals ϕ_{2s} and ϕ_{3s} computed by Hibbert (Private Communication) using his CIV3 programme. The coefficients and exponents for these orbital are tabulated in table (5.1). For calculating the generalised oscillator strength and related first Born matrix, Glauber scattering amplitude, the determinantal wavefunction as given by equation (5.4) is used. However, for the calculations of second Born term and the different terms of the Glauber eikonal series (f_{G2} and f_{G3}). We have considered the lithium atom as a one-electron system with inert core. The absolute value of the product of atomic orbitals can be written as,

$$\phi_{3s}^{\otimes}\phi_{2s} = \frac{1}{4\pi}\Big(\sum_{j=1}^{2} a_j \exp(-\alpha_j r) + \sum_{j=3}^{7} a_j r \exp(-\alpha_j r) + \sum_{j=8}^{12} a_j r^2 \exp(-\alpha_j r) + \sum_{j=13}^{15} a_j r^3 \exp(-\alpha_j r)\Big) \quad \ldots (5.5)$$

The values of a_j and α_j are obtained from the coefficients and exponents of the orbital given in Table (5.1).

(i) Evaluation of first Born term

Within the first Born approximation the differential inelastic scattering cross-section of a target for incoming projection is defined as

$$\frac{d\sigma(\vec{q})}{d\Omega} = \frac{2}{q^2}\frac{k_f}{k_i}\frac{1}{\Delta_{if}} f(\vec{q}) \qquad \ldots (5.6)$$

where $f(\vec{q})$ is the generalised oscillator strength and related to the Born matrix element by,

$$f(\vec{q}) = \frac{2}{q^2}\Delta E_{if} \left|\varepsilon_i^f(\vec{q})\right|^2 \qquad \ldots (5.7)$$

with

$$\varepsilon_i^f(\vec{q}) = \int d\vec{r}\, \psi_f^{\ast}(\vec{r}_1 \ldots \vec{r}_N) \sum_{j=1}^{N} \exp(i\vec{q}.\vec{r}_j)\, \psi_i(\vec{r}_1 \ldots \vec{r}_N) \qquad \ldots (5.8)$$

N is the number of electrons of the atom.

This is referred as length formulation of the Born matrix element. Similarly equation (5.8) can be transformed to the velocity formula

$$\varepsilon_i^f(\vec{q}) = \frac{1}{2\Delta_{if}} \int d\vec{r}\, \psi_f^{\ast} \left[q^2 \left(\sum_{j=1}^{N} \exp(i\vec{q}.\vec{r}_j) \right) \psi_i - 2iq \left(\sum_{j=1}^{N} \exp(i\vec{q}.\vec{r}_j) \frac{\partial \psi_i}{\partial z_j} \right) \right] \qquad \ldots (5.9)$$

The details of these formulations are given in a paper of Tripathi(13).

(ii) Evaluation of Glauber scattering amplitude

The Glauber amplitude for the scattering of a charge particle with an atom can be written as

$$F^{GA}(\vec{q},\vec{k}_i) = \frac{ik_i}{2\pi}\int\Big\langle\psi_f(\vec{r}_1\ldots\vec{r}_N)\Big|\,1-\prod_{j=1}^{3}\Big[\exp(-i\eta\int_{-\infty}^{\infty}V(r,s_j,z_j)dz_j)\Big]\,\Big|\psi_i(\vec{r}_1\ldots\vec{r}_N)\Big\rangle\exp(i\vec{q}.\vec{b})d\vec{b} \qquad \ldots (5.10)$$

where the N electron atom is initially in the state ψ_i (given by equation (5.4)) with energy E_i and the incident electron has a wave vector $\vec{k}_i$. After collision, the atom is in the state ψ_f with energy E_f and scattered electron has a wave vector $\vec{k}_f$. $V(r,r_j)$ is the interaction potential between the incident particle and the j^{th} bound electrons. The momentum transfer $\vec{q}$ is defined as $\vec{q} = \vec{k}_i-\vec{k}_f$ and $\eta = 1/k_i$. Taking the product of the bound state wavefunctions(equation 5.4) to have the form,

$$\psi_f^{\otimes}\psi_i = \prod_{j=1}^{3} P_j \qquad \ldots (5.11)$$

where

$$P_j = a_j\Big[\sum_{k=1}^{N_j} c_{k,j}\, r_j^{n_{k,j}}\exp(-\alpha_{k,j}\, r_j)\Big] \qquad \ldots (5.12)$$

with $a_1=a_2=a_3=\frac{1}{4\pi}$ for s–s transitions and $a_1=a_2=\frac{1}{4\pi}$ and $a_3 = Y^{\otimes}_{1,m'}(\theta_2,\phi_2)/4\pi$ for s–p transition. Use of equation (5.12) in equation (5.10) gives

$$F^{GA}(\vec{q},\vec{k}_i) = \frac{k_i}{2\pi i}\int d\vec{b}\,\exp(i\vec{q}.\vec{b})\prod_{j=1}^{3}P_j\left[\frac{|\vec{b}-\vec{s}_j|}{b}\right]^{2i\eta}d\vec{r}_j \qquad \ldots (5.13)$$

The contribution of the integrals over r_j appearing in equation (5.13) has been discussed by Kumar and Srivastava (155) and

Tayal and Tripathi (167). The same is written as

$$\int P_j \left[\frac{|\vec{b}-\vec{s}_j|}{b}\right]^{2i\eta} dr_j = b^2 E(\eta) \sum_{k=1}^{N_j} C_{k,j}(-1)^{1+\eta_{k,j}} \times \left[\frac{\partial}{\partial \alpha_{k,j}}\right]^{1+\eta_{k,j}} \int_0^\infty dt \frac{t^{-2i\eta}\left[J_1(t)+2tJ_0(t)/(t^2+\alpha_{k,j}^2 b^2)\right]}{(\alpha^2+\alpha_{k,j}^2 b^2)} = T_j(b) \quad \ldots (5.14)$$

where

$$E(\eta) = 2^{2i\eta} \frac{(1+i\eta)}{(1-i\eta)} \quad \ldots (5.15)$$

J_0 and J_1 are the Bessel functions of zeroth and first order respectively. The values of th parameters $C_{k,j}$ and $\alpha_{k,j}$ in equation (5.12) are obtained from the coefficients and exponents of the wavefunction given in table (5.1)

Finally, the scattering amplitude is obtained by putting equation (5.14) and (5.15) in equation (5.13) and carrying out integration over ϕ_b,

$$F^{GA}(\vec{q},\vec{k}_i) = ik_i \int_0^\infty db\, bJ_1(qb)\left[1-\prod_{j=1}^{3} T_j(b)\right] \quad \ldots (5.16)$$

for s–s transition

$$F^{GA}(\vec{q},\vec{k}_i) = k_i e^{\pm i\phi_b} \int_0^\infty db\, b\, J_1(qb) \prod_{j=1}^{3} T_j(b) \quad \ldots (5.17)$$

for s–p transition.

The integrals in equations (5.16) and (5.17) are

evaluated numerically following the procedure of Kumar and Srivastava (155) and Kumar et al(154). With the axis of quantization perpendicular to q, the amplitude F^{GA} for $m_3'=0$ vanishes and $|F^{GA}|^2$ for $m_3'=1$ and $m_3'=-1$ are the same. Thus the Glauber differential cross-section becomes,

$$\left(\frac{d\sigma}{d\Omega}\right)_{GA} = \frac{k_f}{k_i}\left|F^{GA}(q)\right|^2, \qquad \text{s-s transition} \quad \ldots (5.18)$$

$$\left(\frac{d\sigma}{d\Omega}\right)_{GA} = 2\,\frac{k_f}{k_i}\left|F^{GA}(q,m=1)\right|^2, \qquad \text{s-p transition} \quad \ldots (5.19)$$

iii) Evaluation of second Born term

The second Born term has been evaluated by considering the lithium atom as one electron system with inert core. Using the closure approximation and following the procedure outlined by Byron and Latour (70), we get the simplified second Born term (f_{B2})

$$f_{SB2} = 4D(\alpha_j)\, J_j \qquad \ldots (5.20)$$

where $D(\alpha_j)$ is the linear combination of differential operators and is expressed for this transition as

$$D(\alpha_j) = \left[\sum_{j=1}^{2} a_j + \sum_{j=3}^{7} a_j\left(-\frac{\partial}{\partial\alpha_i}\right) + \sum_{j=8}^{12} a_j\left(-\frac{\partial}{\partial\alpha_j}\right)^2 + \sum_{j=13}^{15} a_j\left(-\frac{\partial}{\partial\alpha_j}\right)^3\right] \qquad \ldots (5.21)$$

where

$$J_j = (I_i+I_f)/\alpha_j^3 + \left(\frac{dI_i}{d\alpha_j^2} + \frac{dI_f}{d\alpha_j^2}\right)/\alpha_j - \frac{q^2(q^2+2\alpha_j^2)}{\alpha_j^2(q^2+\alpha_j^2)^2}\, I_{i,f}(\alpha_j=0) \qquad \ldots (5.22)$$

Here

$$I_i(\alpha_j^2) = \int_0^1 \frac{dt}{[\alpha_j^2 t + t(1-t)q^2]^{1/2}\,[(\alpha_j^2+2\omega_{if})t + 2(\bar{\omega}-\omega_{if}) - 2ip(\alpha_j^2 t + t(1-t^2)q^2)^{1/2}]} \quad \ldots (5.23)$$

The expression for I_f is obtained simply by substituting ω_{if} with $-\omega_{if}$ and $\bar{\omega}-\omega_{if}$ with $\bar{\omega}$. ω_{if} is the energy difference between the ground state ω_i and the excited state ω_f of the lithium atom. Also $p^2 = k_i^2 - 2\bar{\omega}$ and $k_f^2 = k_i^2 - 2\omega_{if}$, $\bar{\omega}$ is the average energy of the excitation. The equation (5.23) and (5.22) are evaluated numerically. The value of the integral as given by equation (5.23) is also required in the limit $\alpha \to 0$ for the complete evaluation of equation (5.20). The real and imaginary part of this integral in that limit are taken from the paper of Byron and Latour (70) and are given as

$$\mathrm{Re}I_{i,f}(\alpha=0) = \frac{\pi}{q(p^2q^2 + 4\omega_i\omega_f)^{1/2}} \quad \ldots (5.24)$$

$$\mathrm{Im}I_{if}(\alpha=0) = \frac{1}{q(p^2q^2+4\omega_i\omega_f)^{1/2}} \ln \left[\frac{(p^2q^2+4\omega_i\omega_f)^{1/2} + pq}{4\omega_i\omega_f}\right]^2 \quad \ldots (5.25)$$

The average excitation energy $\bar{\omega}$, required for the calculation of f_{SB2} is chosen following the prescription of Byron and Latour and Wintersand Vanderpoorten(92). We use two different values for the mean excitation energy(i) one lying very near the ionization threshold (5.342 eV) and (ii) the other lying just above the 3P level (3.845 eV).

(iv) Evaluation of f_{G2} and f_{G3}

The expression for second and third order Glauber terms can be obtained in a straightforward way following Yates(3) and Vanderpoorten and Winters(146)

$$f_{G2} = \frac{4i}{k_i} D(\alpha) \left[\frac{1}{\alpha^2 (q^2+\alpha^2)} \ln\left(\frac{q^2+\alpha^2}{q\alpha}\right) \right] \qquad \ldots (5.26)$$

and

$$f_{G3} = -\frac{2}{k_i^2} D(\alpha) \left[\frac{1}{\alpha^2 (q^2+\alpha^2)} \left\{ 2\ln\left(\frac{q^2+\alpha^2}{q\alpha}\right) + \frac{\pi^2}{6} - A(q/\alpha) \right\} \right] \qquad \ldots (5.27)$$

where the function $A(q/\alpha)$ is expressed as

$$A(q/\alpha) = 2\ln^2(q/\alpha) + \pi^2/6 + \sum_{n=1}^{\infty} (-q^2/\alpha^2)^n / n^2, \quad q \leq \alpha$$

$$= -\sum_{n=1}^{\infty} \frac{(\alpha^2/q^2)^n}{n^2}, \quad q > \alpha \qquad \ldots (5.28)$$

Finally, the exchange is taken into account through the Bonham-Ochkur(179, 134) approximation.

5.2.2 Results and discussion

(A) Generalised oscillator strength

In order to assess the reliability of the bound state wavefunction, we have computed the generalised oscillator strength (gos) in the length and velocity formulation equation (5.7-5.9), as defined within the concept of Born approximation. The results of gos using the present wavefunction is compared with the earlier calculations of Tripathi(13) using the Hartree-Fock wavefunction of the Weiss(21). We have also computed the gos

in length formulation using the Rapp and Chang(52) wavefunction obtained with and without frozen core approximation. Most of earlier calculations for this transition (2s-3s) use this wavefunction for simplicity. The figure (5.1) shows the theoretical values of the gos using the variety of wavefunctions along with the measurements of Shuttleworth et al (171). Measured values of the generalized oscillator strength exist over a small region of q lying between 1.3×10^{-1} and 3.4×10^{-2} au. The measurements lie significantly above the Born calculation. This lack of agreements between the theoretical and measured generalised oscillator strength is due to the failure of the Born approximation, owing to coupling to other states. However, the present wavefunction predicts the gos which are in better agreement with those calculated from the Weiss(21) wavefunction than those calculated from the Rapp and Chang(52) wavefunction. To illustrate this point, we present in table 5.2, the values of gos as obtained using various wavefunctions.

(B) Scattering amplitude

Before, we present our results for differential scattering cross-section (DCS), it is worthwhile to examine the variation of the different components of the scattering amplitude. Table 5.3 contains the values of different components of the scattering amplitude. The figure (5.2), displays the variation of the scattering amplitude with scattering angles at 200 eV. It is seen that real part of the simplified second

Born term (f_{SB2}) remain higher throughout the angular region for the first choice ($\bar{\omega}$ = 5.342 eV) of the average excitation energy compared to the second choice ($\bar{\omega}$ = 3.845 eV). Concerning the imaginary part, we see that the different choice of $\bar{\omega}$, do not have any such effect as far as the real part. It is also noted that at large scattering angle, the real part dominates strongly, but at small scattering angle, it deviates from the imaginary part by a factor of 2. The behaviour of f_{G3} and f_{B1} is very similar. They fall off very rapidly in low angular region and pass through the minima and maxima in the angular region of 20^{o}-50^{o} and decreases monotonically with the increase of scattering angle. This feature differs very much in comparison to the elastic results of Tayal et al(163), where f_{G3} dominates the real part for wide range of scattering angles. The trend of variation of the amplitude is not very different at higher energies.

(c) Differential scattering cross-section

The figures (5.3-5.6) display our differential scattering cross-sections at 20, 60, 100 and 200 eV respectively. The calculated differential cross-sections in first Born, Glauber approximation, simplified second Born, modified Glauber and eikonal Born series approximations are given in tables (5.4-5.5) at selected angles in the energy region of 20-200 eV.

Figures (5.3-5.4) show the results of our calculation

for DCS obtained in the first Born, Glauber, second Born, EBS and MG approximation at 20 and 60 eV respectively. The present calculations are compared with recent theoretical calculations of Winters and Vanderpoorten (92) and Sharma et al(142) and with the experimental measurements of Williams et al(187). It is clearly seen that at small angles ($\theta \lesssim 10^{o}$) the first Born results falls off more slowly but that as the scattering angle increases, it decreases far too rapidly. The failure of the first Born approximation at large momentum transfer for inelastic processes is well known. The Glauber approximation also does not give any better representation of the shape of the experimental curve although it falls off more slowly compared with the first Born approximation. The EBS and second Born results are very close to one another and overestimate the cross-section compared with the experimental data indicating the poor convergence of the Born series for s-state excitation. The MG and EBS are in relatively good agreement with experimental data at small angles ($\theta \lesssim 30^{o}$) both giving the forward polarization peak. The MG results falls off sharply at intermediate angles passing through minima around 50^{o} which is more pronounced at 60 eV than 20 eV. The experimental data of Williams et al(18 also show a structure which is less pronounced and appears at a large angle compared with our MG results. At small scattering angles ($\theta \lesssim 30^{o}$) i.e. prior to the dip the DWBA results of Winters and Vanderpoorten (92) tend to underestimate

the experimental data, while beyond the dip i.e. at $\theta \geq 30^{o}$, the results show a secondary maxima around 50^{o}. Beyond 50^{o} DWBA results compare well with the measurements and are in better agreement with experiment than other model calculations presented here. The TPMB results of Sharma et al(142) show an improvement over the first Born approximation but in general follow very nearly the same pattern of variation as observed in the Glauber approximation. As the impact energy increases (see figure 5.3), the Glauber results merge with the TPMB results. At 60 eV, the measurement is only available upto $\theta \leq 30^{o}$, where our MG results compare well with the data.

The behaviour of the DCS at 100 and 200 eV is shown in figures 5.5 and 5.6 respectively. As the incident energy increases, there is hardly any difference between the second Born (SSBA) and EBS results. The MG results show a marked difference compared with EBS results except in the forward direction. Further, sharp minima exhibited at 60 eV become flat with the increase in energy. In the absence of any experimental data available at these energies it is difficult to assess the accuracy of the calculation. It is suggested that new independent measurements for these cross-sections would be highly desirable.

(d) Total cross-section

In figure (5.7) our total cross-sections in various models are compared with experimental measurements of Zajonc and

Gallagher(23) in the energy range 20-200 eV. It is apparent that the results in SSB, EBS and MG approximations overestimates the experimental cross-sections for energies less than 50 eV, whereas for energies $\gtrsim$ 50 eV, our results particularly in MG approximation are in better agreement with experimental data. There do not exist any other calculation in this energy range.

5.3 EXCITATION OF 2s-2p TRANSITION IN LITHIUM BY ELECTRONS

The electron impact excitation of the 2s-2p state of atomic lithium is of particular interest. Firstly, from an experimental point of view i.e. after the excitation of s-p transition in hydrogen and helium, it is the process about which the differential scattering cross-sections over a wide range of energy are available, secondly, the behaviour of perturbative approaches for s-p transition are rather different than that found for s-s transitions (39,65). For the present study, we have employed only modified Glauber (MG) approximation. For evaluating the scattering amplitude in this approximation (equation (5.3)), we need the Glauber amplitude (f_{GA}), the second term (f_{G2}) of the Glauber eikonal series and the second Born term of the Born series. For s-p transitions, the relationship between the various terms of Born and Glauber eikonal series are different in contrast to s-s transitions. For example in the case of s-p transitions, the second Glauber eikonal term f_{G2} is real with a phase factor

and the imaginary part is missing. Thus it is expected that f_{G2} should be comparable to the real part of the second Born term.

The 2s-2p excitation of lithium atom is composed of three processes, 2s-2p$_{\pm 1}$ and 2s-2p$_{o}$ where ± 1 and 0 indicate the eigenvalues ± 1 and 0 of the z-component of the orbital angular momentum of bound electron. The Glauber amplitude for 2s-2p$_{\pm 1}$ processes can be easily computed by using the equations (5.4, 5.17 and 5.19) as discussed earlier in the Section (5.2.1). Here, the z-direction of the system is choser to be perpendicular to the momentum transfer. The second term f_{G2} of GES for this process can also be calculated in the closed form following the procedure of Yates(3). As for the second Born term of the 2s-2p$_{\pm 1}$ processes, we shall evaluate it in the closure approximation and shall follow the approach as outlined by Gein(175) for excitation of hydrogen.

(i) Evaluation of second Born term

We shall consider the lithium atom as one electron system with the use of Hartree-Fock(HF) wavefunction. We have used the wavefunction for the initial (2s) state as given by Clementi and Roetti(55) and of Stone (132) for the final (2p) state. The 2p-state wavefunction is of one term. These are given as

$$\phi_{2s}(\vec{r}) = \left(\sum_{i=1}^{2} A_i e^{-\xi_i r} + \sum_{i=3}^{6} A_i r\, e^{-\xi_i r} \right) Y_{oo}(\hat{r})$$

$$\phi_{2p}(\vec{r}) = c \exp(-\zeta r) Y_{1m_f}(\hat{r}) \qquad \ldots (5.29)$$

with c = 0.228255, ζ = 0.5227 and m_f is the magnetic quantum number for final p-state. A_i's and ξ_i's are taken from element and Roetti(55).

The simplified second Born amplitude is given by (175)

$$f_{SB2} = \frac{2}{\pi^2}\int d\vec{k}\ \frac{1}{k_f^2 k_i^2}\ \frac{1}{(k^2-p_i^2-i\varepsilon)}\ \langle f|\ e^{i\vec{q}.\vec{r}} - e^{i\vec{k}_i.\vec{r}} - e^{-i\vec{k}_j.\vec{r}} + 1\ |i\rangle \qquad \ldots (5.30)$$

where $p_i^2 = k_i^2 - 2\bar{\omega}$.

The absolute value of the product of the radial part of the atomic orbitals as given by equation (5.29) can be written as

$$\phi_{2p}^{\otimes}\phi_{2s} = \sum_{j=1}^{2} c_j r\ e^{-\alpha_j r} + \sum_{j=3}^{6} c_j r^2\ e^{-\alpha_j r} \qquad \ldots (5.31)$$

where the constants c_j's and α_j's are given as

$c_1 = -0.2600714$, $c_2 = -0.0704254$, $c_3 = 9.0417\times10^{-5}$

$c_4 = 0.0915639$, $c_5 = 0.0432158$, $c_6 = -0.0987463$

$\alpha_1 = 2.999$, $\alpha_2 = 5.22143$, $\alpha_3 = 0.90620$

$\alpha_4 = 1.18325$, $\alpha_5 = 1.5927$, $\alpha_6 = 2.1547$

Because of 2p-state, the amplitude for the excitation to a particular magnetic sublevels are given as

$$f_{SB2}^{2p_{\pm1}} = \mp\frac{1}{\sqrt{2}}\left[(f_{SB2}^{2p})_x \pm i(f_{SB2}^{2p})_y\right] \qquad \ldots (5.32a)$$

$$f_{SB2}^{2p_0} = \left[f_{SB2}^{2p}\right]_z \qquad \ldots (5.32b)$$

Considering the first term of the equation (5.31) and substituting the same in equation (5.30) and carrying the integration

over the coordinate variables in the matrix element part (indicated by $\langle\ \rangle$) analytically, one obtains for the first term as

$$f_{SB2}^{I,2p_{\pm1}} = \frac{32\sqrt{2}\,i\pi}{\pi^2} \sum_{j=1}^{2} c_j\alpha_j \left[\int \frac{d^3\vec{k}}{(k^2-p_i^2-i\varepsilon)k_i^2k_f^2} \right.$$
$$\left. \times\left(\frac{q_x \mp iq_y}{(q^2+\alpha_j^2)^3} - \frac{k_{ix} \mp k_{iy}}{(k_i^2+\alpha_j^2)^3} + \frac{k_{fx} \mp k_{fy}}{(k_f^2+\alpha_j^2)^3}\right)\right] \quad \ldots (5.33)$$

$$= 16\sqrt{2}(i\pi) \sum_{j=1}^{2} c_i\alpha_i \frac{\partial^2}{\partial\alpha_j^2}\left(\frac{1}{\alpha_j^2}(J_{ix} \mp iJ_{iy})\right.$$
$$\left. - \frac{1}{\alpha_j^2}(J_{fx} \mp J_{fy}) - \frac{q^2}{\alpha_j^2(q^2+\alpha_j^2)}\times(q_x \mp iq_y)I\right) \quad \ldots (5.34)$$

where J_{ix}, J_{iy}, J_{fx} and J_{fy} are components of the vectors J_i and J_f on the x and y axes respectively. J_i and J_f are given by

$$\vec{J}_i = \frac{1}{\pi^2}\int d^3\vec{k}\ \frac{1}{(k^2-p_i^2-i\varepsilon)}\ \frac{1}{k_f^2}\ \frac{\vec{k}_i}{(k_i^2+\alpha^2)} \quad \ldots (5.35a)$$

$$\vec{J}_f = \frac{1}{\pi^2}\int d^3\vec{k}\ \frac{1}{(k^2-p_i^2-i\varepsilon)}\ \frac{1}{k_i^2}\ \frac{\vec{k}_f}{(k_f^2+\alpha^2)} \quad \ldots (5.35b)$$

Similarly for the second term of equation (5.31), the f_{SB2} can be obtained from the first term and is given as

$$f_{sB2}^{II,2p_{\pm1}} = \sum_{j=3}^{6} c_j\left(-\frac{\partial}{\partial\alpha_j}\right)\left[\alpha_j f_{SB2}^{I,2p_{\pm1}}\right]$$
$$= 2\sum_{j=3}^{6}\alpha_j c_j\left(\frac{\partial}{\partial\alpha_j^2}\right)\left[f_{SB2}^{I,2p_{\pm1}}\right] \quad \ldots (3.36)$$

Using the well known Feymman's (144) Technique of integration and following the procedure given by Gien(175), we can write finally the complete expression of scattering amplitude for $2p_{\pm 1}$ as

$$f^{2p_{\pm 1}}_{SB2} = 16\sqrt{2}(i\pi)\, e^{\pm i\phi q}\left[\sum_{j=1}^{2} c_j\alpha_j\left[\left\{\frac{2(A_1+C_1)}{\alpha_j^6} - \frac{2(A_2+C_2)}{\alpha_j^4} + \frac{(A_3+C_3)}{\alpha_j^2} - \frac{2q^2(q^4+3\alpha_j^2q^2+\alpha_j^4)}{\alpha_j^6(q^2+\alpha_j^2)^3} I\right\} q_\perp + \left\{\frac{2B_1}{\alpha_j^6} - \frac{2B_2}{\alpha_j^4} + \frac{B_3}{\alpha_j^2}\right\} k_{f\perp} + \left\{-\frac{2D_1}{\alpha_j^6} + \frac{2D_2}{\alpha_j^4} - \frac{D_3}{\alpha_j^2}\right\} k_{i\perp}\right] - \sum_{j=3}^{6} c_j\left[\left\{\frac{2(A_1+C_1)}{\alpha_j^6} - \frac{2(A_2+C_2)}{\alpha_j^4} + \frac{(A_3+C_3)}{\alpha_j^2} - \frac{2q^2(q^4+3\alpha_j^2q^2+\alpha_j^4)}{\alpha_j^6(q^2+\alpha_j^2)^3} I\right\} q_\perp + \left\{\frac{2B_1}{\alpha_j^6} - \frac{2B_2}{\alpha_j^4} + \frac{B_3}{\alpha_j^2}\right\} k_{f\perp} + \left\{-\frac{2D_1}{\alpha_j^6} + \frac{2D_2}{\alpha_j^4} - \frac{D_3}{\alpha_j^2}\right\} k_{i\perp} + \left\{-\frac{12(A_1+C_1)}{\alpha_j^6} + \frac{12(A_2+C_2)}{\alpha_j^4} - \frac{6(A_3+C_3)}{\alpha_j^2} + 2(A_4+C_4) + \frac{12q^2(q^6+4q^4\alpha_j^2+6q^2\alpha_j^4+4\alpha_j^6)}{\alpha_j^6(q^2+\alpha_j^2)^4} I\right\} q_\perp + \left\{-\frac{12B_1}{\alpha_j^6} + \frac{12B_2}{\alpha_j^4} - \frac{6B_3}{\alpha_j^2} + 2B_4\right\} k_{f\perp} + \left\{\frac{12D_1}{\alpha_j^6} - \frac{12D_2}{\alpha_j^4} + \frac{6D_3}{\alpha_j^2} - 2D_4\right\} k_{i\perp}\right]\right] \quad \ldots (5.37)$$

where

$$A_1 = I_i(\alpha_j^2) + \int_0^1 \frac{x\,dx}{\Lambda(p_i - P + i\Lambda)(p_i + P + i\Lambda)}$$

$$- \frac{i}{2}\int_0^1 \frac{x\,dx}{P^3} \ln\left(\frac{p_i - P + i\Lambda}{p_i + P + i\Lambda}\right)$$

$$- \frac{i}{2}\int_0^1 \frac{x\,dx}{P^2}\left(\frac{1}{p_i - P + i\Lambda} + \frac{1}{p_i + P + i\Lambda}\right) \quad \ldots (5.38)$$

$$B_1 = -\frac{i}{2}\int_0^1 dx\,\frac{1}{P^3}\,\ell n\left(\frac{p_i-P+i\Lambda}{p_i+P+i\Lambda}\right)$$

$$-\frac{i}{2}\int_0^1 \frac{dx}{P^2}\left(\frac{1}{p_i-P+i\Lambda}+\frac{1}{p_i+p+i\Lambda}\right) \qquad \ldots (5.39)$$

$$A_2 = \frac{d}{d\alpha_j^2}A_1, \qquad A_3 = \frac{d^2}{d(\alpha_j^2)^2}A_1 \text{ and } A_4 = \frac{d^3}{d(\alpha_j^2)^3}A_1$$

$$B_2 = \frac{d}{d\alpha_j^2}B_1, \qquad B_3 = \frac{d^2}{d(\alpha_j^2)^2}B_1 \text{ and } B_4 = \frac{d^3}{d(\alpha_j^2)^3}B_1$$

in which

$$I_i(\alpha_j^2) = \int_0^1 \frac{dx}{\left[\alpha_j^2x+x(1-x)q^2\right]^{1/2}\left\{(\alpha_j^2+2\omega_{if})x+2(\bar{\omega}-\omega_{if})-2ip_i\left[\alpha_j^2x+x(1-x)q^2\right]\right\}}$$

$$I_f(\alpha_j^2) = \int_0^1 \frac{dx}{\left[\alpha_j^2x+x(1-x)q^2\right]^{1/2}\left\{(\alpha_j^2-2\omega_{if})x+2\bar{\omega}-2ip_i\left[\alpha_j^2x+x(1-x)q^2\right]^{1/2}\right\}}$$

$$P = (k_f^2+x^2q^2+2x\vec{k}_f\cdot\vec{q})^{1/2}$$

$$\Lambda = \left\{\left[\alpha_j^2+q^2(1-x)\right]x\right\}^{1/2} \qquad \ldots (5.40)$$

ω_{if} is the energy difference between the 2s and 2p state.

By interchanging the $\vec{k}_i$ with $\vec{k}_f$ everywhere and $I_i(\alpha_j^2)$ with $I_f(\alpha_j^2)$ in the equation (5.38-5.39), one can obtain the expressions for C_1 and D_1. The expressions for C_2, C_3, C_4 and D_2, D_3, D_4 can be obtained by carrying out order order derivatives with respect to α_j^2 of C_1 and D_1 analogous to A_1 and B_1. $q_\perp$, $k_{f_\perp}$ and $k_{i_\perp}$ are algebraic components

of $\vec{q}$, $\vec{k}_f$ and $\vec{k}_i$ on the plane perpendicular to the z-axis. In this plane, $q_\perp$, $k_{f_\perp}$ and $k_{i_\perp}$ are all referred to $\vec{q}$ as the common positive direction of the axis. Thus

$$q_\perp = q$$

$$k_{f\perp} = (k_i\cos\theta - k_f)k_i/q \qquad \ldots (5.41a)$$

$$k_{i\perp} = (k_i - k_f\cos\theta)k_i/q \qquad \ldots (5.41b)$$

where θ is the scattering angle. All the vectors $\vec{q}$, $\vec{k}_{i\perp}$ and $\vec{k}_{f\perp}$ have the same azimuthal angles ϕ_q.

It is worth mentioning that with the usual choice of $\vec{q}$ being perpendicular to z axis, the Glauber amplitude for the process $2s-2P_o$ is vanishing and so is the case with the f_{G2} term. However, the corresponding second Born term is not vanishing. The expression for $f_{SB2}^{2P_o}$ can be derived easily from the equation (5.37) where $q_\perp$ is replaced by q_z. This with the usual choice of z-axis direction, the $f_{fB2}^{2P_o}$ is given by the same equation (5.37), in which $q_\perp = q_z = 0$ and $k_{fz} = k_{iz} = k_i k_f \sin\theta/q$.

(ii) Evaluation of f_{G2} term

The explicit evaluation of f_{G2} for s-p type of transition can be easily carried out following the procedure of Yates(3). Considering the first term of equation (5.31), we can write down the

$$f_{G2}^{I,2P_{\pm 1}} = \frac{8\sqrt{2}\,\pi}{k_i} e^{\mp i\phi_q} \sum_{j=1}^{2} C_j \left[\left(-\frac{\partial}{\partial\alpha_j}\right)\left(-\frac{1}{2\alpha_j}\right) \times \frac{1}{\alpha_j^3} \frac{1}{\xi_j(1+\xi_j^2)} \right.$$

$$\left. \left\{ (\xi_j^2-1)\ln(1-\xi_j^2) - \xi_j^2 \ln \xi_j^4 \right\} \right] \qquad \ldots (5.42)$$

with $\xi_j = q/\alpha_j$

The second term can be easily generated by carrying out one more differentiation with respect to α_j. Thus, finally one can obtain

$$f_{G2}^{2P\pm1} = \frac{8\sqrt{2}\,\pi}{k_i} e^{\pm i\phi_q}\Bigg[\sum_{j=1}^{2} C_j\Big[\Big(-\frac{\partial}{\partial\alpha_j}\Big)\Big(-\frac{1}{2\alpha_j}\Big)\frac{1}{\alpha_j^3\xi_j(1+\xi_j^2)}\Big\{(\xi_j^2-1)\ell n(1-\xi_j^2)^2-\xi_j^2\ell n\xi_j^4\Big\}\Big] + \sum_{j=3}^{6} C_j\Big[\Big(-\frac{\partial}{\partial\alpha_j}\Big)\Big(-\frac{\partial}{\partial\alpha_j}\Big)\Big(-\frac{1}{2\alpha_j}\Big) \times \frac{1}{\alpha_j^3\xi_j(1+\xi_j^2)}\Big\{(\xi_j^2-1)\ell n(1-\xi^2)^2-\xi_j^2\ell n\,\xi_j^4\Big\}\Big]\Bigg] \quad \ldots (5.43)$$

(iii) Evaluation of exchange amplitude

In order to have a better comparison with other calculations which make allowance for electron exchange, and also with experiment, we have calculated eikonal exchange amplitude within the frame work of Bonham-Ochkur approximation following the formulation of Franco and Halpern(177). The advantage of calculating the exchange amplitude in this formulation is that it can be obtained with ease in closed form containing a well defined phase which can be used unambiguously with direct amplitude for calculating the differential scattering cross-section. With the choice of z-axis, the final expression for eikonal exchange amplitude $g_{ex}^{2P\pm1}$ is given as

$$g_{ex}^{2P\pm1} = \frac{C}{4\pi}(\eta+i)\, e^{\pm i\phi_q}\Bigg[\sum_{j=1}^{2} C_j\alpha_j^{-i\eta-1}(\alpha_j^2+q^2)^{i\eta-3}(4\alpha_j^2+i\eta(q^2-\alpha_j^2)) - \sum_{j=3}^{6} C_j\frac{\partial}{\partial\alpha_j}\Big[\alpha_j^{i\eta-1}(\alpha_j^2+q^2)^{i\eta-3}(4\alpha_j^2+i\eta(q^2-\alpha_j^2))\Big]\Bigg] \quad \ldots (5.44)$$

where

$$C = \frac{8\pi^2 \nu_i \exp(\pi\nu/2)}{K^{2+i\nu}\sinh\pi\eta}$$

Here K is equal to $(k_i^2+k_f^2)/\sqrt{2}$ and $\eta = -1/v_i$.

5.3.1 Results and discussions

The differential cross-section (DCS) for the excitation of $2s-2P_{\pm1}$ transition of lithium by electron impact at 100 eV using modified Glauber (MG) approximation is shown in figure (5.8). The present results are compared with the conventional Glauber calculations, first Born results, the unitarised distorted wave polarised (UDPO) results of Kennedy et al(84) along with the recent measurements of Vuskovic et al(104). The other experimental DCS by Williams et al(187) is only available upto 60 eV. The Glauber calculations are in good agreement with the data at low scattering angles ($\theta < 20^o$) but it falls off rapidly at high scattering angles. The same comments also apply to first Born results. The UDPO results show a remarkably good agreement with the measurements of Vuskovic(104) in entire angular region. For the scattering angle $\theta > 20^o$, the present calculation overestimates the DCS by more than an order of magnitude in comparison with the measurements and the UDPO results. The values calculated in the MG approximation are very different than those obtained with conventional Glauber approximation. The removal of the deficiency of the DCS at intermediate and

large scattering angles suffered by the conventional Glauber amplitude by the replacement of f_{G2} by f_{SB2} leads to real improvement. Our comparison of Ref_{SB2} and f_{G2} shows that they agree to well within an order of magnitude at the energy considered here. The consideration of eikonal exchange hardly brings any change in the DCS at this energy. We believe that the poor convergence of the Born series is not responsible for large DCS at $\theta \gtrsim 20^{o}$. The contribution of higher order terms included through the Glauber approximation is not found to be enough. Their full contribution at least for some part of the interaction seems to be imperative.

Table 5.1 Coefficients and exponents for the orbitals appearing in the equation (5.4)

Orbital	Clementi type coefficient	Power of r	Exponent
ϕ_{1s}	0.89652	1	2.47580
	0.11239	1	4.68780
	-0.00039	2	0.75000
	0.00766	2	1.77100
	0.00074	2	0.61830
ϕ_{2s}	-0.14437	1	2.47580
	-0.01602	1	4.68780
	0.50009	2	0.75000
	-0.07864	2	1.77100
	0.56144	2	0.61830
ϕ_{3s}	0.09366	1	2.30142
	-0.92279	2	0.52233
	1.49432	3	0.39659

Table 5.2 Generalised Oscillator strength $f_{if}(q)$ for 2s–3s transition of lithium

Change in momentum q(a.u.)	W_{if}=0.122515(a.u.) Weiss		W_{if}=0.122604(a.u.) CIV3		W_{if}=0.122213 (a.u.) Rapp and Chang	
	Length	Velocity	Length	Velocity	with core length	without core length
0.005	3.1560(-5)	3.2695(-5)	3.2729(-5)	3.2152(-5)	2.9827(-5)	2.9299(-5)
0.020	5.0354(-4)	5.2121(-4)	5.2171(-4)	5.1253(-4)	4.4968(-4)	4.4977(-4)
0.035	1.5299(-3)	1.5833(-3)	1.5847(-3)	1.5569(-3)	1.3631(-3)	1.3645(-3)
0.050	3.0843(-3)	3.1909(-3)	3.1935(-3)	3.1376(-3)	2.7478(-3)	2.7512(-3)
0.110	1.3615(-2)	1.4058(-2)	1.4059(-2)	1.3819(-2)	1.2175(-2)	1.2193(-2)
0.300	4.8914(-2)	4.9841(-2)	4.9617(-2)	4.8907(-2)	4.5128(-2)	4.5226(-2)
0.500	3.3435(-2)	3.3341(-2)	3.3195(-2)	3.2894(-2)	3.2418(-2)	3.2554(-2)
0.700	9.4332(-3)	9.4056(-3)	9.2644(-3)	9.3366(-3)	9.6309(-3)	9.7301(-3)
0.900	1.3462(-3)	1.3375(-3)	1.3329(-3)	1.4574(-3)	1.4650(-3)	1.5111(-3)
1.000	3.7217(-4)	3.6469(-4)	3.7564(-4)	4.6648(-4)	4.3206(-4)	4.5862(-4)
1.300	2.4624(-6)	3.6539(-6)	1.4308(-6)	2.9226(-6)	1.2633(-7)	1.0558(-7)
1.400	9.8252(-6)	1.1736(-5)	7.7400(-6)	3.6330(-10)	4.0319(-5)	1.7538(-6)
1.500	1.2937(-5)	1.4508(-5)	1.0827(-5)	5.1576(-7)	6.5981(-6)	3.5619(-6)
2.000	1.9039(-6)	1.8299(-6)	1.7664(-6)	3.0005(-7)	7.1795(-7)	5.5254(-8)
2.100	5.4116(-7)	6.1782(-6)	8.1304(-7)	1.9090(-7)	2.0863(-7)	1.8120(-8)
2.200	2.9223(-7)	2.9918(-7)	2.8819(-7)	1.2146(-7)	1.5406(-8)	1.9625(-7)
2.400	6.0366(-10)	1.6148(-9)	8.3025(-11)	5.1106(-8)	1.3968(-7)	8.0509(-7)
2.500	4.8943(-8)	1.6279(-8)	4.1193(-8)	3.3744(-8)	3.0201(-6)	1.1022(-6)
3.000	4.3680(-7)	2.3408(-7)	4.2828(-7)	2.9460(-9)	8.8328(-7)	1.7675(-6)
5.000	1.2236(-7)	7.0765(-8)	1.2754(-7)	3.1894(-8)	2.1318(-7)	3.4819(-7)
10.000	1.0878(-9)	2.3097(-10)	1.0245(-9)	2.4095(-7)	1.3341(-9)	2.3618(-9)

Table 5.3 The scattering amplitudes for 2S–3S transition of lithium atom at 20 eV.

Scattering angle (deg)	f_{B1}	Ref_{SB2}	Imf_{SB2}	f_{G2}	f_{G3}	Ref_G	Imf_G
5	3.75	3.35	7.68	6.34	9.19(-1)	2.82	3.54
10	3.20	2.28	4.13	3.37	1.33	1.66	1.45
20	1.75	1.66	1.39	1.20	1.10	1.35(-1)	2.83(-1)
50	1.25(-2)	8.93(-1)	1.09	9.77(-1)	-6.99(-1)	-3.21(-1)	1.05(-1)
80	-1.49(-2)	6.85(-1)	4.95(-1)	4.57(-1)	9.53(-2)	-1.80(-1)	-7.04(-2)
100	-2.08(-3)	6.47(-1)	3.23(-1)	3.04(-1)	1.02(-1)	-1.12(-1)	-9.65(-2)
120	2.96(-3)	6.28(-1)	2.41(-1)	2.28(-1)	8.35(-2)	-7.08(-2)	-9.82(-2)
140	4.53(-3)	6.18(-1)	1.99(-1)	1.89(-1)	7.55(-2)	-4.78(-2)	-9.40(-2)
160	4.94(-3)	6.12(-1)	1.79(-1)	1.70(-1)	6.76(-2)	-3.63(-2)	-9.01(-2)

Table 5.4- Differential cross-sections $\frac{d\sigma}{d\Omega}(a_o^2 Sr^{-1})$ for electron impact excitation of lithium to 3S state at incident energies 20 and 60 eV

Scattering Angle (deg)	FBA	G	SSB	MG	EBS
			E = 20 eV		
5.0	9.74	1.75(+1)	1.19(+2)	7.36(+1)	1.06(+2)
10.0	7.12	4.90	5.60(+1)	2.89(+1)	4.20(+1)
20.0	2.15	1.08	1.69(+1)	6.08	1.01(+1)
50.0	3.32(-4)	1.11(-1)	1.86	3.55(-1)	1.98
80.0	5.08(-4)	3.02(-2)	6.18(-1)	2.22(-1)	5.11(-1)
100.0	3.37(-4)	1.82(-2)	4.64(-1)	2.58(-1)	3.55(-1)
120.0	2.74(-4)	1.26(-2)	4.08(-1)	2.83(-1)	3.14(-1)
140.0	2.39(-4)	9.73(-3)	3.82(-1)	2.96(-1)	3.02(-1)
160.0	2.20(-4)	8.35(-3)	3.70(-1)	3.02(-1)	2.99(-1)
			E = 60 eV		
5.0	9.85	1.18(+1)	2.71(+1)	2.13(+1)	2.39(+1)
10.0	3.65	1.95	8.44	4.95	6.29
20.0	8.53(-2)	1.61(-1)	9.49(-1)	3.18(-1)	9.35(-1)
50.0	3.54(-2)	1.89(-2)	6.36(-2)	2.96(-3)	5.29(-2)
80.0	4.80(-5)	3.36(-3)	3.22(-2)	1.09(-2)	2.78(-2)
100.0	2.69(-5)	1.63(-3)	2.78(-2)	1.46(-2)	2.58(-2)
120.0	1.65(-5)	9.86(-4)	2.59(-2)	1.66(-2)	2.50(-2)
140.0	1.17(-5)	7.09(-4)	2.50(-2)	1.77(-2)	2.46(-2)
160.0	9.57(-6)	5.87(-4)	2.46(-2)	1.82(-2)	2.45(-2)

Table 5.5- Differential cross-sections $\frac{d\sigma}{d\Omega}(a_o^2 Sr^{-1})$ for electron impact excitation of lithium to 3s state at incident energies 100 and 200 eV

Scattering angle (deg)	FBA	G	SSB	MG	EBS
			E=100 eV		
5.0	8.54	8.81	1.55(+1)	1.36(+1)	1.36(+1)
10.0	1.66	1.15	3.37	2.35	2.79
20.0	1.25(-3)	1.09(-1)	2.65(-1)	1.15(-1)	2.72(-1)
50.0	4.20(-5)	4.72(-3)	1.61(-2)	1.13(-3)	1.35(-2)
80.0	1.21(-5)	7.93(-4)	9.41(-3)	3.67(-3)	8.98(-3)
100.0	4.93(-6)	3.87(-4)	8.47(-3)	4.69(-3)	8.44(-3)
120.0	2.60(-6)	2.36(-4)	8.07(-3)	5.27(-3)	8.22(-3)
140.0	1.47(-6)	1.54(-4)	7.85(-3)	5.70(-3)	8.08(-3)
160.0	1.32(-6)	1.43(-4)	7.82(-3)	5.76(-3)	8.06(-3)
			E=200 eV		
5.0	5.22	5.43	7.81	7.75	7.08
10.0	2.11(-1)	2.92(-1)	5.92(-1)	5.29(-1)	5.74(-1)
20.0	5.67	2.86(-2)	5.41	2.18(-2)	5.44
50.0	1.21(-5)	5.93(-4)	2.83(-3)	5.28(-4)	2.66(-3)
80.0	8.81(-7)	1.08(-4)	1.96(-3)	1.03(-3)	2.01(-3)
100.0	2.35(-7)	5.59(-5)	1.85(-3)	1.18(-3)	1.92(-3)
120.0	1.31(-7)	3.58(-5)	1.81(-3)	1.28(-3)	1.88(-3)
140.0	7.81(-8)	2.58(-5)	1.79(-3)	1.35(-3)	1.87(-3)
160.0	5.80(-8)	2.06(-5)	1.78(-3)	1.38(-3)	1.86(-3)

5.4 FIGURE CAPTIONS

Figure 5.1 The generalised oscillator strength for the 2s-3s transition of lithium atom.
Calculations: - - - - : CIV3 wavefunctions; ——— : Weiss wavefunctions; —·—·— : Rapp and Chang wavefunctions with core; — · · — : Rapp and Chang wavefunctions without core.
Experimental results: ⧖ data set 1; ⧗ : data set 2 (Shuttleworth et al(171)).

Figure 5.2 The various components of scattering amplitude for 2s-3s transition of lithium atom at 20 eV.
Calculations: ——— : Ref_{B2} with $\bar{\omega}$ = 5.342 eV; - - - - - - : Ref_{B2} with $\bar{\omega}$ = 3.845 eV; —·— : Imf_{B2} with $\bar{\omega}$ = 5.342 eV; —x— : Im_{fB2} with $\bar{\omega}$ = 3.845 eV; —··— : f_{G3} ; —···—: f_{B1}.

Figure 5.3 The differential scattering cross-section for the 2s-3s excitation of lithium atom by electron impact at 20 eV.
Calculations: - - - - : Present EBS; — · — :Present SSB; —:Present MG; —··—: results in FBA; —x— : results in GA; —x x— : results in TPMB(142); —···— : results in SSB(92); —— —: results in DWBA(92 ;●: Experimental data(187)

Figure 5.4 Same as figure (5.3) but at 60 eV.

Figure 5.5 Same as figure (5.3) but at 100 eV.

Figure 5.6 Same as figure (5.3) but at 200 eV

Figure 5.7 Total cross-sections for the 2s-3s transition of lithium atom.
Calculations: —·— : results in SSB; ——— : results in MG; - - - - - - - : results in EBS; —··—: resultsiin FBA; ●: Experimental data (23)..

Figure 5.8 The differential scattering cross-sections for the 2s-2p transition of lithium atom by electron impact at 100 eV.
Calculations: ——, present results in MG approach; —x— , results in UDWPOII(84); —∘— , results in GA approach (155); □ , first Born results (104); ●, Experimental data (104).

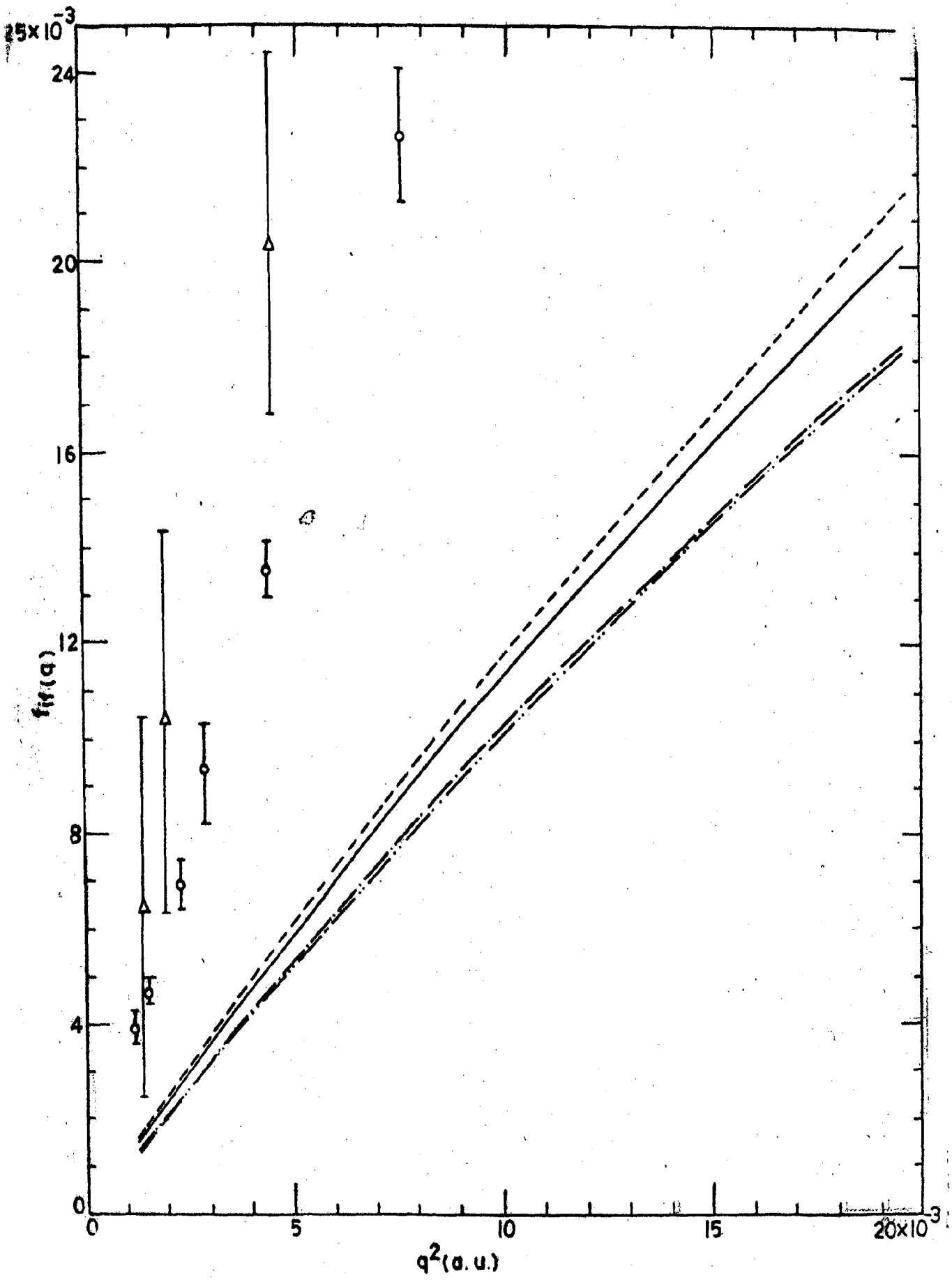

FIG. 5.1

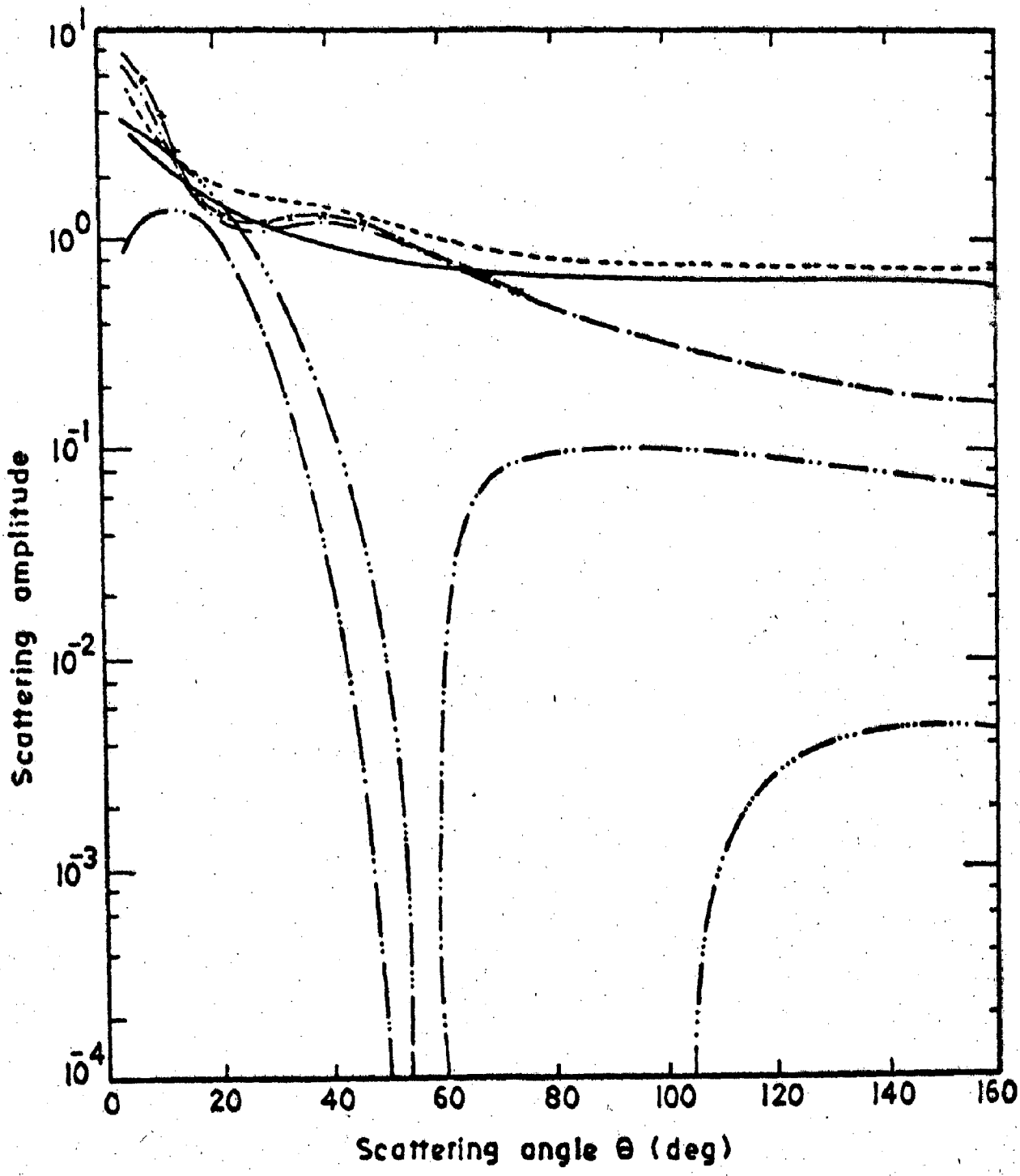
Scattering amplitude
10^{1}
10^{0}
10^{-1}
10^{-2}
10^{-3}
10^{-4}
0
20
40
60
80
100
120
140
160
Scattering angle θ (deg)

FIG. 5.2

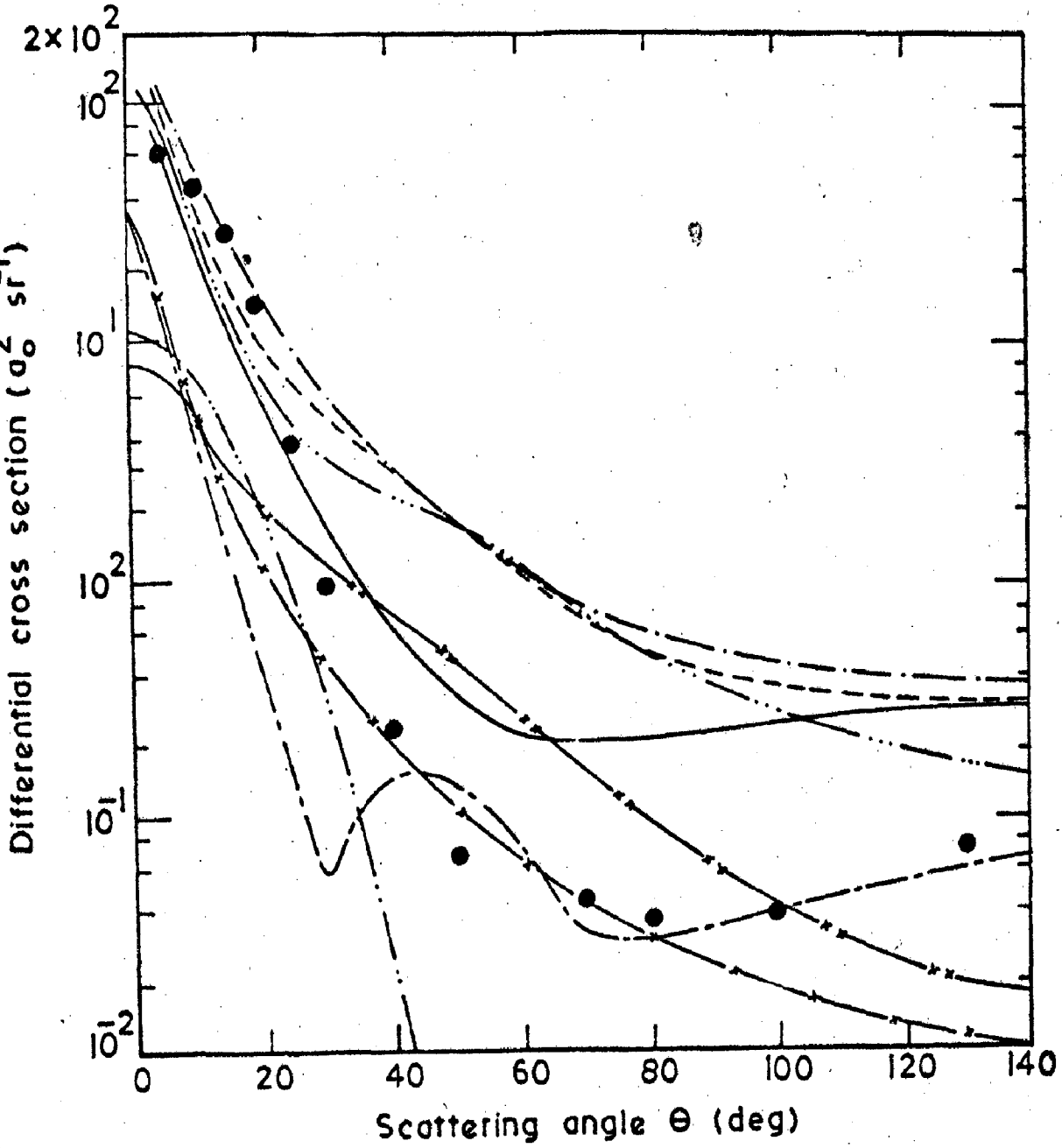
2×10²
10²
10¹
10²
10⁻¹
10⁻²
Differential cross section (a₀² sr⁻¹)
0
20
40
60
80
100
120
140
Scattering angle Θ (deg)

FIG. 5·3

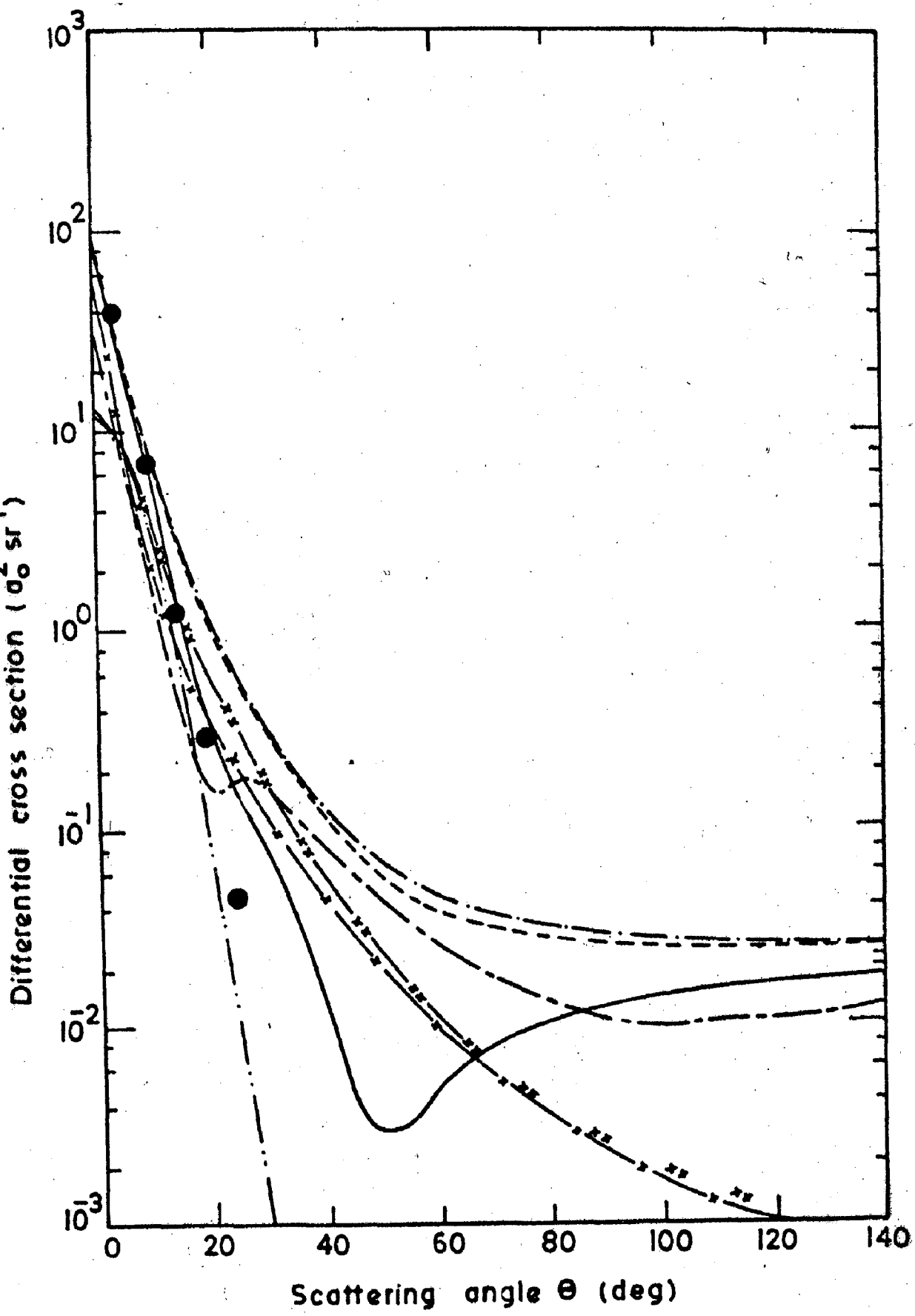
Differential cross section (a_0^2 sr^{-1})
10^3
10^2
10^1
10^0
10^{-1}
10^{-2}
10^{-3}
0
20
40
60
80
100
120
140
Scattering angle θ (deg)

FIG. 5.4

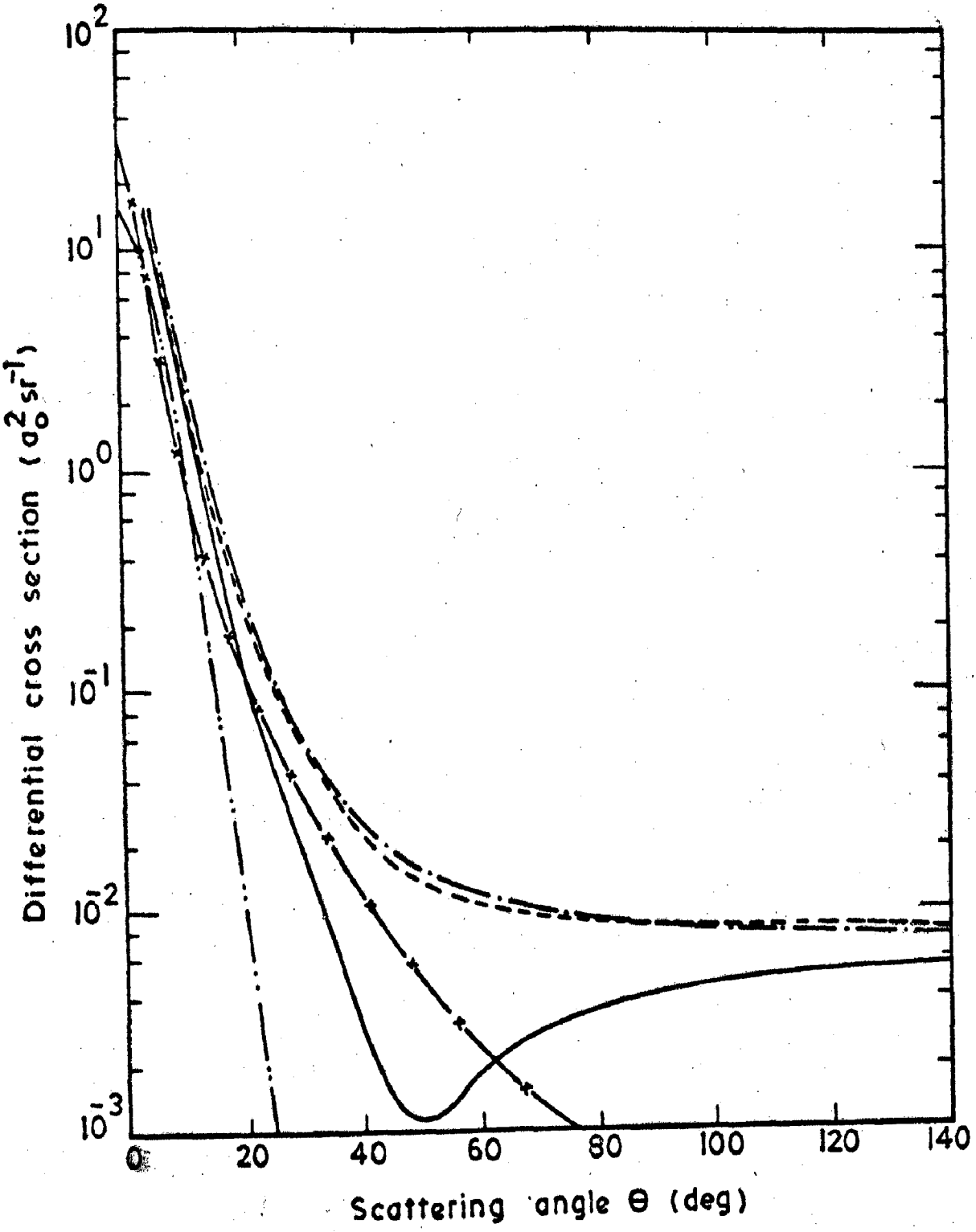
Differential cross section ($a_0^2 sr^{-1}$)
10^2
10^1
10^0
10^{-1}
10^{-2}
10^{-3}
0
20
40
60
80
100
120
140
Scattering angle Θ (deg)

FIG. 5.5

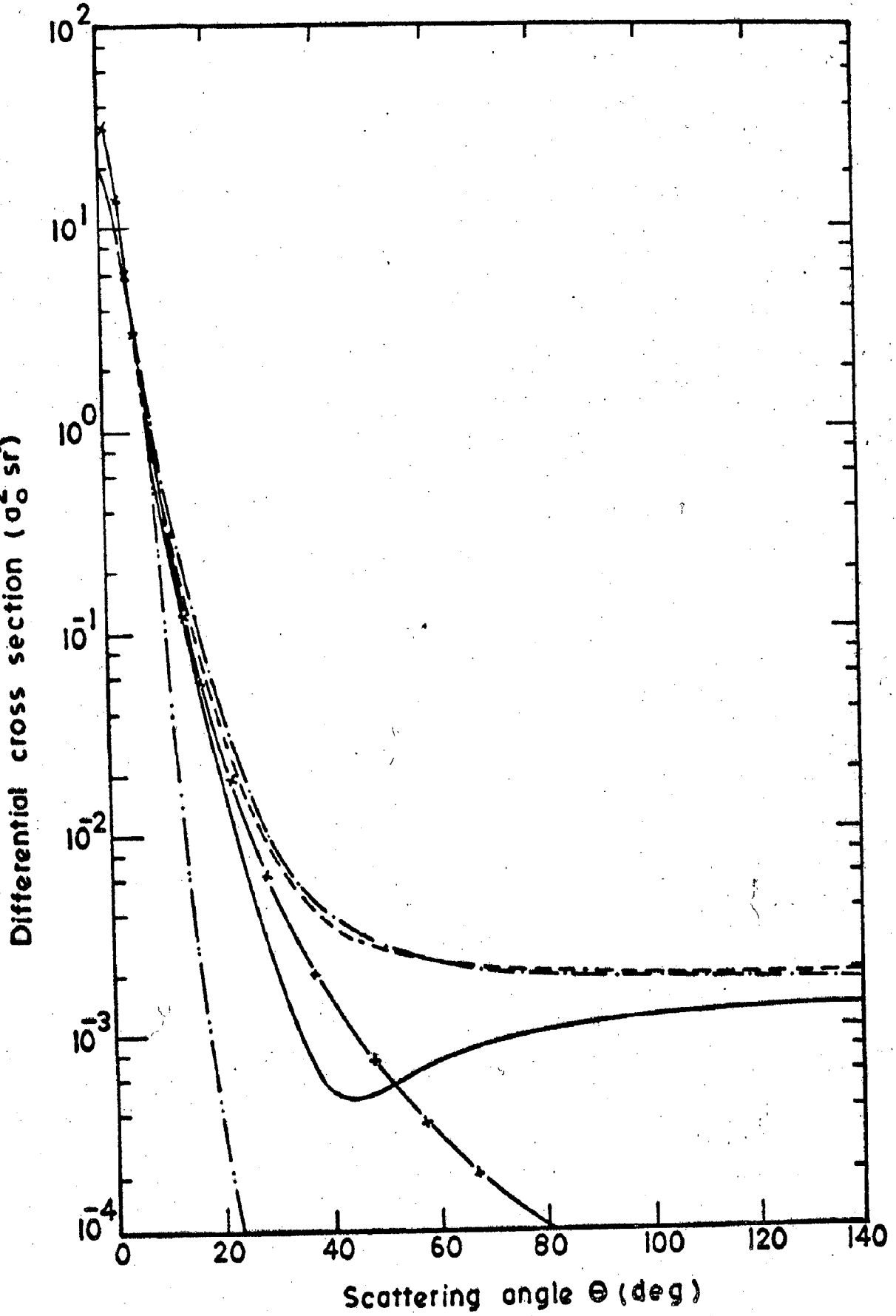
Differential cross section (a_0^2 sr^{-1})
10^2
10^1
10^0
10^{-1}
10^{-2}
10^{-3}
10^{-4}
0
20
40
60
80
100
120
140
Scattering angle Θ (deg)

FIG. 5·6

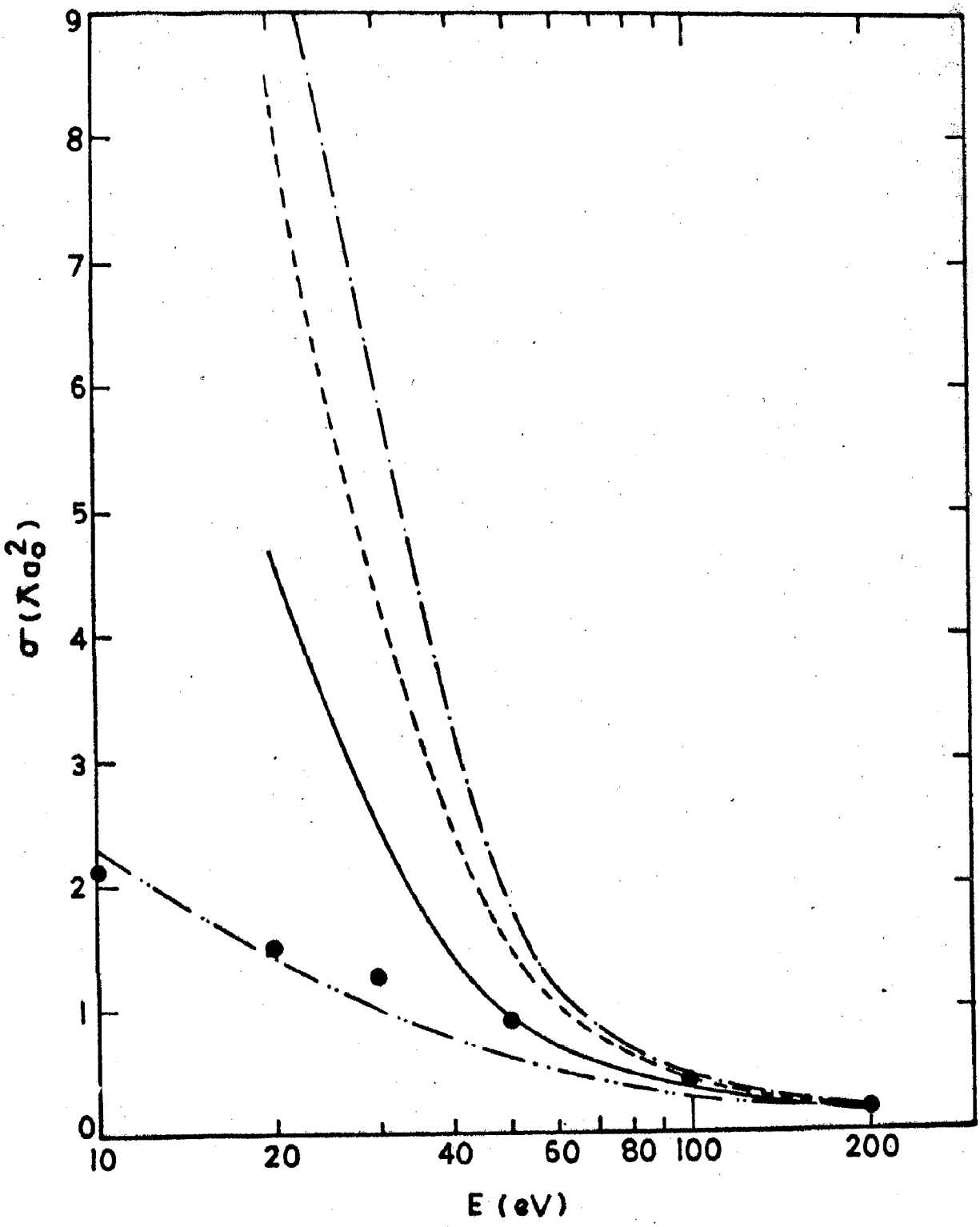

FIG. 5.7

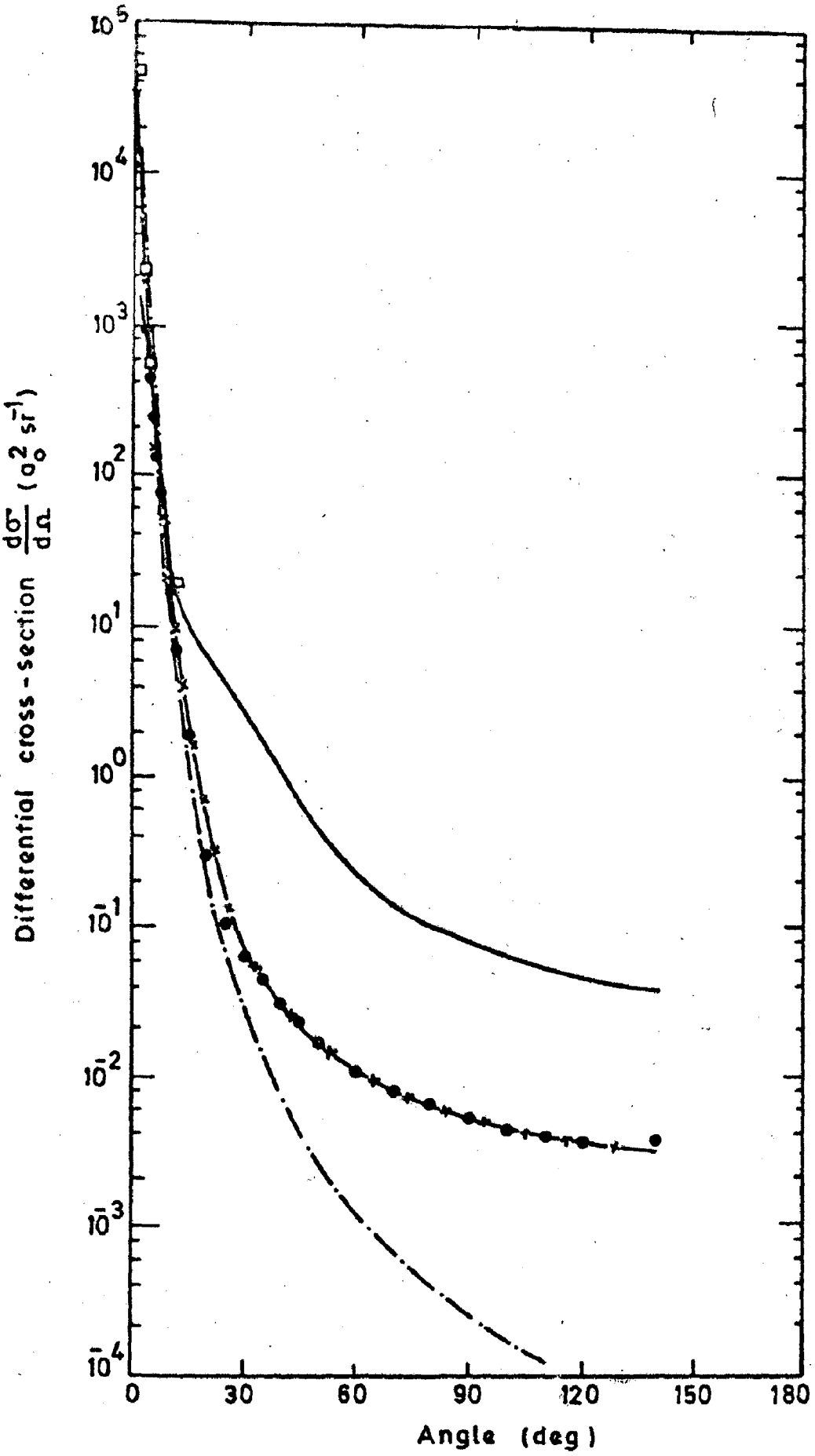
Differential cross-section $\frac{d\sigma}{d\Omega}$ (a_0^2 sr^{-1})
10^5
10^4
10^3
10^2
10^1
10^0
10^{-1}
10^{-2}
10^{-3}
10^{-4}
0
30
60
90
120
150
180
Angle (deg)

FIG.5·8

CHAPTER 6

SCATTERING OF HIGH ENERGY ELECTRONS AND X-RAYS FROM MOLECULES: THE TEN-ELECTRON SERIES: Ne, HF, H_2O, NH_3 AND CH_4

6.1 INTRODUCTION

High energy electron scattering plays an important role in the study of molecular structure (138). It has been well established (see Bonham and Fink(136)) that at high incident electron energies ($\geq$ 25 keV) where the first Born approximation is valid, there exist simple relationships between target properties and the results of a scattering experiment. Consequently such studies provide a wealth of information valuable in assessing the quality of molecular wavefunctions and in understanding chemical binding effects. There have been many experimental measurements for total (elastic + inelastic) cross-sections for scattering from various molecules. However, in recent years a few groups have started measuring the absolute elastic and inelastic intensities separately. In this regard, the work of Lahmam-Bennani et al(11) is worth mentioning. On theoretical side, a few attempts have also been made where high quality abinitio calculations of elastic and inelastic intensities for some simple medium sized molecules are performed.

Among the small and medium sized linear molecules, H_2,

D_2, CO, N_2 and O_2 have been studied the most. The early calculations (85) were based mostly on molecular HF wavefunctions. However, it is generally expected that a better agreement between experimental and theoretical results will be attained by configuration interaction (CI) wavefunctions instead of HF(176). Epstein and Stewart(80) have calculated the total and elastic X-ray scattering intensity for these molecules using a near HF quality wavefunction with extensive basis sets at experimental Re (internuclear separation) values. They have also carried out a multi-configuration self consistent field (MC-SCF) study on CO. However, this wavefunction was able to account for only 21% of correlation energy.

In an attempt to see how important a role electron correlation plays in the computed total and elastic electron scattering intensities, Breitenstein and collaborators (107) have carried out recently a series of moderately high quality CI calculations yielding about 60% of the correlation energy, for a series of linear molecules (CO, N_2, C_2H_2, O_2, F_2 and CO_2). Hirota et al(59) have also carried out an electron correlation study on N_2 but examined only the elastic scattering. It is remarkable to see that as the energetic quality of the wavefunction improves, i.e. as one goes from a near HF to HF and then to a CI type of wavefunction, the total electron scattering intensity functions move in the right direction, i.e. nearer to the experimental measurements.

Apart from considering the role of electron correlation in the target wavefunction, Thakkar, Tripathi and Smith(9)

examined some other aspects of scattering calculations including basis set effects and the difference between the usual elastic intensities for X-ray and electron scattering from nonvibrating but freely rotating diatomic molecules (H_2, N_2) and the fully elastic intensities for scattering from the J=0 state.

The other linear molecule which has been studied somewhat extensively is the CO_2 molecule. Two sets of new measurements one by Sasaki and collaborators(189) and the other by McClelland and Fink(81) have been reported recently. Sasaki and his collaborators(189) have also performed theoretical calculations for the electron scattering intensities using a HF molecular wavefunction while the effect of correlation on the total intensities was estimated through the IAM model. There exists a wide disagreement between theory and experiment particularly in the region of small μ ($0 \leqslant \mu \leqslant 4A^{o-1}$). However, the recent CI calculation of Breitenstein et al(107) goes in the right direction with the measurements of McClleland and the Fink(81).

Among the early calculations on the scattering of electrons by polyatomic molecules was one by Haberl and Hasse(7) on water usimg an abinitio wavefunction and an elastic study by Szabo and Ostlund(18)(H_2O, NH_3 and CH_4) usimg semi-empirical CNDO type wavefunctions. These results showed an improvement over the IAM model calculations but still differed significantly from the experimental data(186). It is only very recently that various groups have initiated

elastic and total electron scattering calculations for medium and large size polyatomic molecules. Hirota et al(59) and Shibata et al(162) have reported elastic electron scattering cross-section calculations on the water and diborane molecules employing several molecular wavefunctions such as double zeta, triple zeta with and without polarization functions and CI wavefunctions. Pulay and coworkers(133) have performed an abinitio Hartree-Fock calculation of the elastic cross-section for electron scattering from the SF_6 molecule. They used a triple zeta basis set augmented with polarization functions and diffuse functions. Kohl et al(45) and Shang de Xie et al (150) have also reported elastic electron scattering cross-sections for CH_4, CF_4 and C_2H_4 respectively, using abinitio HF wavefunctions. Shang de Xie et al(150) have made an extensive study of basis set effects on C_2H_4. They have used six different basis functions ranging from 6-31G to 6-311G**. As there are no experimental measurements available, it is rather difficult to comment on the accuracy of the computed intensities, however, it is believed that the SCF calculations at the level of 6-311G** might be sufficient for the experimental calibration and related routine structure determination.

Sharma and Tripathi(36) have reported elastic and inelastic differential cross-sections for scattering of high energy electrons and X-rays by the NH_3, CH_4 and H_2O molecules. They used an impulse approximations Compton profile (IACP) approach to obtain the inelastic part of the

differential cross-section. The region of validity for such an approach is well known and is explained in the literature (see Bonham(137) and Sharma and Tripathi(35)). The various theoretical results upto 1984 and the present state of the art in comparison with experiment have been reviewed recently by Tripathi and Smith(15). The calculation of elastic and inelastic cross-sections using a configuration interaction (CI) wavefunction which accounts reasonably well for the correlation energy, is relatively difficult compared to that for a Hartree-Fock (HF) wavefunction. It is well known that the experimentalist requires elastic and inelastic intensities separately in order to analyse electron diffraction data in structure determinations. Consequently, the current practice has been to use the result for the elastic intensity calculated at the HF level and the result for the inelastic part by using the independent atom model(IAM). Although the use of HF wavefunctions cannot be expected to yield quantitative accuracy for the calculation of the inelastic intensity, nevertheless its calculation if performed even at the HF level, should be better than the IAM results. The advantage of such a procedure has been that both components are evaluated simultaneously on the same footing. The utility of such an approach has been well demonstrated recently by Thakkar(8). He has shown how the IACP results for the inelastic scattering predict unreliable results in the region of small momentum transfer by carrying out a calculation on CH_4, NH_3 and H_2O. Following this approach

we have carried out detailed calculations of total, elastic and inelastic X-ray and electron intensities for the ten electron systems (Ne, HF, H_2O, NH_3 and CH_4), employing SCF molecular wavefunctions constructed from a double zeta quality basis set of contracted Gaussian orbitals by Snyder and Basch(101). Various trends and systematics in the electron intensities (elastic and inelastic) for these systems have been examined. The effect of molecular binding has also been examined with the help of difference functions computed between the present electron scattering intensities and those for IAM. Before we discuss calculations of electron scattering in comparison with the experimental measurements, it is useful to begin by recalling a few well established relations within the framework of the first Born approximation. In Section 6.2, we describe the theoretical methodology and the numerical procedures. The results and discussion will be given in Section 6.3.

6.2 THEORETICAL PROCEDURE

6.2.1 Theoretical Methodology

In high energy electron scattering the elastic ($I^{ed}_{e\ell}(\mu)$) and total ($I^{ed}_{t}(\mu)$) scattering cross-sections within the framework of the first Born approximation are given respectively by

$$\mu^4 I^{ed}_{e\ell}(\mu)/I_R = I^{xr}_{e\ell}(\mu)/I_T + \bar{\sigma}_{ne}(\mu) + \bar{\sigma}_{nn}(\mu) \quad \ldots (6.1)$$

$$\mu^4 I^{ed}_{t}(\mu)/I_R = I^{xr}_{t}(\mu)/I_T + \bar{\sigma}_{ne}(\mu) + \bar{\sigma}_{nn}(\mu) \quad \ldots (6.2)$$

where I_R is the characteristic Rutherford constant, I_T is the Thomson factor, and $\vec{\mu}$ is the momentum transfer. σ_{ne} and σ_{nn} are the electron-nuclear and nuclear-nuclear interference terms. They are given by

$$\sigma_{ne}(\mu) = -\sum_{A} Z_A \mathrm{Re}\ F(\vec{\mu})\ \exp(-i\vec{\mu}.\vec{R}_A) \qquad \ldots (6.3)$$

and

$$\sigma_{nn}(\mu) = \sum_{A,B} Z_A Z_B j_o(\mu|\vec{R}_A-\vec{R}_B|) \qquad \ldots (6.4)$$

in which the sums are over the nuclei with charges Z_A and position vectors $\vec{R}_A$ and Re $\langle \ldots \rangle$ denotes the real part $\langle \ldots \rangle$. The angular brackets denote the spherical average. $I^{xr}_{e\ell}(\mu)/I_T$ and $I^{xr}_t(\mu)/I_T$ are the elastic and total scattering intensities for X-rays respectively and they are defined in terms of one (P_1) and two electron (P_2) densities with the statistical normalizations N and N(-1) respectively. N is the number of electrons in the molecules.

$$I^{xr}_{e\ell}(\mu)/I_T = \langle |F(\vec{\mu})|^2 \rangle \qquad \ldots (6.5)$$

with

$$F(\vec{\mu}) = \int e^{i\vec{\mu}.\vec{r}} P_1(\vec{r})\,d\vec{r} \qquad \ldots (6.6)$$

$$I^{xr}_t(\mu)/I_T = I^{xr}_{e\ell}(\mu)/I_T + I^{xr}_{inel}(\mu)/I_T \qquad \ldots (6.7)$$

$$I^{xr}_{inel}(\mu)/I_T = \langle S(\vec{\mu}) \rangle \qquad \ldots (6.8)$$

with

$$S(\vec{\mu}) = N + \int [P_2(\vec{r}_1,\vec{r}_2) - P_1(\vec{r}_1)P_1(\vec{r}_2)]\ e^{i\vec{\mu}.(\vec{r}_1-\vec{r}_2)}\ d\vec{r}_1 d\vec{r}_2 \qquad \ldots (6.9)$$

For a closed shell system, the elastic and inelastic components of the intensities can be calculated simultaneously using a self-consistent-field (SCF) molecular wavefunction as demonstrated recently by Thakkar(8).

The elastic intensity defined by eq.(6.1) refers to the situation where the rotational energy differences are not resolved. In practice all the experimental measurements carried out correspond to this situation. However, there is a possibility that one can resolve the rotational levels, i.e. J=0 and then the conventional definition of elastic intensity both for electrons and X-rays needs to be changed. This changed intensity will be referred to as the fully elastic intensity. The expressions for this fully elastic intensity for electron and X-ray scattering are taken from the papers of Kolos et al.(184) and Thakkar et al(9). These are given as

$$I^{xr}_{fel}(\mu)/I_T = \left| \langle F(\vec{\mu}) \rangle \right|^2 \qquad \ldots (6.10)$$

and

$$\mu^4 I^{ed}_{fel}(\mu)/I_R = \left| \langle F(\vec{\mu}) \rangle - \bar{\sigma}_n(\mu) \right|^2 \qquad \ldots (6.11)$$

where

$$\bar{\sigma}_n(\mu) = \sum Z_A j_o(\mu R_A) \qquad \ldots (6.12)$$

A semi-quantitative understanding of the electron molecule scattering cross-section in terms of geometrical and vibrational parameters of the molecule is achieved with the help of the independent atom model(IAM) or promolecule which

assumes that the molecular density is the simple sum of the spherically averaged atomic densities centred at the equilibrium positions of the pertinent nuclei. Although it is an approximate model, nevertheless its simplicity compensates somewhat for what it lacks. Except in the forward direction, predictions of the IAM are always in good agreement with experiment at large scattering angles. This is not surprising as the large scattering angle region is dominated by the nuclear charge and core electron distributions. Accurate electron scattering measurements can be used to deduce the deviations of the correct charge densities from the IAM model.

6.2.2 Calculations

During the last few years, high quality abinitio molecular wavefunctions at the Hartree-Fock level, have become available for many small and medium sized linear and polyatomic molecules and therefore much attention has been devoted to use them in the analysis of high precision electron scattering experiments. Various groups are engaged currently in calculating the elastic and inelastic cross-sections particularly for linear molecules and in a few cases for elastic scatteringg by polyatomic molecules. In principle, there is no restriction in carrying out the calculations for bigger molecules, however in practice the amount of computer time required is very large. It is basically due to the manifold increase in the number of integrals and then to the necessity,

performing the angular integrations over the angular variables. The spherical averaging procedure needed in Eq.(6.1) has not received such attention in the past. There are several possible ways to do this averaging:

(i) Numerical integration using quadrature,

(ii) Expansion of the charge density (one electron density) in Eq.(6.6) in an analytical function in order to facilitate the evaluation of Eq.(6.1) in closed form,

(iii) An accurate analytic approach which does not use any type of numerical approximation.

The problem of spherical averaging is not of great concern as long as one is doing calculations for linear molecules. However, the problem becomes somewhat alarming if the molecule involved is a polyatomic with a large number of atoms. The problem has been recently examined very elegantly by Pulay and coworkers(133,45). They have developed a compact one integral routine for all types of cases occurring in the scattering amplitude with Gaussian based wavefunctions upto and including d functions. Furthermore, they also use the fact that the IAM amplitudes approximate the abinitio results very well, particularly at larger μ. Following this prescription, they define a difference function,

$$\Delta I(\mu) = F(\mu) - F_{IAM}(\mu) \qquad \ldots (6.13)$$

and expand Eq.(6.5) as

$$\left\langle \left| F(\vec{\mu}) \right|^2 \right\rangle = \int d\Omega \left| F_{IAM}(\mu) \right|^2 + 2\,\mathrm{Re} \int d\Omega F^{*}_{IAM}(\mu) \Delta I(\mu) + \int d\Omega \left| \Delta I(\mu) \right|^2 \quad \ldots (6.14)$$

The advantage with Eq.(6.14) is that the first term becomes very trivial and the orientational averaging for the second one is done analytically. Only the last term needs to be evaluated numerically. The integrand, being the square of an already small quantity, practically vanishes above $\mu = 5 a_o^{-1}$, where the numerical integration becomes difficult. In the present study we have evaluated all the integrals numerically using quadrature.

6.3 RESULTS AND DISCUSSION

We have calculated the elastic and fully elastic, inelastic and total electron and X-ray scattering intensities using equations (6.1-6.2, 6.5-6.8) for the HF, H_2O, NH_3 and CH_4 molecules. The indicated spherical averaging has been done numerically. These molecules are ten electron systems and therefore, we have also calculated the elastic and inelastic intensity for the Ne atom for the purpose of intercomparison of the intensities and its related behaviour on charge density. For the neon atom we have used the small size geometrical Gaussian basis set wavefunction of Clementi and Corongiu(56). The results for X-ray and electron elastic and inelastic intensities are presented in tables (6.1-6.4) in the range of μ (momentum transfer) $0 \leqslant \mu \leqslant 10$ au.

6.3.1 Difference elastic and fully elastic intensity

The difference function between elastic and fully elastic intensities for X-rays and electrons are shown in Figures (6.1)(a-d) and 6.2(a-d). It is seen that the differences are greater for X-ray scattering compared to those for electron scattering. The IAM differences which are displayed (dotted line) along with the differences computed using the molecular wavefunctions, reveal the true nature of molecular differences. In the case of X-rays, the IAM differences increase at small μ and then fall off very rapidly with μ whereas in the case of electron scattering, the IAM differences show a rapid increase in the small angular region and thereafter approach to a constant value at very large μ in an oscillatory fashion. This behaviour is very similar to what has been observed and explained by Thakkar, Tripathi and Smith(9) for homonuclear diatomic molecules. In general, it is found that the deviation decreases with the increase in number of hydrogen atoms in the constituent molecule, i.e. it is maximum for HF and minimum for CH_4. This fact can be rationalised by noting that hydrogen is a weak scatterer and so its addition along the sequence does not produce any significant difference between the SCF and IAM results. On the other hand, it is observed that the more extended the atomic form factor (presently in the order F, O, N, C), the more it produces the difference between SCF and IAM results. The electron scattering results are relatively better accounted for in shape but not in magnitude by

the IAM compared to the X-Ray scattering results. The differences arise due to the electron-nuclear term. This is relfected in Figure 6.3 where the σ_{ne}^{-} term in the IAM always underestimates it contribution in comparison with the molecular σ_{ne}^{-} upto μ = 4.0 au. Beyond 4.0 au both σ_{ne}^{-} become very small and they almost merge into each other.

6.3.2 Differences between the I_t^{xr}, I_{el}^{xr} and σ_{ne}^{-} intensities

Figures 6.3(a-d) show the difference between the SCF and IAM results for I_t^{xr}, I_{el}^{xr} and σ_{ne}^{-} for the HF, H_2O, NH_3 and CH_4 systems. From these figures it is observed that the calculated SCF results for all these molecules show a similar oscillatory behaviour but differ in magnitude and period of the oscillations. There exists a large discrepancy for I_t^{xr}, I_{el}^{xr} and σ_{ne}^{-} between the SCF and IAM results in the small angular region and thus the use of IAM results for I_t^{xr} would effect conventional structural analysis. Therefore, we believe that the present SCF inelastic results (shown in table 6.2) when combined with I_{el}^{xr} to obtain I_t^{xr} may be more useful than those of the IAM. However, if the present inelastic results are properly corrected for the correlation contributions to the residual atoms using the standard procedure, i.e.,

$$S_{inel}^{CORMO}(\mu) = S_{inel}^{SCFMO}(\mu) + S_{inel}^{IAMCI}(\mu) - S_{inel}^{IAMHF}(\mu) \quad \ldots (6.15)$$

then these results may perhaps become as reliable as those obtained with high quality molecular wavefunctions accounting for a large amount of the correlation energy. Table (6.3)

lists the corrected SCFMO (CORMO) results for all these molecular systems.

6.3.3 NH_3 molecule

Very recently Duguet et al.(5) have measured the elastic and inelastic components separately for the NH_3 molecule. We therefore constructed the difference functions between the present elastic and inelastic electron intensities and those for the IAM. The results are presented in Figure 6.4 (a-b), along with the experimental measurement(5) and other theoretical calculations. The present elastic scattering results (Figures 4a) are in good agreement with recent data between $0.3 \leqslant \mu \leqslant 3.0$ a.u. Beyond $\mu = 1.2$ a.u., the experimental measurements favour more than the abinitio molecular calculations of Ostlund (see Ref.5). This theoretical calculation uses the d-type polarisation functions in the basis set. The augmentation of the basis set by d-functions influences the charge density resulting in a significant change in the elastic intensity. Figure (6.4b) displays the several difference functions for the inelastic intensity. They are defined as follows:

$$S_1 = S_{inel}^{SCFMO}(\mu) - S_{inel}^{IAMHF}(\mu) \quad \ldots (6.16)$$

$$S_2 = S_{inel}^{CORMO}(\mu) - S_{inel}^{IAMHF}(\mu) \quad \ldots (6.17)$$

$$S_3 = S_{inel}^{IAMCI}(\mu) - S_{inel}^{IAMHF}(\mu) \quad \ldots (6.18)$$

$$S_4 = S_{inel}^{EXP}(\mu) - S_{inel}^{IAMHF}(\mu) \quad \ldots (6.19)$$

$$S_5 = S_{inel}^{EXP}(\mu) - S_{inel}^{IAMCI} \quad \ldots (6.20)$$

In the present calculations the theoretical $S_{inel}^{IAMHF}(\mu)$ and $S_{inel}^{IAMCI}(\mu)$ values are obtained using the atomic incoherent scattering factors given by Tavard et al.(43) for HF and Tanaka and Sasaki(97) for CI. It is clear that the present calculations using molecular wavefunctions at the SCF level (SCFMO) does not reproduce the experiment (See Curve S_4). However, when this calculation is corrected (CORMO curve S_2) using curve S_3 partly for the residual electron correlation in the atoms, then it lies in between the experimental measurements (see Curves S_4 and S_3). The experimental curves are taken as it is from the paper of Duguet et al(5). The correlated independent atom model IAMCI (Curve S_3) shows a large deviation compared to IAMHF (curve S_4) results for μ values lying between 1 and 3 au. This deviation suggests that the inelastic cross-sections are strongly influenced by the quality of atomic cross-sections.

Table 6.1 Calculated SCFMO $I_{el}^{xr}(\mu)/I_T$ for X-ray scattering

μ(a.u.)	Ne	HF	H_2O	NH_3	CH_4
0.0	100.00	100.00	100.00	100.00	100.00
0.04	99.951	99.928	99.898	99.858	99.809
0.10	99.694	99.551	99.362	99.119	98.814
0.20	98.782	98.219	97.479	96.531	95.351
0.30	97.287	96.052	94.442	92.400	89.886
0.40	95.246	93.125	90.392	86.975	82.835
0.50	92.707	89.536	85.511	80.564	74.694
0.60	89.728	85.400	80.002	73.506	65.988
0.70	86.374	80.840	70.077	66.133	57.202
0.80	82.716	75.984	67.942	58.750	48.749
0.90	78.823	70.955	61.784	51.610	40.936
1.0	74.768	65.865	55.763	44.908	33.963
1.2	66.428	55.894	44.607	33.288	22.833
1.4	58.162	46.682	35.102	24.307	15.243
1.6	50.324	38.573	27.424	17.769	10.420
1.8	43.145	31.692	21.453	13.198	7.4811
2.0	36.746	26.002	16.922	10.075	5.7188
2.2	31.162	21.379	13.529	7.9556	4.6560
2.4	26.369	17.662	10.998	6.5107	4.0039
2.6	22.306	14.689	9.1041	5.5100	3.5942
2.8	18.893	12.315	7.6743	4.8004	3.3260
3.6	16.047	10.418	6.5821	4.2815	3.1359
3.2	13.684	8.8973	5.7365	3.8881	2.9831
3.4	11.729	7.6751	5.0707	3.5765	2.8454
3.0	10.114	6.6887	4.5392	3.3201	2.7093
3.8	8.7816	5.8887	4.1081	3.1016	2.5721
4.0	7.6807	5.2365	3.7534	2.9105	2.4352
4.4	6.0147	4.2605	3.2082	2.5887	2.1756
4.8	4.8611	3.5872	2.8142	2.3306	1.9517
5.2	4.0496	3.1097	2.5212	2.1232	1.7651
5.6	3.4681	2.7613	2.2972	1.9528	1.6034
6.0	3.0430	2.4990	2.1192	1.8052	1.4535
6.5	2.6582	2.2496	1.9352	1.6355	1.2728
7.0	2.3794	2.0540	1.7739	1.4720	1.1006
7.5	2.1667	1.8893	1.6228	1.3137	0.94309
8.0	1.9948	1.7425	1.4780	1.1638	0.80452
8.5	1.8477	1.6065	1.3397	1.0257	0.68515
9.0	1.7159	1.4782	1.2090	0.90101	0.58264
9.5	1.5939	1.3564	1.0872	0.78937	0.49420
10.0	1.4789	1.2409	0.97475	0.68971	0.41780

Table 6.2 Calculated SCFMO $S_{inel}(\mu)$ for X-ray and high energy electron scattering

μ(a.u.)	Ne	HF	H_2O	NH_3	CH_4
0.00	0.0000	0.0000	0.0000	0.0000	0.0000
0.04	0.0032	0.0047	0.0066	0.0085	0.0103
0.10	0.0197	0.0293	0.0408	0.0530	0.0638
0.20	0.0782	0.1163	0.1612	0.2088	0.2504
0.30	0.1741	0.2575	0.3550	0.4575	0.5468
0.40	0.3051	0.4477	0.6129	0.7845	0.9336
0.50	0.4679	0.6805	0.9231	1.1722	1.3878
0.60	0.6590	0.9483	1.2730	1.6019	1.8857
0.70	0.8743	1.2432	1.6499	2.0562	2.4059
0.80	1.1096	1.5575	2.0422	2.5198	2.9305
0.90	1.3607	1.8840	2.4398	2.9806	3.4456
1.0	1.6235	2.2165	2.8350	3.4299	3.9419
1.2	2.1696	2.8794	3.5957	4.2724	4.8553
1.4	2.7230	3.5167	4.2969	5.0242	5.6473
1.6	3.2653	4.1126	4.9290	5.6798	6.3133
1.8	3.7847	4.6606	5.4906	6.2405	6.8573
2.0	4.2741	5.1587	5.9832	6.7102	7.2887
2.2	4.7298	5.6068	6.4090	7.0957	7.6217
2.4	5.1500	6.0061	6.7722	7.4062	7.8737
2.6	5.5344	6.3586	7.0782	7.6532	8.0630
2.8	5.8835	6.6672	7.3336	7.8484	8.2064
3.0	6.1984	6.9354	7.5457	8.0029	8.3181
3.2	6.4808	7.1675	7.7217	8.1267	8.4091
3.4	6.7329	7.3678	7.8683	8.2281	8.4869
3.6	6.9569	7.5407	7.9913	8.3134	8.5568
3.8	7.1554	7.6901	8.0958	8.3877	8.6219
4.0	7.3310	7.8196	8.1859	8.4543	8.6839
4.4	7.6238	8.0316	8.3356	8.5738	8.8025
4.8	7.8543	8.1978	8.4594	8.6829	8.9156
5.2	8.0387	8.3334	8.5683	8.7862	9.0231
5.6	8.1810	8.4491	8.6682	8.8848	9.1243
6.0	8.3176	8.5518	8.7620	8.9788	9.2186
7.0	8.5735	8.7752	8.9770	9.1926	9.4222
8.0	8.7800	8.9698	9.1666	9.3735	9.5809
9.0	8.9594	9.1423	9.3308	9.5214	9.7000
10.0	9.1189	9.2937	9.4692	9.6385	9.7869

Table 6.3 Corrected CORMO $S_{inel}(\mu)$ for X-ray and high energy electron scattering

μ(a.u.)	HF	H_2O	NH_3	CH_4
0.00	0.0000	0.0000	0.0000	0.0000
0.04	0.0045	0.0056	0.0086	0.0103
0.10	0.0281	0.0388	0.0514	0.0599
0.20	0.1109	0.1540	0.1998	0.2331
0.30	0.2446	0.3376	0.4365	0.5100
0.40	0.4233	0.5821	0.7464	0.8682
0.50	0.6423	0.8746	1.1113	1.2889
0.60	0.8911	1.2033	1.5147	1.7492
0.70	1.1646	1.5542	1.9386	2.2307
0.80	1.4537	1.9176	2.3693	2.7180
0.90	1.7516	2.2843	2.7963	3.2003
1.00	2.0542	2.6473	3.2134	3.6707
1.20	2.6553	3.3467	4.0004	4.5569
1.4	3.2321	3.9993	4.7207	5.3567
1.6	3.7786	4.6006	5.3701	6.0571
1.8	4.2937	5.1540	5.9491	6.6504
2.0	4.7790	5.6581	6.4535	7.1322
2.2	5.2333	6.1114	6.8821	7.5119
2.4	5.6535	6.5116	7.2380	7.7994
2.6	6.0383	6.8585	7.5260	8.0158
2.8	6.3853	7.1538	7.7565	8.1793
3.0	6.6940	7.4044	7.9393	8.3045
3.2	6.9670	7.6127	8.0860	8.4035
3.4	7.2051	7.7871	8.2022	8.4856
3.6	7.4125	7.9325	8.2988	8.5573
3.8	7.5898	8.0535	8.3803	8.6239
4.0	7.7433	8.1568	8.4525	8.6872
4.4	7.9899	8.3228	8.5770	8.8052
4.8	8.1778	8.4549	8.6864	8.9169
5.2	8.3255	8.5688	8.7886	9.0252
5.6	8.4459	8.6692	8.8873	9.1255
6.0	8.5525	8.7628	8.9814	9.2197
7.0	8.7763	8.9777	9.1935	9.4230
8.0	8.9704	9.1676	9.3742	9.5811
9.0	9.1426	9.3312	9.5218	9.7006
10.0	9.2933	9.4691	9.6391	9.7869

Table 6.4 Calculated SCFMO $\mu^4/I_R\ I_{el}^{ed}(\mu)$ for high energy electron scattering

μ(a.u.)	Ne	HF	H_2O	NH_3	CH_4
0.00	0.0000	0.0000	0.0000	0.0000	0.0000
0.04	0.00001	0.00047	0.00061	0.00047	0.00002
0.10	0.00024	0.00323	0.00417	0.00351	0.00097
0.20	0.00373	0.01658	0.02208	0.02204	0.01496
0.30	0.01866	0.05063	0.06896	0.07766	0.07174
0.40	0.05790	0.12157	0.16716	0.20115	0.21029
0.50	0.13807	0.24927	0.34225	0.42461	0.46667
0.60	0.27830	0.45498	0.61872	0.77404	0.86294
0.70	0.49878	0.75901	1.0161	1.26361	1.4005
0.80	0.81938	1.1786	1.5460	1.8928	2.0594
0.90	1.2583	1.7265	2.2108	2.6467	2.8034
1.0	1.8311	2.4097	3.0041	3.4996	3.5888
1.2	3.4214	4.1821	4.9149	5.3746	5.1266
1.4	5.6340	6.4477	7.1222	7.2860	6.4814
1.6	8.4451	9.1075	9.4747	9,1124	7.6819
1.8	11.775	12.051	11.882	10.868	8.8846
2.0	15.509	15.185	14.329	12.648	10.235
2.2	19.516	18.450	16.849	14.560	11.795
2.4	23.667	21.807	19.487	16.672	13.561
2.6	27.847	25.232	22.273	18.997	15.514
2.8	31.960	28.696	25.196	21.500	17.645
3.0	35.930	32.158	28.208	24.115	19.934
3.2	39.700	35.559	32.701	28.026	23.453
3.4	43.234	38.828	34.138	29.265	24.551
3.6	46.508	41.888	36.834	31.536	26.421
3.8	49.514	44.665	39.201	33.401	27.616
4.0	52.253	47.098	41.142	34.720	27.929
4.4	56.965	50.802	43.532	35.422	26.025
4.8	60.765	52.981	43.993	33.910	22.835
5.2	63.802	53.995	43.216	31.775	21.620
5.6	66.222	54.428	42.320	30.925	23.535
6.0	68.155	54.864	42.302	32.199	26.911
6.5	69.709	55.965	43.996	35.609	29.884
7.0	71.529	57.721	46.727	38.441	30.546
7.5	72.727	59.625	48.928	39.275	29.874
8.0	73.748	61.036	49.705	38.629	28.624
8.5	74.662	61.653	49.320	37.688	28.301
9.0	75.517	61.700	48.724	37.570	30.492
9.5	76.344	61.739	48.841	39.051	33.766
10.0	77.157	62.280	50.078	41.756	34.893

6.4 FIGURE CAPTIONS

Figure 6.1 Difference between the elastic and fully elastic X-ray intensities for HF, NH_3, H_2O and CH_4 molecules. ——— : Calculated using molecular wavefunctions, - - - -: Calculated in the IAM

Figure 6.2 Difference between the elastic and fully elastic electron intensities HF, NH_3, H_2O and CH_4 molecules. ————: Calculated using molecular wavefunctions, - - - - - -: Calculated in the IAM.

Figure 6.3 Difference between the SCFMO and IAM intensities corresponding to I_t^{xr}, I_{el}^{xr} and $\bar{\sigma}_{ne}$ for HF, NH_3, H_2O and CH_4 molecules. ——— ; ΔI_{el}^{xr}; - - - - ; ΔI_t^{xr}, —·— ; $\Delta\bar{\sigma}_{ne}$.

Figure 6.4 Difference between the SCFMO and IAM results for NH_3, corresponding to elastic and inelastic intensities.

(a) Elastic: ——— , calculated using SCFMO and the IAM-HF; (o) 6-31G*, (Δ) 6-31G**, (+) 4-31G basis set results of Ostlund (Ref.(5); experimental: ∅ data of Duguet et al.(Ref.5).

(b) Inelastic: —— S_1; —·—·— S_2; ——xx—— S_3; - - -ǂ- - - S_4; ——— S_5.

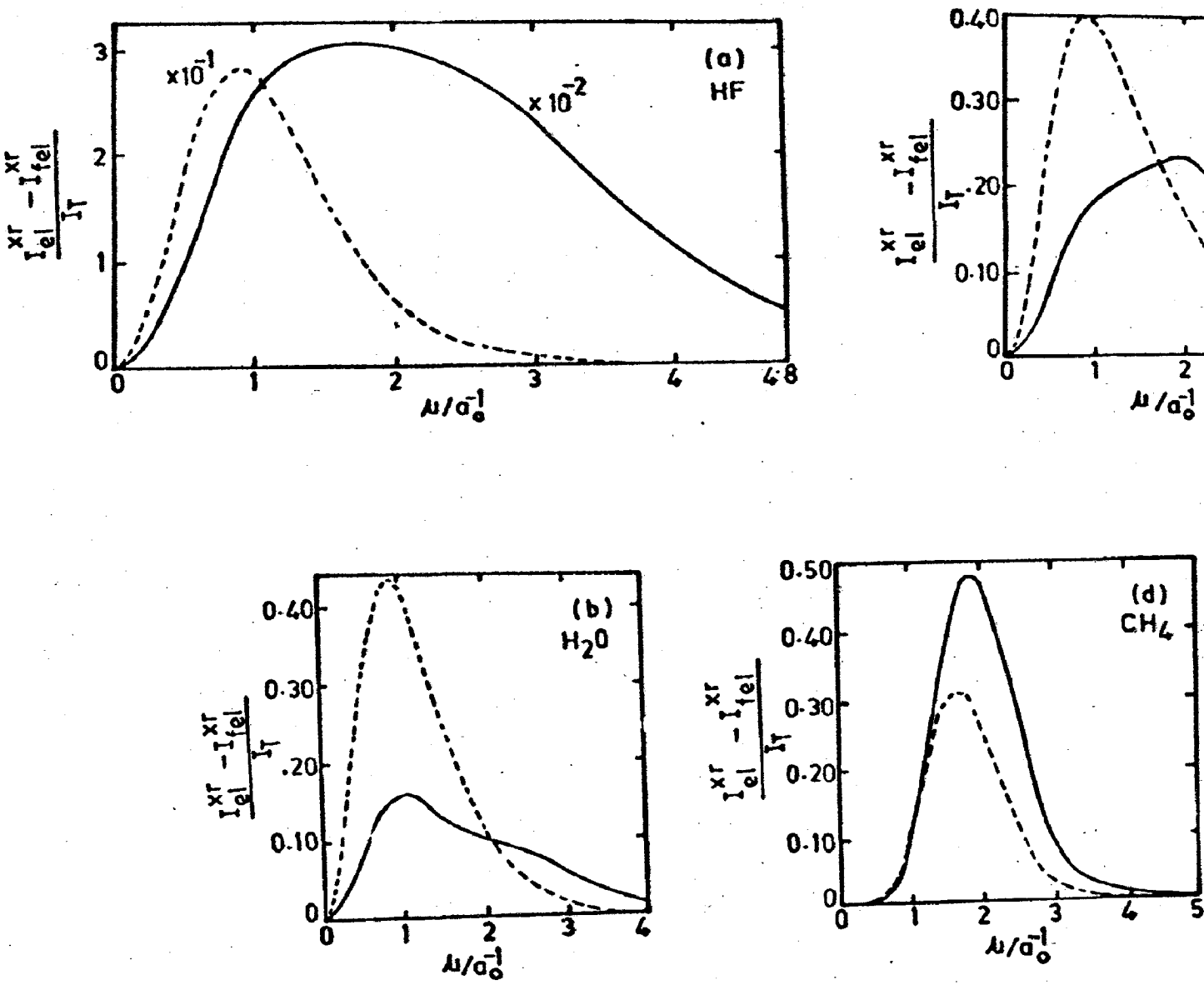

Fig. 6·1

wavefunctions along with the HF type wavefunctions as well. The distorted waves for each partial wave were generated by solving the radial Schrödinger equation by a non-iterative procedure of Marriot and Percival. To achieve the proper convergence of the transition matrix element, 6 to 5 number of partial waves were needed for s-s type transitions at 100 and 200 eV respectively. For s-p type transitions, 15 to 25 number of partial waves were required at these energies to achieve the same accuracy. It is seen that this approach is quite successful in reproducing the differential and total cross-section results. Further, we also noticed that the target correlation has only a minor effect on the final results. The comparison of different distorted wave models among themselves as well as with the present approach clearly shows that the inclusion of target polarization in both channels and exchange contribution is important and is in right direction.

The Chapter 4 presents a comparative study for positron impact excitation of helium to 2^1S, 2^1P states using the Coulomb-Born and distorted wave polarised orbital methods. The present positron-atom scattering is one of the first such calculations where we have explored the effect of utilization of accurate MPC wavefunction within the framework of distorted wave approximation itself. One of the attraction of our Coulomb-Born approach is its simplicity for obtaining the reasonable results. Further our study in distorted wave polarised method is as reliable as obtained by other distorted wave calculations at intermediate and high

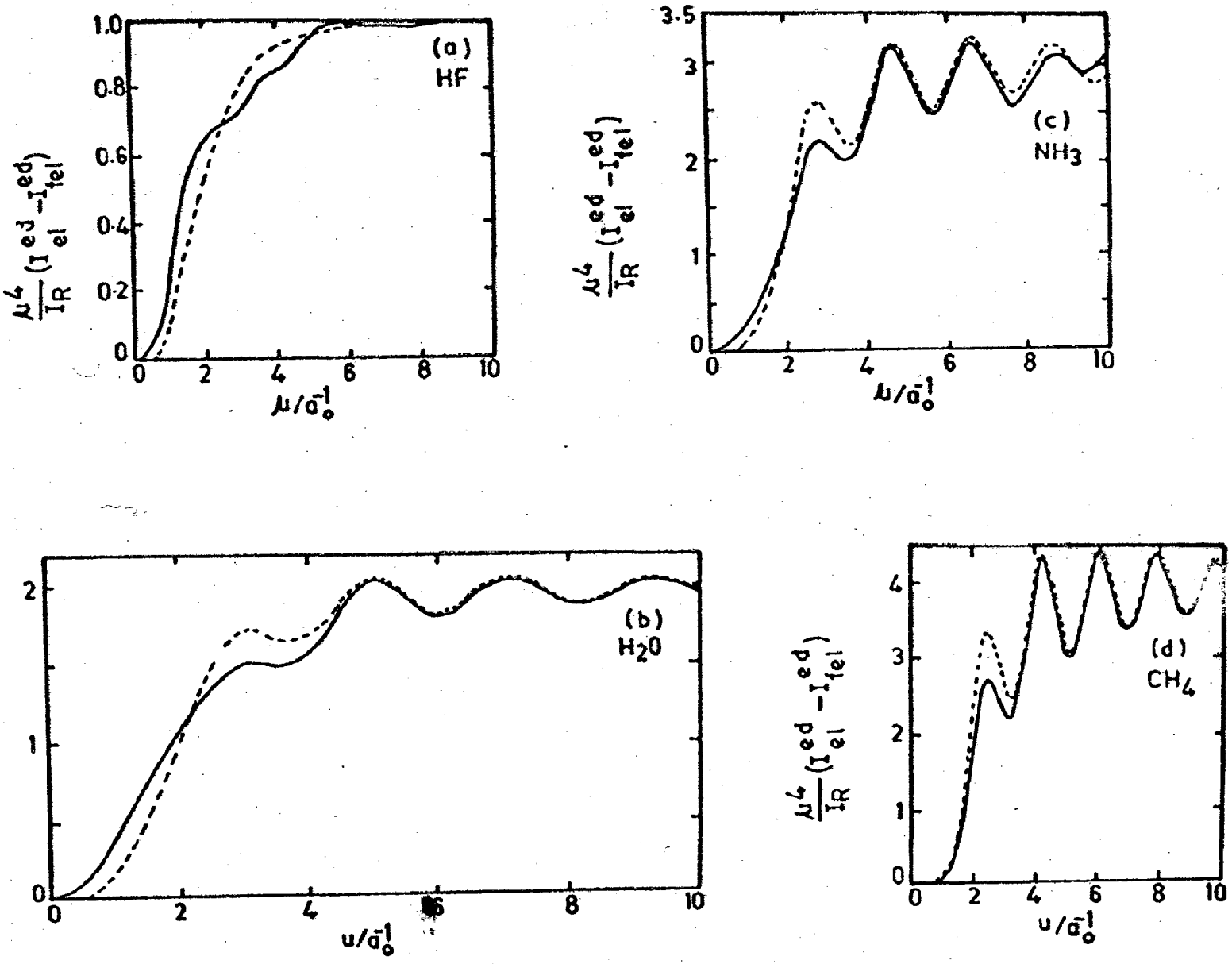

Fig. 6·2

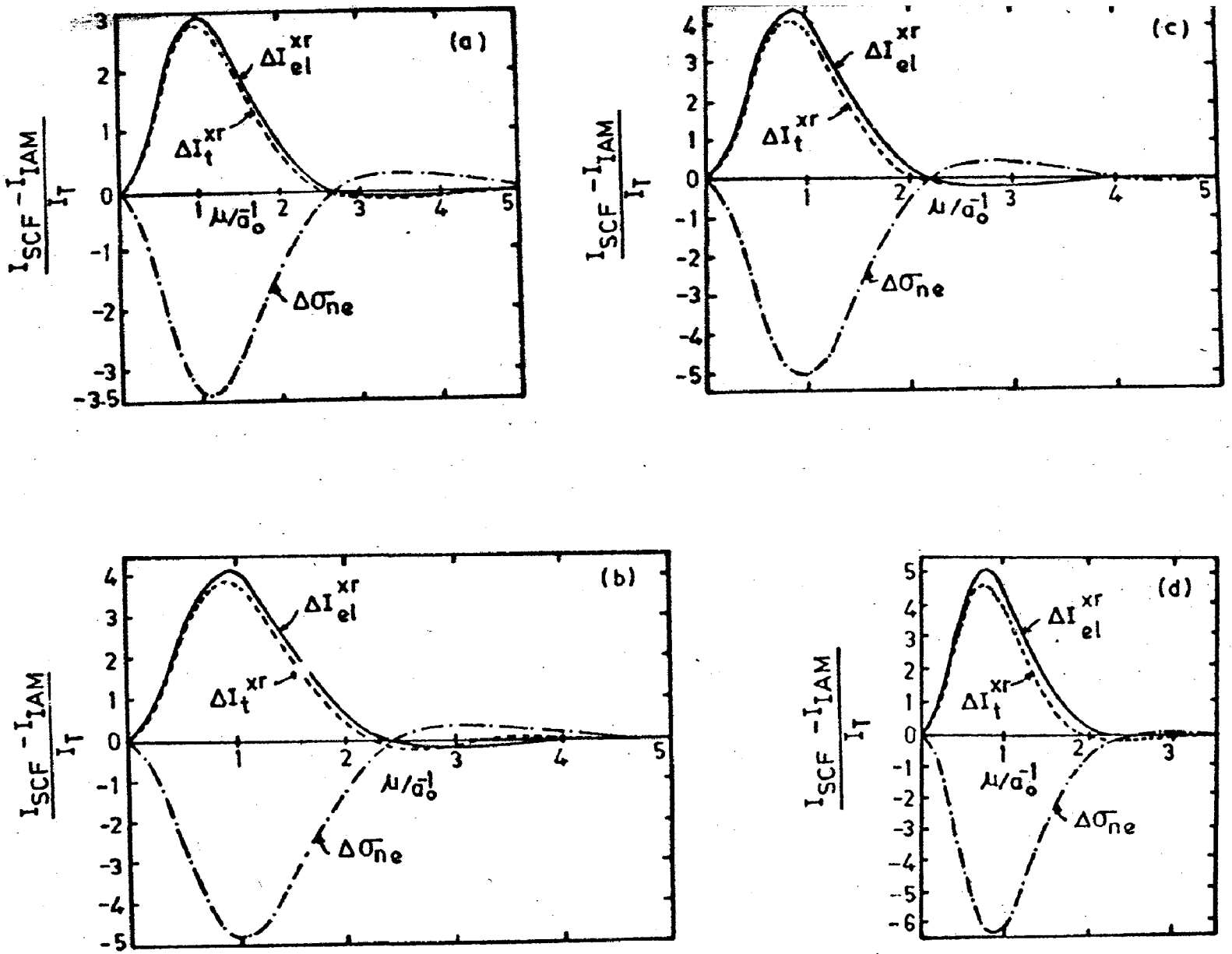
(a)
(b)
(c)
(d)
$\frac{I_{SCF} - I_{IAM}}{I_T}$
ΔI_{el}^{xr}
ΔI_t^{xr}
$\Delta\sigma_{ne}$
μ/a_o^{-1}

Fig. 6·3

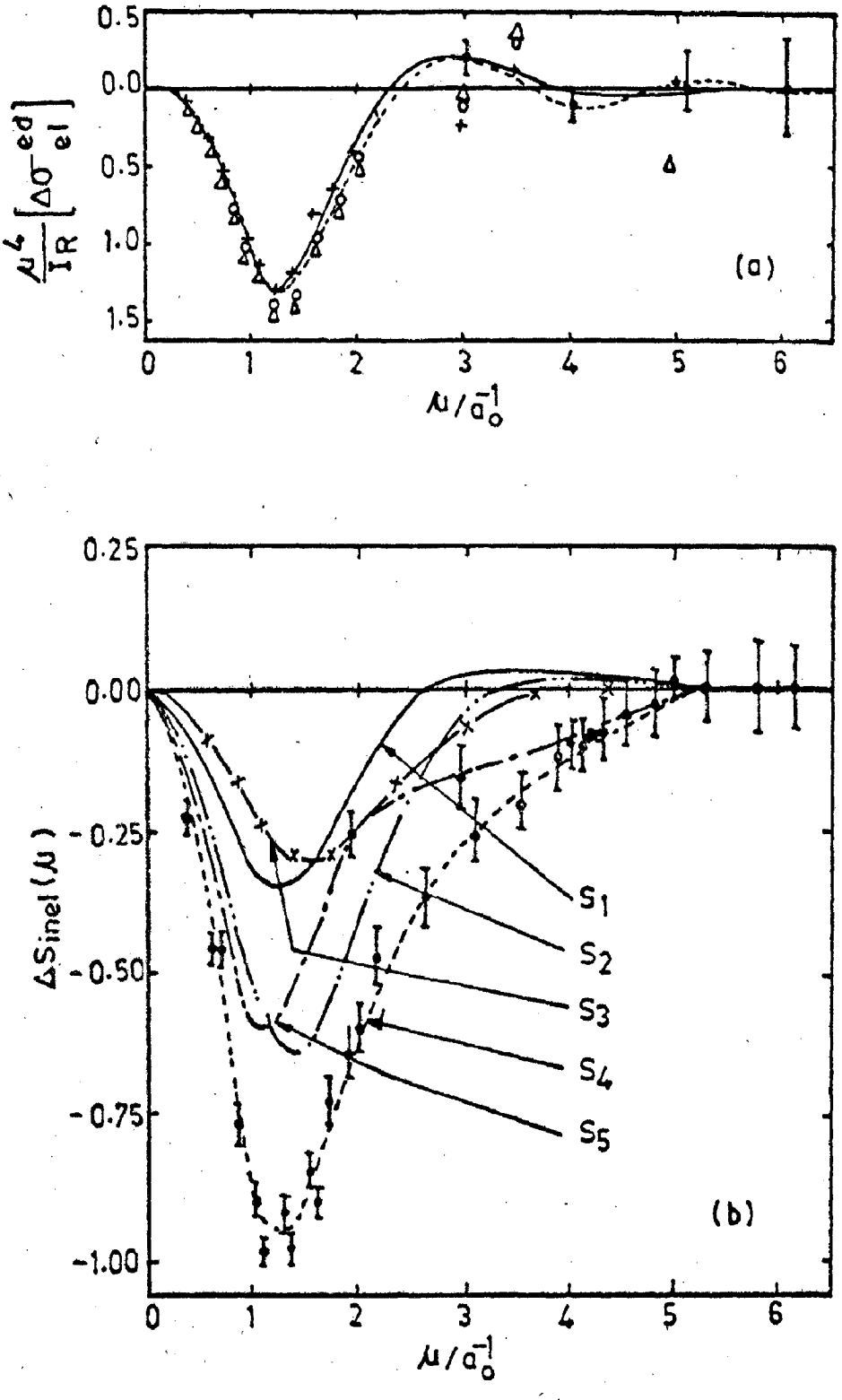
0.5
0.0
0.5
1.0
1.5
0
1
2
3
4
5
6
$\frac{\mu^4}{I_R}\left[\Delta\sigma_{el}^{ed}\right]$
μ/a_o^{-1}
(a)
0.25
0.00
-0.25
-0.50
-0.75
-1.00
$\Delta S_{inel}(\mu)$
S_1
S_2
S_3
S_4
S_5
(b)
μ/a_o^{-1}

Fig. 6·4

CHAPTER-7

SUMMARY, CONCLUSIONS AND COMMENTS

In the following we summarise the work presented in Chapters 2 to 6. These include (i) the study of differential scattering cross-sections and total cross-sections for electron/positron impact excitation of helium as studied by using the Coulomb-Born and distorted wave polarised orbital methods (ii) the DCS and total cross-sections for electron impact excitation of lithium, to 2s-3s transition employing various perturbative approaches such as eikonal-Born series, modified Glauber approximation, second Born, Glauber and Born approximation and also to the resonance transition 2s-2p of lithium in Modified Glauber approximation (iii) the scattering of high energy electron and X-rays from the ten electron molecule series, such as Ne, HF, H_2O, NH_3 and CH_4 in the first Born approximation.

Our aim throughout this work has been to investigate, extend and propose simple and consistent methods so that the results could be improved without unduly complicating the procedures at intermediate and high energy region. The accent is on simplicity of the approach and computational feasibility.

In Chapter 2 we have studied the electron impact excitation of 2^1S, 2^1P states of helium in the Coulomb-Born model.

In the present model we have considered the distortion due to the nucleus of target in both the channels. Closed form expression for scattering amplitude have been obtained with Fourier decomposition of the interaction potential along with the use of accurate many parameter correlated (MPC) bound state wavefunctions. We have also carried out the calculations in this model using the commonly used Hartree-Fock(HF) wavefunctions to see the changes in the cross-sections compared to the cross-sections obtained using the MPC wave functions. It is seen that the effect of correlated wavefunctions has been mostly in the region of large scattering angles. The differences in the results among the distorted wave models can be attributed due to the different choice of distorting potential. The present model, except for taking the distortion by the fixed Coulomb field of the target, has all the precise feature required. Another advantage of the present approach lies in its simplicity and do not require any numerical solution for generation of distorted wave function and thereby use of less computer time.

The Chapter 3 deals with the excitation of same transition in helium beyond Coulomb-Born level, referred as distorted wave polarised orbital approach. It is often seen that not much consistent effort is made to include in both channels the distortion of the incident particle, polarization of target and contribution due to exchange. In view of these, we have attempted to include these features in a systematic manner in both the channels. In addition, we have also used the MPC

impact energies. Due to lack of experimental data for differential cross-sections and total cross-sections at higher energies, it is rather difficult to comment on the accuracy and adoptability of any specific model.

In Chapter 5, we have applied various perturbative approaches such as eikonal-Born series, Modified Glauber method, simplified second Born, Glauber approximation and first Born methods to study the electron impact excitation of lithium (2s-3s) transition. The resonance transition (2s-2p) is studied only in Modified Glauber approximation. One of the important features here, has been that we give special attention to the second order term of the multiple scattering series and attempt to calculate it as accurately as possible. For the 2s-3s transition, the EBS and second Born results are very close to one another and overestimate the cross-section compared to experimental data indicating a poor convergence of the Born series for this process. The modified Glauber approximation are found to reproduce the experimental results better than eikonal-Born series and second Born results. It is perhaps due to the presence of higher order terms in modified Glauber approximation. For the case of resonance transition (2s-2p), we find that the results of calculation in modified Glauber approximation show a marked improvement over the conventional Glauber and first Born calculations. The present calculation overestimates the differential cross-section by more than order of magnitude in comparison with experimental data. This shows

that the inclusion of higher order term in modified Glauber approximation through Glauber approximation is not sufficient. Their full contribution at least for some part of the interaction (for example static, polarisation potential etc) seems to be imperative.

Finally, we report our calculations for the elastic, inelastic and total intensities for high energy electrons and X-ray from the ten electron systems Ne, HF, H_2O, NH_3 and CH_4. We note the following points.

i) For each molecule, the differences between the calculated total (elastic and inelastic) and the experimental cross-section have similar nodal pattern but differ in the amplitude of oscillation.

ii) At Hartree-Fock level, one can calculate with a little additional effort the inelastic scattering cross-section along with the elastic scattering cross-section. Thus both components can be calculated at the same footing. Consequently for the calculation of total intensity the use of inelastic component taken from the IAM can be avoided. Further, the present inelastic calculations can be easily corrected for the correlation contribution to the residual atoms using the standard procedure (see Eq.(6.15)), making this result more reliable.

iii) It is also seen that the elastic scattering cross-

section is not very sensitive to the selection of basis set, however, one should include the d-functions in its representation (not taken in the present study see fig.6.4(a)).

(iv) The calculation beyond HF level is always more demanding and worth pursuing.

(v) Further, in order to have a better understanding of electron correlation effects and also how well a HF level calculation predicts the cross-section, new measurements are needed separately for elastic and inelastic components of the cross-section.

REFERENCES

1. A.Birman and S.Rosendroff,

   'Elastic electron-hydrogen scattering in a modified approach to the Glauber approximation', Phys.Rev. A21 556(1980).

2. A.Burgess,

   'The determination of Phase and amplitudes of wave-functions', Proc. Phys. Soc. (London), 72, 121(1956).

3. A.C.Yates,

   'On the term-wise analysis of the Glauber eikonal series', Chem.Phys.L25, 480(1974).

4. A.C.Yates,

   'High-energy higher-order Born approximation:Theoretical development', Phys.Rev.A19 1550-8(1979).

5. A.Duguet, A.Lahmam -Bennani and M. Roualt,

   'High energy elastic and inelastic electron scattering by NH_3 molecule-bending effect', J.Chem.Phys. 78, 6595 (1983)

6. A.E.Kingston and H.R.J.Walters,

   'Electron scattering by atomic hydrogen: The distorted-wave second Born approdimation', J.Phys.B13 4633-62(1980).

7. A.Haberl and J.Hasse,

   Z.Naturforsch, 29a, 1033(1974) (quoted from Int.J.Qn.Chem. 1976(in press) by V.H.Smith, Jr.).

8. A.J.Thakkar,

   'Incoherent scattering factors', J.Chem.Phys.81, 1943(1984).

9. A.J.Thakkar, A.N. Tripathi and V.H.Smith, Jr.,

   'Molecular x-ray- and electron-scattering intensities', Phys.Rev.A29 1108-1113(1984).

10. A.K. Bhatia, A.Temkin and A.Silver,

'Photoionization of lithium', Phys.Rev.A12 2044(1975).

11. A.Lahmann-Bennani, A Duguet, H.E.Wellenstein and N.Roualt,

'Bethe surface and compton profile of NH_3 obtained by 35 keV electron impact', J.Chem.Phys.72, 6398(1980).

12. A.Nordseick,

'Reduction of an integral in the theory of Bremsstrahlung', Phys.Rev.93, 785-7(1954).

13. A.N. Tripathi,

'Generalised oscillator strengths and inelastic scattering cross sections for allowed and non-allowed transitions in lithium atoms', Phys.Rev. A23, 1801(1981).

14. A.N. Tripathi,

'Theoretical methods for electron atom scattering at intermediate and high energy', Fourth National Workshop on Atomic and Molecular Physics, edited by S.C.Mukerjee, 21-34(1984).

15. A.N. Tripathi and V.H.Smith Jr.,

'In comparison of abinitio quantum chemistry with experiment: state-of-the Art', edited by R.Bartlett (Beidel 1985),A.N. Tripathi and V.H.Smith,Jr., 'Scattering of x-rays and high-energy electrons from molecules: comparison of abinitio calculations with experiment. Int.J.Quantum Chem.(1986) (in press).

16. A.R.Holt and B.L.Moisewitch,

'Application of a simplified second Born approximation to the scattering of electrons and protons by hydrogen atom I.', J.Phys B1 36-47(1968).

17. A.R.Holt, J.Hunt and B.L.Moisewitsch,

'Application of a simplified second Born approximation to the scattering of electrons and protons by helium atoms', J.Phys.B4, 1318-31(1971), Forward elastic scattering of electron by helium', J.Phys.B4 L41-3(1971).

18. A.Szabo and N.S.Ostlund,

'Calculation of high energy elastic electron-molecule scattering cross-sections with CNDO wavefunctions', J. Chem.Phys.60, 946(1974).

19. A.Temkin,

'Polarization and exchange effects in the scattering of electron from atom with application to oxygen', Phys. Rev 107, 1004-12(1957); Non-adiabatic theory of the scattering of electrons from hydrogen', Phys.Rev.L4, 566-8(1960).

20. A.Temkin and J.C.Lamkin,

'Application of the method of polarized orbitals to the scattering of electrons from hydrogen', Phys.Rev.121, 785-94. (1961).

21. A.W.Weiss,

'Wave function and oscillator strengths for the lithium isoelectronic sequence', Astrophysic J.135,1262-1276(1963).

22. A.W. Weiss,

J.Res.Nat.Bur Stand 71A 163(1967) (quoted from Ref.113)

23. A.Zajonc and Alan Gallagher,

'Electron excitation of Li S and D states', Phys.Rev.A20 1393(1979).

24. B.D.Buckley and H.R.J.Walters,

'Second-Born approximation to electron and positron impact excitation of the 1^1S-2^1S transition in helium', J.Phys.B8 1693-715(1975).

25. B.D.Buckley and H.R.J.Walters,

'Second Born approximation of the elastic scattering of electrons and positrons by helium atoms', J.Phys.B7, 1380-1400(1974).

26. B.H.Branden, J.J.Smith and K.H.Winters,

'Distorted wave approximation for the triple differential cross-sections for ionization of helium by electron impact', J.Phys.B11 3095(1978).

27. B.H.Bransden and J.P.Coleman,

'The use of second order potential in the theory of the scattering of charge particles by atoms I.General theory', J.Phys.B5 537-45(1972).

28. B.H.Bransden and K.H.Winters,

'The use of second-order potentials in the theory of scattering of charged particles by atoms IX. The excitation of hydrogen and helium to the n=2. S level by electron impact', J.Phys.B8, 1236-1244(1975).

29. B.H.Bransden and M.R.C.McDowell,

'Electron scattering by atoms at intermediate energies I, theoretical models', Phys.Rep.30C, 207-303(1977).

30. B.H.Bransden and M.R.C.McDowell,

'Theoretical and experimental data for light atoms', Phys. Rep.46C, 249-394(1978).

31. B.L. Moiseiwitsch,

'Recent progress in atomic collisions theory', Rep. Prog.Phys. 40, 843-904(1977).

32. B.L.Moiseiwitsch, and S.J.Smith,

'Electron impact excitation of atoms', Review of Modern Phys.Vol.40, 238-353(1968).

33. B.Padhy,R.Srivastava and D.K. Rai,

'Double electron excitation in helium like ions', Phys.Rev.A28, 1825-1828(1983).

34. B.R.Junker,

'Modified Born model for excitation of atoms by electrons', Phys.Rev.A11 1552-9(1975).

35. B.S. Sharma and A.N. Tripathi,

'Impulse approximation Compton Profile incoherent scattering factors for Na, Al, Ar and Kr', J.Phys. B13, 2947(1980).

36. B.S.Sharma and A.N. Tripathi,

'Elastic and inelastic scattering of high energy electrons and X-ray by NH_3, CH_4 and H_2O molecules', J.Phys. B16, 1827(1983)

37. C.B.Opal and E.C.Beaty,

'Measurements of large angle inelastic scattering cross-sections for electron on helium', J.Phys B5 627-35(1972).

38. C.J.Joachain and C.Quigg,

'Multiple scattering expansions in several particle dynamics', Rev Mod.Phys.46, 279-324(1974).

39. C.J. Joachain and K.H.Winters,

'The electron impact excitation of the 2^1P state of helium in eikonal-Born series approximation' J.Phys. B10 L727-730(1977).

40. C.J.Joachain,

'Quantum Collision Theory (North-Holland Amsterdam, 1985).

41. C.J.Jeachain and R.Vanderpoorten,

'Inelastic scattering of electrons and positrons by atoms at intermediate energies', J.Phys.B6, 622-416 (1973), Inelastic scattering of electrons and positrons by atoms at intermediate energies II', J.Phys. B7, 817-30(1974).

42. C.S.Singh, R.Srivastava and D.K. Rai,

2^1S excitation of the helium atom, Phys.Rev.A27, 302 (1983).

43. C.Tavard and D.Nicolas and M.Roualt,

'Diffraction Des Rayons XET DES electrons Molecules IV. Calcul du factor de diffusion et de I', inlensite incoherente pour trente six peremiers atoms', J.Chem. Phys 64 540(1967).

44. D.A.Kohl, D.P.Duncon, F.W.Tuley Jr. and M.Fink,

'Application of the eikonal approximation to electron scattering II inelastic scattering from helium', J.Chem.Phys 56, 3769-3772(1971).

45. D.A.Kohl, P.Pulay and M.Fink,

'On the calculation of elastic electron scattering cross-sections from molecules wavefunctions CF_4 and CH_4', Theochem.17,149(1984).

46. D.H.Madison and K.H.Winters,

'A second order distorted wave model for the excitation of the 2^1P state of helium by electron and positron impact' J.Phys.B16, 4437-50(1983).

47. D.H.Madison and W.N.Shelton,

'Distorted wave approximation and its application to the differential and integrated cross-sections for electron impact excitation of the 2^1P state of helium', Phys. Rev A7, 499-513(1973).

48. D.Leep and A.Gallagher,

'Electron excitation of the lithium 6708-$\AA$ resonance line', Phys.Rev.A10, 1082(1974).

49. D.L.Moores,

Proc. 13th Int.Conf. on Physics and electronic and Atomic collisions Berlin ed.J.Eichler et al (Amsterdam North-Holland), Abs.9.123(1983).

50. D.P.Dewangen,

'A higher-order model for inelastic electron-atom scattering', J.Phys.B16, L595(1983).

51. D.P.Dewangen and H.R.Walters,

'The elastic scattering of electrons and positrons by helium and neon: The distorted-wave second Born approximation', J.Phys. B10 637-61(1977).

52. D.Rapp and C.M.Chang,

'Wavefunctions and pseudo potential for alkali charge transfer', J.Chem.Phys.57, 4283-6(1972).

53. D.S.F.Crothers,

'Analytic curves fits to helium transition integrals', J.Phys.B3 , 976(1970).

54. D.S.F. Crothers and R.P.McEachran,

'Excitation of the helium S levels by hydrogen impact', J.Phys.B2, 976(1970).

55. Enrico Clement and Carla Roetti,

'Roothaun-Hartree-Fock Atomic wavefunctions', Atomic data and Nuclear data tables', 14, 177-478(1974).

56. E.Clementi and Corongiu,

'Geometrical Basis for Molecular Computations IBM, IS and TG April 27(1982).

57. E.Gerjuoy and B.K. Thomas,

'Applications of the Glauber approximation to atomic collision', Rep.Prog.Phys.37, 1345-1431(1974).

58. E.N. Lassettre,

'Power series representation of generalised oscillator strength', J.Chem.Phys.43, 4479(1965).

59. F.Hirota, H.Terada and S.Shibata,

Bulletin of the Faculty of Education,' Shizuoki University, National Science Series, Vol.31, p.49 (1980).

60. F.J. deHeer and R.J.Jansen,

'Total cross sections for electron scattering by He', J.Phys.B10, 3741(1977).

61. F.K.Canter and A.P.Mills Jr.,

'Slow positron beam design notes', Con.J.Phys.60, 551-64(1982).

62. F.T.Chan, C.H.Chang and M.Lieber,

'Comparison of Born and Glauber generalized oscillator strengths for the 2s-2p transition of atomic hydrogen', Phys. Rev.A17, 1869-73(1978).

63. F.T.Chan, M.Lieher, G.Foster and W.Williamson Jr.,

'Applications of Glauber and eikonal approximations to atomic collisions', Adv.Electronics and electron Phys.49, 133-204(1981).

64. F.W.Byron Jr. and C.J.Joachain,

'Correlation effects in atoms I.Helium', Phys.Rev.146, 1-8(1966).

65. F.W.Byron, Jr. and C.J.Joachain,

'Electron impact excitation of the 2^1S state of helium at intermediate and high energies', J.Phys B8, L284-8 (1975).

66. F.W.Byron Jr. and C.J.Joachain,
'Eikonal theory of electron and positron-atom collisions, Phys: Rep 34C, 233-324(1977).

67. F.W.Byron Jr. and C.J.Joachain,
'Elastic electron-atom scattering at intermediate energies', Phys. Rev.A8, 1267-82(1973);Elastic scattering of electrons and positrons by atomic hydrogen and helium at intermediate energies', J.Phys.B10, 207-226(1977).

68. F.W.Byron Jr., C.J.Jeachain and R.M.Polvliege,
'Unitarisation of the eikonal-Born series method for electron and positron-atom collisions', J.Phys.B14 L609(1981).

69. F.W.Byron Jr. and C.J.Joachain and R.M.Polvliege,
'Elastic and inelastic scattering of electrons and positrons by atomic hydrogen at intermediate and high energies in the unitarised eikonal Born series method', J.Phys.B18, 1637(1985).

70. F.W.Byron Jr. and L.J.Latour,
'Excitation of atomic hydrogen in the eikonal Born-Series approximation', Phys.Rev.A13, 649(1976).

71. G.P.Gupta and K.C.Mathur,
'Electron impact excitation of the 2^1S state of helium at intermediate energies', J.Phys.B12, 1733-9(1979).

72. H.R.J.Walters,
'Electron scattering by Li, Na and K in the forgen core Glauber approximation', J.Phys.B6 1003-19(1973).

73. H.R.J.Walters,
'Perturbative methods in electron and positron-atom scattering', Phys Repts.116, 1-102(1984).

74. H.S.W.Massey and C.B.O.Mohr,
Proc. Roy.Soc.A146, 880(1934).

75. H.Suzuki and T.Takayanagi,
Abstracts of papers, Eighth International Conference on the Physics of Electronic and Atomic Collisions,' edited by B.C. Cabic and M.V.Kurepa (Institute of Physics, Belgrade. Yugoslavia,1973), p.286.

76. I.P.Zapesochnyi, I.V. Postoi and I.S. Aleksakin, Sov.Phys. JETP 41, 865(1975).

77. J.Callaway, 'Electron-atom scattering', Adv.Phys.29, 771-867(1980).

78. J.C.K. Chan, C.J.Joachain and K.M. Watson, 'Eikonal theory of inelastic electron atom scattering at intermediate energies', Phys. Rev.A5, 2460-74 (1972).

79. J.Callaway, M.R.C. McDowell and L.A.Morgen, 'Scattering of electrons by hydrogen atoms at intermediate energies: Total and differential cross-sections for excitation of n=2 states', J.Phys B8, 2181-90(1975); Inelastic differential scattering of electrons by hydrogen, J.Phys.B9, 2043-51(1976).

80. J.Epstein and R.F.Stewart, '(i) x-ray and electron scattering from diatomic molecules, (ii) in the First Born approximation. A study of calculated x-ray and electron diffraction scattering intensities by Co($1\frac{+}{-}$):electron correlation', J.Chem. Phys.66,4057,abid,67, 238(1977).

81. J.J.McClelland and M.Fink, 'Electron Correlation and binding effects in measured electron-scattering cross-section of CO_2 Phys.Rev.Lett 54, 2218-2221(1985).

82. J.N.Gau and J.Mack, 'Inelastic electron hydrogen scattering in the unrestricted Glauber approximation', Phys.Rev.A12 1760(1975).

83. J.O.Phelps, J.E.Saloman, D.F.Korff, C.C. Lin and E.T.P. Lee, 'Electron impact excitation of potassium atom,' Phys. Rev.A20, 1418(1979).

84. J.V.Kennedy, V.P.Myerscough and M.R.C. McDowell, 'Electron impact excitation of the resonance transition of Li, Na and K', J.Phys.B10, 3759-3780(1977).

85. J.W.Liu,

'Electron scattering from molecules in the first Born approximation', J.Chem.Phys.59,1988(1973).

86. K.A.Berrington, P.G.Burke and A.L.Sinfailam,

'Low-energy scattering of electrons by helium atom',J.Phys B8,1459-73(1975).

87. K.Bhadra, J.Callaway and R.J.W.Henry',

'Electron impact excitation of the n=2 levels of helium at intermediate energies', Phys.Rev.A19,1841-51(1979). S.Trajmar, Phys.Rev.A8,191(1973); R.J.Hall, G.Joyez, J.Mazeau, J. Reinhardt and C.Schermann, J.Phys.(Paris) 34,327(1973);D.G. Truhlar, S.Trajmar, W.Williams, S. Ormonde and B.Torres, Phys.Rev.A8 2475(1973); A.Chutjin and S.K.Srivastava, J.Phys B8, 2360(1975)(quoted from first Ref); G.E.Chamberlain, S.R.Mielezarck and C.E.Kuyall, Phys. Rev.A2,1905-22(1970)(quoted from Ref.180).

88. K.Floeder, D.Fromme, W.Raith, A.Schwab and G.Sinapins,

'Abstracts of papers', Positron impact ionization of helium, Seventh International Conference on Positron Annihilation (6-11, Jan.1985, New Delhi), p.D4.

89. K.H.Winters, C.D.Clark, B.H.Bransden and J.P.Coleman,

'The use of second order potentials in the theory of scattering of electrons by hydrogen and helium atoms', J.Phys.B6, L247-51(1973); The use of second order potentials in the theory of scattering of charge particles by atom VII. The partial wave formalism and elastic scattering of electrons by hydrogen and helium', J.Phys.B7, 788-98(1974).

90. K.H.Winters,

'On distorted wave approximations for excitations', J.Phys. B11,149-65(1978).

91. K.H.Winters,

Ph.D. Thesis, University of Durham, England 1974.

92. K.H.Winters and R.Vanderpoorten,

'The excitation of Li(3s) by electron impact', J.Phys. B15,3945-58(1982).

93. K.L.Bell and A.E.Kingston,

'First Born approximation', Adv.At.Mole Phys.10,53(1974).

94. K.L. Bell, D.J.Kennedy and A.E. Kingston,

'Accurate first Born approximation cross-sections for the excitation of helium by fast electrons', J.Phys.B2 26-43(1969).

95. K.L. Boluja and M.R.C. McDowell,

'Electron impact excitation of the 2^1P and 2^3S levels of helium', J.Phys.B12, 835-45(1979).

96. K.Omidvar,

'2s and 2p electron impact excitation in hydrogen' Phys.Rev.133, 970-85(1964); Behaviour of the ionization cross-section in collision of high energy electrons with hydrogenic atoms:Phys.Rev.177, 218-8(1969).

97. K.Tanaka and F.Sasaki,

'Configuration interaction study of X-ray and fast electron scattering factors for high systems', Int.J.Qu. Chem. 5, 157(1971).

98. L.A. Morgan,

'Positron impact excitation of the n=2 levels of hydrogen', J.Phys. B15, L25-9(1982).

99. L.A.Parcell, R.P.McEachran and A.D.Stauffer',

'Positron excitation of the 2^1S state of helium', J. Phys. B16, 4249-57(1983).

100. L.C.Green, M.M.Mulder, M.N. Lewis and J.W.Woll, Jr.,

'A discussion of analytic and Hartree-Fock wavefunctions for $1s^2$ configuration from H to VI', Phys.Rev.93 757-61(1954).

101. L.C.Snyder and H.Basch,

'Molecular wavefunctions and properties, (Wiley, New York 1972).

102. L.D. Thomas, Gy.Csanak, H.S. Taylor and B.S. Yarlagadda,

'The application of first order many-body theory to the calculation of the differential and integral cross-sections for the electron impact excitation of the 2^1S, 2^1P, 2^3S and 2^3P states of helium', J.Phys.B7, 1719-33(1974).

103. L.I. Schiff,

'Approximation method for high energy potential scattering' Phys.Rev.103, 443(1956).

104. L.Vuskovic, S.Trajmar and D.F.Register,

'Electron impact cross-section for the 2^2P state excitation of lithium', J.Phys. B15, 2517-29(1982).

105. M.A.Dillion and E.M.Lassettre,

'A collision cross-section study of the 1^1S-2^1P and 1^1S-2^1S transitions in helium at kinetic energies from 200-700 eV. Failure of the Born approximation at large momentum changes; J.Chem.Phys. 62, 2373-90(1975).

106. M.A. Dillon and M.Inokuti,

'Precise test of Coulomb-projected Born approximation for the 2^1S and 3^1S excitation of helium by electron impact', J.Chem.Phys.76, 5887(1982).

107. M.Breitenstein, A.Endesfelder, H.Meyer, A.Schweig and W.Zittlau,

'Electron correlation effects in electron-scattering cross-section calculation of N_2', Chem.Phys.Lett 97, 403(1983), M.Breitenstein, A.Endesfelder, H.Meyer and A.Schweig, 'CI calculations of electron scattering cross-sections for some linear molecules', Chem.Phys. Lett 108, 430(1984); M.Breilenstein, R.J.Manwharder, H.Meyer and A.Schweig, 'Phys.Rev.Lett 53,2398(1984).

108. M.E.Rose,

'Elementary theory of angular momentum', John Wiley and Sons, New York, 1957.

109. M.Inokuti,

'Rev.Mod.Phys.43, 297(1971).

110. M.J.Wollings and M.R.C. McDowell,

'Collisions of fast electrons with helium I. Various forms of the second Born approximation', J.Phys. B5 1320-31(1972).

111. M.J.Woolings,

Ph.D. Thesis University of London (1972).

112. M.K. Srivastava

'Simple two piece procedure for electron atom elastic scattering at low intermediate energies', Phys.Lett. A79 61(1980).

113. M.Kumar, R.Srivastava and A.N. Tripathi,

Systematic approach for discrete excitation of helium in Coulomb-Born model', Phys.Rev.A31, 652(1985).

114. M.Kumar, R.Srivastava and A.N. Tripathi,

'Study of e^+-He scattering: A distorted wave approximation', J.Phys.B18, 4169(1985), Excitation of helium by positron: A distorted wave polarized orbital appr oach approach, J.Chem. Phys. Lett 192(1986)(in press).

115. M.Kumar, S.S. Tayal and A.N. Tripathi,

'Electron impact excitation of the 3s state of lithium at intermediate and high energies', J.Phys. B18,135-40 (1984).

116. M.Lal and M.K. Srivastava,

'Elastic scattering of electron by atomic hydrogen and helium', J.Phys.B14, 1857-1873(1981).

117. M.R.C. McDowell and J.P.Coleman,

'Introduction to theory of Ion-Atom Collisions'(North-Holland, Amsterdam, 1970), p.341.

118. M.R.C. McDowell, L.A.Morgen and V.P.Myerscough,

'Electron impact excitation of H and He^+I 1s-ns transition', J.Phys.B6 1435-51(1973); Electron impact excitation of H and He^+ III 1s-np transitions, J.Phys. B8 1053-72(1975); Electron impact excitation of H and He^+ V. Differential cross-sections for the excitation of the n=2 levels of atomic hydrogen at intermediate energies',J. Phys. B8 1838-50(1975).

119. M.R. Flannery,

'Multi-state impact-parameter treatment of hydrogen-helium excitation collisions', J.Phys.B2, 913(1969).

120. M.R.Flannery and K.J.McCann,

'A ten-channel eikonal treatment of differential and integral cross-sections and of the (λ,χ)parameters for the n=2 and n=3 excitation of helium by electron impact', J.Phys.B8, 1716-33(1975).

121. P.G.Burke, D.F.Gallahar and S. Geltmans,

'Electron scattering by atomic hydrogen using pseudo-state expansion I.Elastic scattering', J.Phys.B2, 1142-52(1969).

122. P.G.Burke and J.F.Williams,

'Electron scattering by atoms and Molecules', Phys. Rep.30, 325-69(1977).

123. P.G.Burke and J.F.B.Mitchell,

'Electron scattering by atomic hydrogen using a pseudo-state expansion IV. The convergence of s-state expansion at intermediate energies', J.Phys.B6 320-8(1973).

124. P.G.Burke and K.Smith,

'The low energy scattering of electron and positron by hydrogen atoms', Rev. Mod.Phys.34, 358-502(1962).

125. P.G.Burke, S.Ormonde and W.Whittecker,

'Low energy electron scattering by atomic hydrogen I. The close-coupling approximation', Proc. Phys.Soc. (London) 92, 319-35(1967).

126. P.G.Burke and T.G.Webb,

'Electro scattering by atomic hydrogen using a pseudo-state expansion III. Exc .tation of 2s and 2p states at intermediate energies', J.Phys. B8, L131-34(1970).

127. P.G.Burke and W.D.Robb,

'The R-matrix of atomic processes; Adv.Mol.Phys.41, 143(1975).

128. P.G.Coleman,

'Abstracts of papers, Seventh International Conference on positron annihilation' 6-11, Jan 1985, New Delhi, p.R5.

129. P.G.Coleman, J.T.Hutton, D.R.Cook and C.A. Chandler, Can. J.Phys.60,584-90(1982).

130. P.G. Coleman and McNutt,

'Measurement of differential cross-sections for the elastic scattering of positrons by argon atoms', Phys. Rev. Lett 42, 1130-3 (1979).

131. P.M. Morse, L.A.Young and E.S.Haurwitz,
Phys. Rev. 48,948(1935).

132. P.M.Stone,
'Polarisation potentials for low-energy scattering e^{+}+H and e^{-}+Li', Phys.Rev.141,137-45(1966).

133. P.Pulay, R.Mawhorter, D.A.Kohl and M.Fink,
'Abinitio Hartree-Fock calculation of the elastic scattering cross-section of sulphur hexafluoride', J. Chem.Phys.79, 185 (1983).

134. R.A. Bonham,
'Inelastic scattering from atoms at medium energies I Bound states', J.Chem.Phys.36, 3260-9(1962).

135. R.A.Bonham,
'Infinite-channel close-coupling theory in the second-Born approximation I. charge polarization in the elastic electron scattering from H and He', Phys.Rev.A3 298-309(1971), II. Treatment of charge polarization in elastic scattering by used T-matrix formalism, Phys.Rev.A3 1958-68(1971).

136. R.A.Bonham and M.Fink,
'High energy electron scattering', Van Nostrand, New York, 1974.

137. R.A.Bonham,
'Calculation of total inelastic x-ray scattering cross-sections $(d\sigma/d\Omega)_{total}$', Phys.Rev.A23, 2950-2956 (1981).

138. R.Benesch and V.H. Smith Jr.,
'In wave Mechanics. The First fifth years', edited by W.C.Price, S.S.Shissick and T.Ravensdale (Butterworths, London,1973) p.357-377, Acta Cryst A.26, 579(1970).

139. R.J.Glauber,

'In lectures in theoretical physics', Vol.I, edited by W.E.Brittin (Interscience, New York), p.135(1959).

140. R.J.Drachman and A.Temkin,

'Case studies in atomic collision physics', (North-Holland, Amesterdum, 1972), Vol.2, 399.

141. R.J.W.Henry,

'Excitation of atomic positive ions by electron impact', Phys.Rep.68, 1-91(1981).

142. R.K. Sharma, G.P. Gupta and K.C.Mathur,

'Differential cross-sections for the 2s-3s excitation of the lithium atom by positron-impact Phys.Rev.A26, 1122-4 (1982).

143. R.Marriot, '

'Calculation of the 1s-2s electron excitation of hydrogen', Proc. Phy.Soc.(London), 72, 121(1958).

144. R.P.Feynman,

Phys.Rev.76, 709(1949); R.H.Dalitz Proc. R.Soc. A206, 509(1951); R.R.Lewis, Phys.Rev.102,537(1956).

145. R.Srivastava, M.Kumar and A.N. Tripathi,

'2^1S excitation of helium' A precise distorted wave approach', J.Chem. Phys.82, 1818(1985).

146. R.Vanderpoorten and K.H. Winters,

'Off-diagonal potentials in the distorted-wave expansion for electron-atom scattering', J.Phys.B12, 473-488(1978).

147. R.V.Calhaun, D.H.Madison and W.N.Shelton,

'Angular correlation parameters for 1S-2P excitation of hydrogen calculated in the distorted wave approximation', J.Phys.B10, 3523-33(1977).

148. R.W.LaBahn and J.Callaway,

'Distortion effects in the elastic scattering of 100 to 400 eV electron from helium, Phys.Rev.180, 91-6(1964); Addendum to distortion effects in the elastic and inelastic scattering of 100 to 400 eV electrons from helium', Phys. Rev.188 520-1(1969).

149. Sung Dahm Oh, J.Mack and Ed Kelsey,

'Electron excitation of hydrogenlike ions in the Coulomb-Born approximation', Phys.Rev.A17, 873-879(1978).

150. Shang-deXie, M.Fink and D.A.Kohl,

'Basis set dependence of abinitio SCF elastic, Born, electron scattering cross-sections for C_2H_4', J.Chem. Phys.81, 1940(1984).

151. S.Geltman,

'A high energy approximation I. Proton hydrogen charge transfer', J.Phys.B4, 1288-98(1971).

152. S.J.Wallace,

'Ann.Phys.NY 78, 190-257(1973).

153. S.K. Srivastava and L.Vuskovic,

'Elastic and inelastic scattering of electron by Na', J.Phys.B13, 2633-43(1980).

154. S.Kumar, A.N. Tripathi, and M.K. Srivastava,

'e-H^- elastic scattering in eikonal approximation', J. Phys.B8, 1082(1975).

155. S.Kumar, M.K. Srivastava and A.N. Tripathi,

'Glauber cross-sections for the 2s-2p resonance excitation in helium by electron impact', Phys.Rev.A13, 1307 (1976).

156. S.L. Willis, J.Hata, M.R.C. McDowell, C.J.Joachain and F.W.Byron, Jr.,

'Positron collisions with helium at intermediate energies', J.Phys.B14, 2687-704(1981).

157. S.N.Singh and A.N.Tripathi,

'Elastic and inelastic scattering of electron by helium atoms based on the Glauber eikonal-series', Phys.Rev.A21, 105(1980).

158. S.P.Khare,

'Angular distribution of electrons elastically scattered by helium atoms, Phys.Lett.29A, 355-356(1969).
'Differential cross-sections for electrons elastically scattered by helium atom; Proc. Phys.Soc.86, 25-9(1965).

159. S.P.Khare and P.Shobha,

'Elastic scattering of electrons by helium atoms', Phys.Lett A31, 571-2(1970); Differential cross-sections for the elastic of electrons by helium atoms', J.Phys.B4, 208-14(1971).

160. S.Saxena and K.C.Mathur,

'Angular correlation parameters and differential cross-sections in electron-lithium scattering', J.Phys. B18, 509-522(1985).

161. S.Saxena, G.P.Gupta and K.C.Mathur,

'Positron impact excitation of helium at intermediate and high energies', Phys.Rev. A27 225-235(1983).

162. S.Shibata, F.Hirota, N.Kakuta and T.Muramatsu,

Int. J.Quantum Chem.18, 281(1980) (quoted from Ref.15)

163. S.S.Tayal, A.N. Tripathi and M.K. Srivastava,

'Elastic scattering of electrons and positrons by lithium Phys. Rev.A24,1817(1981).

164. S.S.Tayal, A.N. Tripathi and M.K. Srivastava,

'Comments on the eikonal Born series approach to electron-atom scattering', J.Phys. B12 L167(1979).

165. S.Tayal, S.N.Singh and A.N.Tripathi,

'Comparison of eikonal-Born series and modified Glauber approach for the study of elastic electron-hydrogen scattering', Praman 13, 89(1979).

166. S.S.Tayal, A.N.Tripathi and M.K. Srivastava,

'Elastic scattering of electrons and positrons by lithium', Phys.Rev.A24,1817(1981).

167. S.S.Tayal and A.N. Tripathi,

'Glauber generalized oscillator strength for allowed transitions of lithium atom', J.Chem.Phys.75,4385(1981).

168. T.F.O.Malley, P.G.Burke and K.A.Berrington,

'R-matrix calculation of low-energy, e-He scattering', J.Phys.B12, 953-65(1979).

169. T.Ishihara and J.C.Y.Chen,
'Two-potential eikonal approximation for electron atom collisions', Phys.Rev.A12, 370-4(1975).

170. T.Noro,F.Sasaki and H.Tatewaki,
'R-matrix study of resonance spectra of the neon atom,' J.Phys.B12, 2217(1979).

171. T.Shuttleworth, D.E.Burgess, M.A.Hender and A.C.H.Smith,
'Inelastic scattering of electron by lithium atoms', J.Phys.B12, 3967-3978(1979).

172. T.Scott and M.R.C.McDowell,
'Electron impact excitation of n^1S and n^3S states of He at intermediate energies', J.Phys.B8, 1851-1865(1975), also see M.R.C.McDowell, L.A.Morgen and V.P.Myerscough 'Electron impact impact excitation of H and He I:1S-nS transitions', J.Phys.B6 1435-1451(1973).

173. T.S.Stein and Kauppila,
'Physics of Electronic and Atomic Collisions,' edited by S.Datz (Amsterdam North Holland, (1982)),p.311.

174. T.Scatt and M.R.C. McDowell,
'Electron impact excitation of n^1S and n^3S states of He at intermediate energies', J.Phys.B8, 1851-1865(1975).

175. T.T.Gein,
'Elastic scattering of electron by hydrogen at intermediate energies: a modified Glauber theory', J.Phys.B9, 3203-12(1976); Elastic scattering of electrons by helium at intermediate energies, Phys Rev.A16 1793-8(1977), Elastic electron hydrogen scattering in Modified Glauber method with the inclusion of Glauber exchange, Phys.Rev.A16 123-8(1977); Excitation of the hydrogen atom in a modified theory, Phys. Rev.A20, 1457-67(1979); Excitation of He^+ by electron impact in the modified Glauber approximation II-1s-2p transition, J.Phys.B17, 3575-85(1984); 1s-2s excitation of He^+ by electron impact in modified Glauber approximation, J.Phys. B17, 1123-35(1984).

176. V.H.Smith, Jr.,
Phys. Script 15, 147(1977).

177. V.Franco and A.M.Halpern,
'Eikonal exchange amplitude', Phys.Rev.A21, 1118(1980).

178. V.Franco,

'Diffraction theory of scattering by hydrogen atom', Phys.Rev.Lett 20, 709-12(1968).

179. V.I.Ochkur, Z

Zh.Eksp. Teo.Fiz.46, 734(1963); The Born Oppenheimer method in the theory of atomic collision', Sov.Phys.JETP 18, 503(1964).

180. W.C.Fon, K.A.Barrington and A.E.Kingston,

'The 1^1S-2^1S and 1^1S-2^1P excitation of helium by electron impact', J.Phys B13, 2309-25(1980).

181. W.C.Fon, K.A.Barrington and A.Hibbert,

'The elastic scattering from inert gases I.Helium, J.Phys.B14, 307-21(1981).

182. W.C.Fon, K.A.Barrington, P.G.Burke and A.E.Kingston,

'The 1^1S-2^3S and 1^1S-2^3P excitation of helium by electron impact', J.Phys.B12, 1861-72(1979), Elastic scattering of electrons by atomic hydrogen at intermediate energies', J.Phys.B14, 1041-51(1981).

183. W.E.Kappila and T.S.Stein,

'Positron-gas cross-section measurements', Can.J.Phys.60 471-493(1982).

184. W.Kolas, H.J. Monkhorst and K.Szalewicz,

'Energy unresolved differential cross-section for electron scattering by H_2', J.Chem.Phys.77, 1323(1982), ibid, 80, 1435(1984), 'Effect of vibrations on the energy unresolved electron scattering by H_2 and D_2.

185. W.N.Shelton, E.S.Leherissey and D.H.Madison,

'Excitation of the 2s state of atomic hydrogen by electron impact in the distorted-wave approximation angular distributions', Phys.Rev.A3, 242-50(1971).

186. W.R.Harshbarger, A.Skerbele and E.N. Lassettre,

'Generalized oscillator strength of the $\tilde{A} - \tilde{X}$ Transition of Ammonia', J.Chem.Phys.54, 3784-3789(1971).

187. W.Williams, S.Trajmar and D.Bozinis,

'Electron scattering from Li at 5.4, 10, 20 and 60 eV impact energies', J.Phys.B9, 1529-36(1976).

188. Y.K.Kim and M.Inokuti,

'Generalised oscillator strength of the helium atom II. Transitions from the metastable states', Phys.Rev.181, 205-14(1969).

189. Y.Sasaki, S.Konaka, T.Iijima and M.Kimta,

'Small-angle electron scattering and electron density in Carbon dioxide', Int.J.Qu.Chem.21,475(1982).